GEOLOGICAL SURVEY OF CANADA
BULLETIN 362

THE EARLY PROTEROZOIC RICHMOND GULF GRABEN, EAST COAST OF HUDSON BAY, QUEBEC

F.W. Chandler

1988

Energy, Mines and Resources Canada
Énergie, Mines et Ressources Canada

©Minister of Supply and Services Canada 1988

Available in Canada through

authorized bookstore agents and other bookstores

or by mail from

Canadian Government Publishing Centre
Supply and Services Canada
Ottawa, Canada K1A 0S9

and from

Geological Survey of Canada offices:

601 Booth Street
Ottawa, Canada K1A 0E8

3303-33rd Street N.W
Calgary, Alberta T2L 2A7

A deposit copy of this publication is also available
for reference in public libraries across Canada

Cat. No. M42-362E Canada: $16.00
ISBN 0-660-12861-6 Other countries: $19.20

Price subject to change without notice

Cover Photo

LANDSAT image #1553-15391 courtesy of
Paul Lowman, Goddard Space Flight Centre,
N.A.S.A., Greenbelt MD. 20771 USA.

Critical Reader

K. Card
H. Geldsetzer

Preface

The eastern shore of Hudson Bay consists of granitoid rocks of the Archean Superior Province that is largely surrounded by an Early Proterozoic supracrustal fold belt, the Circum-Superior belt. The dominant feature of the east shore of the bay is its shape, for it forms a smooth, east-convex arc with a 500 km perimeter centred on the Richmond Gulf Graben at latitude 56° North. This 75 km wide, east-striking graben structure contains two Aphebian sedimentary-volcanic sequences, and appears to die out eastward into the Superior Province.

In this bulletin the detailed stratigraphy, paleocurrent patterns and sedimentary environments of the rocks of the graben are described. Mineralization includes occurrences of apatite in redbeds, stratabound copper, lead-zinc in carbonates, and iron-manganese formation. The report is accompanied by a geological map of the graben at 1:100 000 scale.

The origin of the great arc on the east coast of Hudson Bay, and its associated graben, has been a subject of much speculation. Although they have been attributed to meteorite impact, Dr. Chandler favours a plate tectonic model. An important aspect of this model is continental rifting, evidence of which is seen in aulacogens, sediment-filled cratonic grabens that strike at high angles to craton margins and terminate at bends in adjacent fold belts that fill re-entrants in the craton margin.

Testing the relevance of plate tectonic theory to Proterozoic fold belts of the Canadian Shield is an important part of understanding the Canadian landmass and of providing a predictive model for finding mineral resources.

R.A. Price
Assistant Deputy Miinister
Geological Survey of Canada

Préface

La rive est de la baie d'Hudson se compose de roches granitoides de la province archéenne du lac Supérieur, il s'agit de roches en grande partie entourées d'une zone de plissement supracrustale, soit la zone de plissement de la province du lac Supérieur. La rive est de la baie se caractérise par sa forme, qui présente l'aspect d'un arc uni, convexe vers l'est, dont le périmètre de 500 km est centré sur le graben de Richmond Gulf à une latitude de 56°N. Ce graben, dont la largeur atteint 75 km et à orientation est, contient deux séries sédimentaires et volcaniques d'âge aphébien et semble se terminer en biseau vers l'est, dans la province du lac Supérieur.

Le présent bulletin décrit en détail la stratigraphie, les cours suivis par les paléocourants ainsi que les milieux de sédimentation des roches du graben. La minéralisation comprend des venues d'apatite dans les couches rouges, du cuivre trouvé à l'intéveiur d'une seule strate, du plomb et du zinc dans les roches carbonatées et une formation de fer et de manganèse. Le rapport est accompagné d'une carte géologique du graben à une échelle de 1/100 000.

L'origine du grand arc sur la côte est de la baie d'Hudson et du graben connexe a donné lieu à de vives discussions. Bien qu'il pourraient être le résultat de l'impact d'un météorite, l'auteur croit plutôt en un modèle de tectonique de plaques. Un aspect important de ce modèle est à noter, soit la création de fossés continentaux, que traduit la présence d'aulacogènes, grabens cratoniques remplis de sédiments dont la direction forme un angle élevé avec les marges du craton et qui se terminent à des inflexions dans les zones de plissements contigues qui remplissent les rentrants de la marge du craton.

Il est essentiel d'évaluer la pertinence de la théorie de la tectonique de plaques par rapport aux zones de plissement d'âge protérozoique du Bouclier canadien pour mieux comprendre la partie continentale du Canada et fournir un modèle conjectural susceptible de servir à la recherche des ressources minérales.

R.A. Price, sous-ministre adjoint
Commission géologique du Canada

CONTENTS

1 Abstract/Résumé

2 Summary/Sommaire

7 Introduction
7 Location and access
7 Previous work
8 Fieldwork and acknowledgments

9 Regional tectonic framework

10 General geology
10 Archean granitic basement
11 Aphebian supracrustal rocks
11 Richmond Gulf Group
11 Pachi Formation
11 Description of sandstones
12 Description of lacustrine units
14 Persillon Formation
14 Description
16 Ellipsoidal structures
18 Petrography and chemistry
19 Qingaaluk Formation
19 Description of members 1-3, (alluvial sedimentary rocks)
22 Description of member 4, (local basalt flows)
24 Description of member 5, (marine sandstone)
24 Interpretation of the sedimentary rocks of the Richmond Gulf Group
24 Sandstones
25 Lacustrine unit of the Pachi Formation
26 Intrusive rocks
26 Wiachuan Sills
26 Dykes, igneous and sedimentary
27 Nastapoka Group
27 Introduction
30 Sub-Nastapoka Group basement
30 Basal unconformity and basal clastics (member A)
30 Graded, laminated carbonate (member B)
32 Quartz arenite (member C)
32 Lower biolaminite (member D)
32 Chert breccia (member E)
33 Lead-zinc-bearing stromatolitic biostrome (member F)
34 Wavy stromatolite zone (member G)
35 Upper biolaminite (member H)
35 Top sandstone (member I)
36 Nastapoka basalt ("Caprock"; member J)
36 Summary of sedimentology
37 Stromatolites and environment-sensitive sedimentary structures

42 Structure and age of the graben
42 Faulting and folding
45 Evidence from paleocurrents
49 Geochronology
51 Mineral occurrences
51 Apatite and sedimentary copper in the Richmond Gulf Group
53 Lead-zinc in the Nastapoka Group
53 Iron formation and manganese in the Nastapoka Group
55 Discussion
55 Aphebian geological history of the Richmond Gulf Graben
56 Aphebian regional tectonics and correlation with the Belcher Foldbelt
58 Implications of the Richmond Gulf Graben for the Archean tectonics of northern Quebec

60 References

Appendices

65 1. Description of three vertical facies sequences from sandstones of the Qingaaluk Formation
67 2. Stratigraphic sections (1-12) through the Nastapoka Group, with illustrations

Table

17 1. Chemical analyses of basalts

Figures

in pocket 1. Geological map of the Richmond Gulf Graben; scale 1:100 000
11 2. View toward mafic sill(s) in the Richmond Gulf Group
11 3. Granite-boulder conglomerate at base of the Pachi Formation
11 4. Matrix-supported granite breccia smeared on basement cliff
12 5. Photomicrograph of feldspathic sandstone, Pachi Formation
12 6. A 6 m high cliff section of trough-crossbedded arenite of the Pachi Formation
13 7. Four metre thick unit, probably lacustrine, within pink feldspathic crossbedded grit of the Pachi Formation
13 8. Detail of grey and green lacustrine member, Pachi Formation
13 9. Detail of 1.25 m thick varved, red mudstone-rippled siltstone unit, Pachi Formation
13 10. Interlayered graded volcanogenic red grit and desiccation-cracked mudstone from interflow sediments, Persillon Formation
14 11. Flow-top breccia sandwiched between vesicular flow top and overlying flow base, Persillon Formation
14 12. Pillow-like bodies at base of lava flow overlying clastic sediments, Persillon Formation
15 13. Eastward-leaning spiracles indicating basalt flow direction, at base of Persillon Formation
15 14. Typical scarp face of Persillon Formation capping cuesta of crossbedded Pachi Formation sandstone

15	15.	View of columnar jointed Persillon Formation volcanics capping cuesta of Pachi Formation sandstone
15	16.	View of hematitic alteration of columnar joints, Persillon Formation
16	17.	Detail of weathered joint column in Persillon Formation
16	18.	Ropy flow structure, upper surface of flow unit, Persillon Formation
16	19.	Highly oxidized set of basalt flows in the gently dipping Persillon Formation
16	20.	Contact between spheroidally weathered basalt of the Persillon Formation and overlying basalt-cobble Qingaaluk Formation conglomerate
18	21.	Vertical exposure of oxidized columnar joints in loose block of basalt, Persillon Formation
18	22.	Qingaaluk Formation arkose overlain by sediments and basalt of the Nastapoka Group
19	23.	Basal conglomerate (member 1), Qingaaluk Formation, with angular basalt clasts
19	24.	View of members 1-3 of the Qingaaluk Formation
19	25.	Mudcracked bedding surface of siltstone, redbed member, Qingaaluk Formation
19	26.	Typical coarse grained pebbly feldspathic sandstone of the upper part of the Qingaaluk Formation
20	27.	Strongly exfoliated boulder of basalt in basal conglomerate, Qingaaluk Formation
20	28.	Contact between the Pachi Formation and the Qingaaluk Formation where the normally intervening Persillon Formation is missing but is marked by a basalt-pebble conglomerate
20	29.	Red mud-chips in trough-crossbedded sandstone at the top of the redbed member, Qingaaluk Formation
30	30.	Carbonate layer within desiccation-cracked current-lineated and rippled maroon siltstone, redbed member, Qingaaluk Formation
21	31.	Fining-upward waning-current cycle in medium grained sandstone to mudstone, redbed member, Qingaaluk Formation
21	32.	Parts of five fining-upward alluvial cycles from the redbed member, Qingaaluk Formation
21	33.	Thick- and wavy- to planar-bedded, crossbedded feldspathic sandstone typical of the third member of the Qingaaluk Formation
22	34.	Trough-crossbedded arkose with basal scours (facies A) and interbedded rippled, current-lineated and mudcracked arkose (facies B), Qingaaluk Formation
22	35.	Stratigraphic section of typical braided fluvial sandstone of the third member of the Qingaaluk Formation
23	36.	Two basalt flows separated by flow-top breccia and red sandstone, member 4, Qingaaluk Formation
23	37.	Flow-top breccia on lower basalt flow, member 4, Qingaaluk Formation
23	38.	Tidal marine sandstone (member 5), Qingaaluk Formation, overlain by interbedded herringbone-crossbedded sandstone and rippled siltstone. Carbonates and basalt of the Nastapoka Group disconformably overlie these units

23	39.	Herringbone-crossbedded sandstone and interbedded lenticular and wavy-bedded siltstone, tidal (5th) member, Qingaaluk Formation
24	40.	Photomicrograph of beach grit, tidal member, Qingaaluk Formation
24	41.	Sediment transport directions from trough and planar crossbeds, tidal marine sandstone member, Qingaaluk Formation
25	42.	Ripple-topped sandstone beds and wavy to lenticular-bedded siltstone, upper part of tidal member (member 5), Qingaaluk Formation
25	43.	Herringbone crossbedding in sandstone bed tidal member, Qingaaluk Formation
27	44.	Sandstone conglomerate zone separating two nonvesicular basalt dykes, Qingaaluk Formation
27	45.	Brecciated sandstone of the third member of the Qingaaluk Formation
28	46.	Generalized column to show stratigraphic subdivision of Nastapoka Group
in pocket	47.	Stratigraphic sections (1-12) of the Nastapoka Group
29	48.	Location of stratigraphic sections (1-12) of the Nastapoka Group
30	49.	General view of the Nastapoka Group in a 400 m high cliff. The group overlies the tidal (fifth) member of the Qingaaluk Formation with gentle angular unconformity
30	50.	Paleocanyon eroded into Qingaaluk Formation at the base of the Nastapoka Group
31	51.	Vertical section of base of the Nastapoka Group
31	52.	Cliff of graded laminite of member B of the Nastapoka Group
31	53.	Lenticular turbidite (member B) and quartz arenite (member C) filling depression on unconformity surface beneath carbonates of Nastapoka Group
32	54.	Vertical section of straight and crinkly laminated biolaminite with edgewise laminite breccia layers, Nastapoka Group
33	55.	Detail of chert-breccia zone (member E), Nastapoka Group
33	56.	Four metre thick black-chert breccia (member E), Nastapoka Group
33	57.	Irregular mass of pyrite in lead-bearing zone (member F), Nastapoka Group
33	58.	Cavity in dolomite (member F), Nastapoka Group
34	59.	Cliff of strongly brecciated, cavernous, limonite-stained, galena-bearing member F, Nastapoka Group
34	60.	Disoriented stromatolites in pyritic transitional zone immediately above member F, Nastapoka Group
34	61.	Branched columnar stromatolites peculiar to member F of the Nastapoka Group
34	62.	Vertical section of member G (wavy stromatolite zone), Nastapoka Group
35	63.	Plan view of member G (wavy stromatolite zone), Nastapoka Group
35	64.	Vertical section of low domal stromatolites in laminated dolomite, upper biolaminite (member H), Nastapoka Group
36	65.	Parallel-bedded sandstone (member I) overlain by basalt (member J), Nastapoka Group
39	66.	Plan view of edgewise laminite breccia replaced by white chert in wavy stromatolite zone (member G), Nastapoka Group

40	67.	Tepee structure in unit 1 (member H), Nastapoka Group
40	68.	Geological and gravity profile across the Richmond Gulf Graben
43	69.	Graben-margining fault north of Lac Guillaume-Delisle. Qingaaluk Formation is downthrown against granitic basement. Unfaulted basalt, underlain by arkose, both of the Nastapoka Group overlie the faulted rocks
43	70.	View towards paleohill of Archean granitic basement (G) upon which rest, sandstone of the Qingaaluk Formation, and carbonates and basalt of the Nastapoka Group
43	71.	View toward the central horst, a west-plunging 300 m high hogsback of Archean basement
43	72.	Cliff-forming Archean granite basement upthrown against the Qingaaluk Formation. The faulted rocks are overlain by unfaulted Nastapoka Group
44	73.	Orientation of faults cutting the Richmond Gulf Group, Richmond Gulf Graben
44	74.	West-plunging drag syncline in Pachi and Persillon formations, formed on downthrow side of normal fault at south margin of Richmond Gulf Graben
45	75.	Gentle angular unconformity separating Qingaaluk Formation from gently west-dipping Nastapoka Group
45	76.	Paleocurrents, Pachi Formation
46	77.	Paleocurrents, redbed (2nd) member, Qingaaluk Formation
46	78.	Paleocurrents, arkosic 3rd member, Qingaaluk Formation
47	79.	Trough crossbed in pink arkose of the 3rd member, Qingaaluk Formation
47	80.	Flow directions of Persillon Formation, from leaning pipe amygdules and vesicles at base of flow unit
48	81.	Microtrough-crosslamination (rib and furrow marks), a section of current ripples in the bedding surface, second (redbed) member, Qingaaluk Formation
48	82.	Comparison of some paleocurrent data from trough crossbeds and current ripples from the second (redbed) member, Qingaaluk Formation
49	83.	Geological map with paleocurrent data, to show lack of effect of present granitic basement horst on fluvial paleocurrent trend of Qingaaluk Formation
50	84.	Stratigraphic correlations of the Aphebian supracrusal rocks of the east Hudson Bay region, Richmond Gulf Graben and Belcher Islands
51	85.	Some major structural elements of the northeast Superior Structural Province and adjacent areas
65	86.	Current crescents in fine grained sandstone, second (redbed) member, Qingaaluk Formation
68	87.	Unique zone of finger-shaped and sized stromatolites, Nastapoka Group
71	88.	Stromatolite bun, lower biolaminite, Nastapoka Group
71	89.	Detail of layer of spherical stromatolites with interdome edgewide laminite breccia, Nastapoka Group

71	90.	Stromatolite-rich dolomite layer with pyrite nodules, Nastapoka Group
72	91.	General view of the Nastapoka Group on the west shore of Lac Guillaume-Delisle, to show irregular unconformity surface
73	92.	Vertical section of crossbedded and rippled quartz arenite interbedded with lenticularly bedded siltstone-shale, Nastapoka Group
73	93.	Vertical section of 1 m high tepee structure, lower biolaminite, Nastapoka Group
74	94.	Vertical section of 60 cm high single stromatolite layer, lower biolaminite, Nastapoka Group
74	95.	Vertical section of chertified low domal stromatolites growing on elevations of edgewise laminite breccia in biolaminite, Nastapoka Group
74	96.	Oncolites in vertical section in wavy stromatolite member (member G), Nastapoka Group
74	97.	Fifty-five centimetre high vertical section of conophyton-like stromatolites, Nastapoka Group
75	98.	Laminated dolomite with low domal stromatolite domes, edgewise laminite breccia layers, and chert layers, upper biolaminite, Nastapoka Group
75	99.	Photomicrograph of bimodal quartz arenite, Nastapoka Group

THE EARLY PROTEROZOIC RICHMOND GULF GRABEN, EAST COAST OF HUDSON BAY, QUEBEC

Abstract

The 75 km wide Richmond Gulf Graben is of mid-Aphebian age. Sedimentary facies, paleocurrents, mafic intrusives, gravity and structural data support a failed arm model connected with rifting in the Circum-Superior Belt. The graben strikes toward a similar feature across the Superior Province. This with other regional geological features suggests that it formed along a weakness in the Archean crust. The Aphebian Richmond Gulf Group was derived from thermal doming in the west and northwest, and is now restricted to the graben. The overlying miogeoclinal Nastapoka Group is much more widespread. The basal formation of the Richmond Gulf Group, the Pachi, up to 500 m of fluvial arkose, contains authigenic apatite mineralization in basal redbeds. Up to 70 m of oxidized, weathered subaerial basalt, the Persillon Formation overlies the Pachi and is succeeded by the Qingaaluk Formation, 500 m of braided fluvial arkose with local basalt flows. East- trending mafic dykes intruded the Richmond Gulf Group, probably during graben-formation. Later uplift produced a rugged surface upon which were deposited unconformably south- and west- thickening peritidal carbonates, clastics and sub-aerial basalt of the Nastapoka Group. A pyritic zone, up to 200 m thick, at the unconformity is the site of local copper-cobalt mineralization. A brecciated stromatolitic horizon hosts lead-zinc mineralization. Volcanogenic iron formation and manganese, higher in the Nastapoka Group, are related to compressive tectonics.

Résumé

Le graben de Richmond Gulf, d'âge aphébien, est large de 75 km. Les faciès sédimentaires, les paléocourants, les intrusions mafiques et les données gravimétriques et structurales militent tous en faveur d'un modèle de bras affaissé lié à la création de fossés dans la zone de plissement de la province du lac Supérieur. Le graben est orienté vers une structure similaire en travers de la province du lac Supérieur. Cette situation, avec d'autres éléments géologiques, semble indiquer que le graben s'est formé le long d'une faiblesse de la croûte archéenne. Le groupe aphébien de Richmond Gulf est dérivé du bombement thermique à l'ouest et au nord-ouest et maintenant se trouve uniquement dans le graben. Le groupe miogéoclinal sus-jacent de Nastapoka a une répartition beaucoup plus vaste. La formation de Pachi, formation basale du groupe de Richmond Gulf, se compose d'un maximum de 500 m d'arkose fluviatile, et contient une minéralisation authigène d'apatite dans les couches rouges basales. La formation de Persillon, qui comprend jusqu'à 70 m de basalte subaérien altéré et oxydé, repose sur la formation de Pachi et est recouverte par la formation de Qingaaluk, composée de 500 m d'arkose fluviatile anastomosée avec, par endroits, des coulées de basalte. Des filons mafiques à orientation est ont fait intrusion dans le groupe de Richmond Gulf, probablement au cours de la formation du graben. Un soulèvement plus récent a produit une surface accidentée sur laquelle se sont accumulés en discordance des roches carbonatées de nature péritidale, des sédiments clastiques et un basalte subaérien du groupe de Nastapoka; ces roches s'épaississent vers le sud et vers l'ouest. Le long de la discordance, une zone pyriteuse dont l'épaisseur atteint jusqu'à 200 m, est une zone de minéralisation cupro-colbatifère locale. Un horizon stromatolitique bréchifié contient une minéralisation plombo-zincifère. Une formation ferrifère et de la manganèse volcanogénique, situées plus haut dans le groupe de Nastapoka, sont liées à la compression tectonique.

SUMMARY

The Richmond Gulf Graben lies on the east coast of Hudson Bay at about latitude 56°N. It is separated from the Archean basement to the north and south by east-striking listric normal faults that downthrow Aphebian supracrustal rocks creating a basin about 80 km across in which lies a large body of brackish water, Lac Guillaume Delisle. Two to three hundred metres below the level of the surrounding Archean peneplane, the topography within the graben is rough and exposure is excellent.

The Aphebian rocks associated with the graben include two sedimentary-volcanic sequences, the Richmond Gulf Group and the overlying Nastapoka Group as well as some mafic sills and dykes. The older group consists of three formations, in ascending order, the arkosic Pachi, the basaltic Persillon and the arkosic Qingaaluk. The group is restricted to the graben and was much faulted during graben formation. The Nastapoka Group is informally divided into ten members consisting mainly of carbonate, quartz and feldspar-rich sandstone and basalt. It is unfaulted, dips gently west, unconformably overlies the Richmond Gulf Group and extends north and south beyond the Archean shoulders of the graben.

The Archean basement gneiss, which is also locally present as horsts in the graben, is peneplaned and unweathered. The Pachi Formation, 0 to possibly 500 m thick, consists mainly of weakly upward- coarsening arkosic sandstone to grit with granitic and quartz pebbles probably deposited on a braided alluvial plain. Very minor orthoconglomerate and paraconglomerate at the basal unconformity are not related to graben faults. Local redbed units up to 20 m thick occur at the base of the formation. Trough and planar crossbeds dominate the arkose. Rare mud chips and desiccation-cracked mud wisps are ubiquitous. At the outcrop level paleocurrents based on trough crossbeds are strongly unidirectional. In the southern part of the graben they indicate transport to the east and southeast. In the north, associated with quartz- pebble conglomerate, dispersal was as a south-directed fan. Possible other evidence of a disturbed paleocurrent pattern in the north is the presence of units, up to several metres thick, of thinly bedded sandstone and mudstone of shallow lacustrine origin.

SOMMAIRE

Le graben de Richmond Gulf se situe sur la côte est de la baie d'Hudson à une latitude d'environ 56°N. Il est séparé du socle archéen au nord et au sud par des failles listriques normales à orientation est responsables de l'affaisement des roches supracrustales aphébiennes, lequel a ainsi créé un bassin d'environ 80 km de diamètre au sein duquel repose une vaste nappe d'eau saumâtre, le lac Guillaume Delisle. La topographie à l'intérieur du graben est accidentée et on y trouve d'excellents affleurements à deux ou trois cent mètres sous le niveau de la pénéplaine archéenne environnante.

Les roches aphébiennes associées au graben comportent deux séries sédimentaires et volcaniques, le groupe de Richmond Gulf et le groupe sus-jacent de Nastapoka, ainsi que quelques filons-couches et filons mafiques. Le groupe plus ancien se compose de trois formations soit, en ordre ascendant: la formation arkosique de Pachi, la formation basaltique de Persillon et la formation arkosique de Qingaaluk. Le groupe se trouve uniquement dans le graben et a été largement faillé au cours de la formation de ce dernier. Le groupe de Nastapoka est divisé officieusement en dix termes composés surtout de carbonate, se quartz et de grès feldspathique, ainsi que de basalte. Dépourvu de failles, il s'incline légèrement vers l'ouest et repose en discordance sur le groupe de Richmond Gulf; il se prolonge au nord et au sud au-delà des épaulements archéens du graben.

Le gneiss du socle archéen, qui se trouve également par endroits dans le graben sous forme de horsts, est pénéplané mais non altéré. La formation de Pachi, dont l'épaisseur varie de 0 à près de 500 m, se compose surtout de grès arkosique qui se transforme vers le haut de la section en grès grossier à cailloux de granite et de quartz vraisemblablement accumulés sur une plaine alluviale anastomosée. De très petites quantités d'orthoconglomérat et de paraconglomérat trouvés à la discordance basale ne sont pas liées aux failles du graben. Par endroits, des unités de couches rouges pouvant atteindre 20 m d'épaisseur se présentent à la base de la formation. L'arkose se caractérise par une stratification oblique en auge et planaire. Quelques rares fragments de boue et de minces volutes de boue fissurés par dessiccation se retrouvent partout. À l'échelle de l'affleurement, la stratification oblique en auge témoigne de la nature fortement unidirectionnelle des paléocourants. Dans la partie sud du graben, les paléocourants indiquent que le transport s'est fait vers l'est et vers le sud-est. Au nord, la présence de conglomérats à cailloux de quartz indique que la dispersion a eu lieu vers le sud, sous forme de cône. Au nord, la présence d'unités de grès et de pélite finement stratifiées, d'origine lacustre peu profonde, pourrait être une autre indication de paléocourants perturbés; ces unités peuvent atteindre plusieurs mètres d'épaisseur.

The overlying Persillon Formation consists of several columnar-jointed subaerial basalt flows with desiccation-cracked interflow sediments. The formation is present throughout almost the entire graben and is up to 70 m thick. Flow tops are vesicular and show ropy flow structure. East-leaning pipe amygdules at the base of the unit indicate eastward flow. The basalt is black to green and texturally very altered. Flow tops are reddened and the top of the formation is strongly weathered and red so that the joint columns are reduced to exfoliated corestones. Together with angular blocks, these cobbles provide the material for a conglomerate about 1 m thick at the base of the succeeding formation.

The overlying Qingaaluk Formation, apart from the basal conglomerate (member 1) contains a 80 m thick redbed unit (member 2), a weakly reddened arkose (member 3) up to 500 m thick, and a locally preserved grey sandstone (member 5). Within the formation local subaerial basalt flows (member 4) also occur. The redbed member consists of fine grained sandstone to mudstone with abundant current ripples and desiccation cracks. Locally, small scale (10 cm) upward fining alluvial cycles are preserved. Paleocurrents in this member, based separately on current ripples and trough crossbeds indicate uniform eastward sediment transport. Member 3 is composed of feldspathic sandstone to grit like the bulk of the Pachi Formation. It contains waning current cycles of stacked crossbedded sandstone, with rare preservation of cycle- top members of rippled silt and desiccation-cracked mudstone. The formation is interpreted as of braided fluvial origin. Member 5 consists of a lower part, about 30 m thick, of flat-bedded feldspathic grit and sandstone with opposed crossbedding, probably of beach origin. The upper part, 70 m thick, is composed of alternating herringbone-crossbedded sandstone and fine sandstone to siltstone of tidal marine origin. The unit is present in an east-facing cliff on the west shore of Lac Guillaume Delisle in the form of an open syncline, over a north-south strike length of 11 km.

La formation sus-jacente de Persillon se compose de plusieurs coulées subaériennes de basalte prismatique caractérisé par la présence de sédiments intercalaires fissurés par dessiccation. La formation se manifeste presque partout dans le graben et son épaisseur peut atteindre 70 m. Les sommets des coulées sont vésiculaires et font voir une structure cordée. La présence, à la base de l'unité, de petites cavités allongées et inclinées vers l'est, indique que l'écoulement s'est produit vers l'est. La couleur du basalte varie de noir à vert et sa texture est fortement altérée. Les sommets des coulées ont une couleur rougeâtre et le sommet de la formation, de couleur rouge, est fortement altéré, de sorte que les prismes sont réduits à des boules exfoliées. Ces gros cailloux, combinés à des blocs angulaires, forment un conglomérat d'environ 1 m d'épais à la base de la formation suivante.

Outre le conglomérat basal (membre 1), la formation sus- jacente de Qingaaluk se compose d'une unité de couches rouges de 80 m d'épaisseur (membre 2), d'un arkose rougeâtre dont l'épaisseur peut atteindre 500 m (membre 3) et, par endroits, d'un grès gris (membre 5). La formation contient également, par endroits, des coulées basaltiques subaériennes (membre 4). Le membre 2 se compose de grès fin et de pélite que caractérise la présence d'abondantes rides de courant et fentes de dessiccation. De petits (10 cm) cycles alluviaux à granoclassement vertical sont conservés par endroits. Dans ce membre, les rides de courant et la stratification oblique en auge indiquent que les sédiments ont été transportés uniformément vers l'est. Le membre 3 se compose de grès fedspathique ou de grès grossier, tout comme la plus grande partie de la formation de Pachi. Il contient des grès empilés à stratification oblique, déposés par des courants moins puissants; on y trouve quelques rares pélites fissurées par dessiccation et limons ondulés qui représentent le sommet des cycles de courant. La formation aurait une origine fluviatile anastomosée. La partie inférieure du membre 5 a environ 30 m d'épaisseur et se compose de couches horizontales, vraisemblablement d'origine littorale, de grès grossier de nature feldspathique et de grès caractérisé par une stratification oblique opposée. La partie supérieure du membre de 70 m d'épaisseur se compose de couches alternées de grès à stratification oblique en chevrons et de grès fin ou d'aleurolite d'origine marine tidale. L'unité se trouve dans une falaise à orientation est sur la rive ouest du lac Guillaume Delisle, sous forme d'un synclinal ouvert; elle a une orientation nord-sud et se prolonge sur une distance de 11 km.

Mafic sills up to 30 m thick occur in the central and southern parts of the graben. Sparse mafic dykes, commonly oriented east-west are concentrated in the axial part of the graben and coincide with a positive gravity anomaly that has been interpreted as due to a mafic intrusion at depth, possibly related to graben formation.

On the mainland the Nastapoka Group occurs in east-facing cliffs up to 400 m high on the west side of Lac Guillaume Delisle. In the south part of the graben it consists of ten mappable members. At the northern limit of the graben the group is reduced to a few metres of feldspathic sandstone. The Nastapoka overlies the Richmond Gulf Group with a generally rugged surface and gentle angular unconformity. Both the Richmond Gulf and the Archean basement are bleached and pyritized beneath the Nastapoka Group, locally to a depth of 200 m.

The unconformity surface on the Richmond Gulf Group is overlain locally by crossbedded sandstone and conglomerate and graded carbonate turbidite rhythmites and mass flow conglomerates, overlain by crossbedded quartz arenite. These rocks are followed by several chertified carbonate units of "algal" mat origin that contain stromatolitic layers, oolites, oolitic sand waves, tepee structures desiccation and syneresis cracks and edgewise laminite breccia – features of peritidal origin. Other units within the carbonate sequence include a discordant chert breccia, probably related to emergence of the carbonate depositional environment and several markedly pyritic stromatolite- rich layers. The best developed of these is brecciated, cavernous and mineralized by lead and zinc. The carbonates are overlain by up to 30 m of quartz-rich to feldspathic crossbedded sandstone, probably of tidal marine origin. The Nastapoka Group on the mainland is capped by several subaerial basalt flows.

The graben strikes eastward into the craton and could be explained as a random rift, an impactogen or an aulacogen. Its position, striking into the craton at a high angle from a convex salient in the Circum Superior Foldbelt, and lack of disturbance of the mioclinal Nastapoka Group suggest origin as an aulacogen. The aulacogen model predicts that the graben should have been located at a re-entrant in the rifted craton margin.

Des filons-couches mafiques dont l'épaisseur peut atteindre 30 m se manifestent dans les parties centrale et sud du graben. Quelques filons mafiques épars, à orientation généralement est- ouest, sont concentrés dans la partie axiale du graben et coincident avec une anomalie gravimétrique positivequi serait due à une intrusion mafique en profondeur, possiblement liée à la formation du graben.

Dans la zone continentale, le groupe de Nastapoka se trouve dans des falaises à orientation est dont la hauteur peut atteindre 400 m, sur la rive ouest du lac Guillaume Delisle. Dans la partie sud du graben, le groupe se compose de dix membres que l'on peut porter sur carte. À l'extrémité nord du graben, le groupe se limite à quelques mètres de grès feldspathique. Le groupe de Nastapoka recouvre le groupe de Richmond Gulf; la surface de contact, généralement accidentée, accuse une discordance angulaire douce. Le groupe de Richmond Gulf et le socle archéen ont été lessivés et pyritisés sous le groupe de Nastapoka, jusqu à une profondeur atteignant par endroits 200 m.

La surface de discordance sus-jacente au groupe de Richmond Gulf est recouverte, par endroits, par des grès à stratification oblique, des conglomérats, des séquences rythmiques de turbidites carbonatées classées et des conglomérats formés par écoulement en masse, sur lesquels repose, à son tour, une arénite quartzeuse à stratification oblique. Viennent ensuite plusieurs unités carbonatées, transformées en chert, formées au départ par des tapis d'algues et contenant des couches stromatolitiques, des oolites, des dunes sous-marines oolitiques, des structures en forme de chevron (tepee structures), des fentes de dessiccation et de synérèse et des brèches à laminites disposées de côté; ces éléments accusent tous une origine péritidale. La séquence carbonatée contient d'autres unités, y compris une brèche de chert discordante, probablement associée à l'émersion du milieu de sédimentation carbonaté, et plusieurs couches stromatolitiques fortement pyriteuses. La mieux développée de ces couches est bréchifiée, vacuolaire et a subi une minéralisation plombifère et zincifère. Les couches carbonatées sont recouvertes d'un grès quartzeux ou feldspathique à stratification oblique dont l'épaisseur peut atteindre 30 m et dont l'origine est vraisemblablement marine tidale. La partie continentale du groupe de Nastapoka est recouverte de plusieurs coulées subaériennes de basalte.

Le graben a une direction est et pénètre dans le craton; il pourrait s'agir d'un fossé formé au hasard, d'un fossé formé par impact ou d'un aulacogène. Le graben pénètre dans le craton à un angle élevé à partir d'une saillie convexe dans la zone de plissement de la province du lac Supérieur et il y a absence de perturbations dans le groupe mioclinal de Nastapoka, ce qui semble indiquer qu'il s'agirait d'un aulacogène. Selon le modle de l'aulacogène, le graben aurait été la latitude du graben.

re-entrant in the rifted craton margin. During later cratonic convergence, thrusting of a thickened miogéoclinal prism eastward into the re-entrant could have contributed to the form of the great arc defined by the east coast of Hudson Bay about the latitude of the graben.

The geological evolution of the graben may be summarized as follows. Alluvial arkose of the Pachi Formation was transported eastward from a thermally domed Archean craton that lay west of the Belcher Islands. Irregular paleocurrents suggest rough topography. Widespread occurrence of the Persillon Formation subaerial basalt suggests some smoothing of the land surface. This surface was composed of a sandy alluvial plain with some granitic hills and shallow lakes. The Persillon Formation with its weathered mantle of exfoliated corestones was covered by alluvial arkose of the Qingaaluk Formation, derived again from a granitic source in the west. The greater simplicity of the paleocurrent pattern of the Qingaaluk could be related to increasing smoothing of the topography. The uppermost unit (member 5) of marine flooding of the area in the Richmond Gulf Group.

The Richmond Gulf Group is extensively faulted and tilted by listric normal faults mostly oriented east- west. There is no evidence in the area of other post- Archean faulting. No coarse facies in the arkoses are present near any of these faults, nor are paleocurrents affected by the presence of the faults. Thus the graben was formed after deposition of the Richmond Gulf Group. Mafic dykes, dominantly east-striking, and mafic sills cut the Richmond Gulf Group, but not the Nastapoka, and are probably related to graben formation. Preservation of the marine unit (member 5) of the Qingaaluk Formation only in the axial zone of the graben points to maximum downwarp in this zone.

Following graben formation, uplift carved a locally jagged landscape upon the Richmond Gulf Group within the graben. Deposited on this surface with gentle angular unconformity and on the granitic rocks margining the graben, the rocks of the Nastapoka Group are evidence of the second marine transgression in the Aphebian sequence. An unknown part of the record has been eroded at this unconformity and might include fluvial sediments that the aulacogen model predicts should have been transported westward to the sea along the aulacogen.

situé à l'emplacmeent d'un rentrant dans la marge fissurée du craton. Au cours de la covergence cratonique subséquente, le chevauchement, vers l'est dans le rentrant, d'un prisme miogéoclinal épaissi aurait contribué à la forme arquée qu'affiche la côte est de la baie d'Hudson, plus ou moins au niveau de la latitude du graben.

L'évolution géologique du graben se résume ainsi: l'arkose alluviale de la formation de Pachi a été transportée vers l'est à partir d'un craton archéen thermiquement bombé qui se situait à l'ouest des îles Belcher. L'irrégularité des paléocourants semble indiquer que la topographie était accidentée. La vaste répartition du basalte subaérien de la formation de Persillon indique qu'il y a eu régularisation de la surface terrestre. Cette surface se composait d'une plaine alluviale sableuse et de quelques collines granitiques et lacs peu profonds. La formation de Persillon, avec son manteau altéré de boules exfoliées, a été recouverte par l'arkose alluviale de la formation de Qingaaluk qui, elle aussi, provenait d'une source granitique à l'ouest. La plus grande simplicité du cours suivi par les paléocourants de la formation de Qingaaluk pourrait être attribuable à un relief de moins en moins accentué. L'unité supérieure (membre 5) de la formation de Qingaaluk a enregistré la première inondation marine de la région dans le groupe de Richmond Gulf.

Ce dernier est fortement faillé et a été basculé par des failles listriques normales dont la plupart sont orientées d'est en ouest. La région ne contient pas d'autres indices de la formation de failles post-archéennes. Aucun faciès grossier des arkoses ne se mainfeste près de ces failles et les paléocourants n'ont pas été touchés par la présence des failles. Le graben a donc été formé après la mise en place du groupe de Richmond Gulf. Des filons mafiques, généralement à direction est, et des filons-couches mafiques traversent le groupe de Richmond Gulf, mais non celui de Nastapoka, et sont donc vraisemblablement liés à la formation du graben. La conservation, uniquement dans la zone axiale du graben, de l'unité marine (membre 5) de la formation de Qingaaluk indique que l'affaissement maximal s'est produit dans cette zone.

Suivant la formation du graben, le soulèvement a taillé un paysage parfois accidenté sur le groupe de Richmond Gulf, à l'intérieur du graben. Les roches du groupe de Nastapoka se sont accumulées sur cette surface en formant une discordance angulaire douce; elles se sont également accumulées sur les roches granitiques en marge du graben. Ces dernières témoignent de la deuxième transgression marine dans la série aphébienne. À l'endroit de cette discordance, une section indéterminée de la séquence des événements a été effacée suite à l'érosion; il pourrait s'agir de sédiments fluviatiles qui, selon le modèle de l'aulacogène, auraient dû être transportés vers l'est le long de l'aulacogène jusqu'à la mer.

Mineral occurrences associated with the graben include apatite in redbeds, stratabound copper, lead- zinc in carbonates and iron formation and manganese carbonate. One occurrence of apatite that cements feldspathic redbeds is present at the base of the Pachi Formation. Disseminated copper sulphide mineralization is present locally at the unconformity between the weakly oxidized sandstone of the Qingaaluk Formation and the carbonates of the overlying Nastapoka Group. The post-graben age of the carbonates suggests that thermal effects of the graben were not involved in formation of the mineralization. Copper may have been derived diagenetically from basaltic debris from the Persillon Formation in the Qingaaluk Formation. There is no evidence with the copper of evaporites that might have enhanced transport of the metal.

Galena and sphalerite occur in a brecciated, pyrite-rich stromatolitic zone in the carbonates of the Nastapoka Group. Thin iron formation and associated manganese carbonate in clastic rocks of the Nastapoka Group, offshore in the Nastapoka Islands, are probably of hydrothermal origin and related to a compressive tectonic regime. Although a current tectonic model of the Aphebian evolution of the area favours an island arc regime, the composition of the thick volcanic rocks overlying correlative iron formation is better explained by release of magma from subducting a lithospheric plate into the ocean trench.

The position of the graben opposite the Castignon Lake Graben at a similar latitude in the Labrador Trough on the eastern side of the Superior Craton in Quebec suggests that the two grabens might define a line of Archean crustal weakness. This line separates an Archean terrane in the north that was probably more deeply eroded than one to the south. This and the fact that the Circum-Superior Foldbelt lies also to the north of the Richmond Gulf Graben (Cape Smith Belt) might explain southward components in sediment transport during tensional tectonics that led to deposition of the Richmond Gulf Group and might also have caused facies changes in the Nastapoka Group.

Des venues minérales associées au graben renferment, notamment, l'apatite dans les couches rouges, le cuivre trouvé à l'intérieur d'une seule strate, le plomb et le zinc dans le roches carbonatées, la formation ferrifère et le carbonate de manganèse. Une venue d'apatite cimente les couches rouges feldspathiques à la base de la formation de Pachi. Des sulfures de cuivre disséminés se manifestent par endroits le long de la discordance entre le grès faiblement oxydé de la formation de Qingaaluk et les roches carbonatées du groupe sus-jacent de Nastapoka. La mise en place des roches carbonatées a eu lieu après la formation du graben, phénomène qui semble indiquer que la minéralisation n'est pas attribuable aux effets thermiques du graben. Le cuivre pourrait avoir été produit par diagenèse des débris basaltiques de la formation de Persillon que renferme la formation de Qingaaluk. Le cuivre ne présente aucune trace d'évaporites qui auraient pu faciliter le transport du métal.

Ou trouve de la galène et de la sphalérite dans une zone stromatolique de nature pyriteuse et bréchifiée, dans les roches carbonatées du grupe de Nastapoka. Au large de la côte, dans les îles Nastapoka, une mince formation ferrifère et du carbonate de manganèse connexe trouvés dans les roches clastiques du groupe de Nastapoka ont probablement une origine hydrothermale associée à un régime tectonique de compression. Bien qu'un modèle tectonique actuel de l'évolution aphébienne de la région favorise un régime d'arc insulaire, une libération de magma à partir d'une plaque lithosphérique en subduction dans le fossé océanique expliquerait mieux la composition des roches volcaniques épaisses sus-jacentes à la formation de fer corrélative.

La position du graben en face du graben de Castignon Lake à une latitude similaire dans le fossé du Labrador, sur le côté est du craton du lac Supérieur, au Québec, semble indiquer que les deux grabens pourraient définir une ligne de faiblesse de la croûte archéenne. Cette ligne sépare un terrain archéen au nord qui aurait été plus profondément érodé que celui au sud. Ce phénomène, ainsi que le fait que la zone de plissement de la province du lac Supérieur se trouve également au nord du graben de Richmond Gulf (zone de Cape Smith), pourrait expliquer la direction sud de certains éléments du transport sédimentaire au cours de la tectonique de tension qui aurait mené à la mise en place du groupe de Richmond Gulf et qui pourrait également avoir causé des changements de faciès dans le groupe de Nastapoka.

INTRODUCTION

Location and access

The Richmond Gulf Graben forms an 80 km wide area depressed about 200-300 m below the level of the surrounding Archean peneplain. It lies on the east coast of Hudson Bay at latitude 56°N and is largely occupied by a triangular brackish body of water with a navigable opening to Hudson Bay at its southwest corner. This body of water, about 45 km across, is called Lac Guillaume-Delisle (Richmond Gulf). It is separated from Hudson Bay by 300-400 m high coastal cliffs and on the other sides of the gulf the topography is rough, dominated by fault cuestas and horsts within the graben and by rounded hills within the Archean terrane with a local relief of 100-300 m.

Exposure is excellent except in a swampy area near, and to the northeast of, the mouth of Petite rivière de la Baleine (Little Whale River; see Fig. 1, in pocket).

Vegetation, limited to valleys, is composed of spruce up to 10 m high and with trunks upto 15 cm across, rare aspen and thickets of impassable alder and willow. Waterfowl and ptarmigan are abundant. White whales visit the gulf and seal are common. Char and trout can be taken in the rivers and lakes that drain into the gulf. Land mammals are rare and include black bear, deer, moose and arctic hare. The area now lacks year-round human inhabitants, the original Cree and Inuit population having removed itself, with the Mission and Hudson Bay Post to Poste-de-la-Baleine (Great Whale River), a settlement of several hundred people and transportation centre, 120 km to the southwest on the Hudson Bay coast. Fishing parties visit the gulf from that settlement to camp during the summer season.

Daily access from the south to Poste-de-la-Baleine is given by commercial air carriers (Nordair, Austin Airways). For travel from Poste-de-la-Baleine to Lac Guillaume-Delisle a float-equipped aircraft is required. During the break-up season in the gulf a float plane can be landed early near the opening to Hudson Bay where tidal flow disturbs the ice cover. Availability of float-equipped aircraft at Poste-de-la- Baleine and nearby settlements to the south is very much dependent on current economic activity. The gulf can also be reached from Poste-de-la-Baleine by small boat if due respect is given to the storms which occur on Hudson Bay with only a few hours' warning and to wind-controlled move- ment of pack ice on Hudson Bay during the break-up season.

Ideal sites for field survey camps of a dozen or more people, with safe anchorage for float planes are very rare. The best combination occurs at the old Hudson Bay Post at the southeast corner of Lac Guillaume-Delisle. This site has a plentiful supply of summer-long stream water and a still habitable large Mission house. Beaches are generally very shallow and water levels are subject to tidal change particularly during wind storms. Some good sites for small camps exist at the foot of the coastal cuesta, with easy approach for float planes, though conditions can be very turbulent in the air to the east of the cliffs when a strong west wind is blowing.

Because of the rugged topography foot travel is slow and a helicopter is an ideal mode of transport, although wind and low cloud can hamper air travel. On the gulf itself a float plane is of use as is a small boat during calm weather. But weather in the gulf is changeable. Much of the writers' fieldwork was hampered by strong winds and rough water which prevented free use of small boats. Rain, fog and ceilings often as low as 30-50 m hampered air travel and work on land especially near the coastal cliffs.

Previous work

Early geological work at Lac Guillaume-Delisle included that of Low (1889) who journeyed from Hudson Bay to the Clearwater Lakes, making some brief observations in the gulf en route. Low (1902) described stratigraphic sections along the coastal cuesta and proposed a tectonic hypothesis wherein, following widespread formation of granite, the Aphebian sediments were thrust eastward over the cooling and contracting granitic terrane. Leith (1910) described briefly, and named, the Nastapoka and Richmond (now Richmond Gulf) groups recognizing the unconformity separating them. Harwood (1949) and Parks (1949) described the Pb-Zn occurrences in the Nastapoka Group, the former proposing a granite and thrusting-related hydrothermal model, thought by Chandler (1984) to be unlikely.

Kranck (1951) was the first to suggest that the depression is a graben. Mapping of the structure commenced with surveys by Eade (1966) and Stevenson (1968) at a scale of 1:1 000 000 and that of Woodcock (1960) who mapped the shores of the gulf at 3 miles to the inch (1:190 000). Woodcock gave a more detailed description of the sedimentary and igneous rocks of the gulf proposing a hypothesis for the structural development of the graben. Hews (1976) made an inconclusive Rb-Sr geochronological study of the supracrustal rocks of the graben. Correlations with Aphebian sequences elsewhere in the Hudson Bay region have been made on geological grounds (Dimroth et al., 1970; Ricketts and Donaldson, 1981) and on paleomagnetic grounds (Schwarz and Fujiwara, 1981).

The writer's field program in the area since 1977 has yielded publications by Chandler (1978), a report

on the uranium potential of the supracrustals by Miller, (1978), three preliminary geological maps at 1:50 000 scale (Chandler, 1979; Chandler et al., 1982) and a hypothesis (Chandler and Schwarz, 1980; Chandler et al., 1982) suggesting that the graben structure might be an east- striking failed arm. This model was later supported by a gravity study (Gibb et al., 1983). Two reports (Chandler, 1982, 1984) deal with mineral occurrences in the region, the latter placing these within a tectonic framework.

Chandler and Schwarz (1980) gave a preliminary account of the Aphebian geology of the Lac Guillaume- Delisle area. Salient aspects included brief description and interpretation of the supracrustal rocks, their nomenclature and correlation, and an account of the structure of the graben and its interpretation as an aulacogen.

The supracrustal rocks consist of the Richmond Gulf Group, an arkosic alluvial sequence overlain unconformably by the Nastapoka Group, a marine carbonate- sandstone-shale sequence. Woodcock (1960), placing an unconformity within the arkosic sequence, divided it into a lower Pachi Group and an upper Richmond Gulf Formation. The writer, like Stevenson (1968), for reasons explained in this report thought the division of the arkosic sequence unwarranted, suggesting that it should be named Richmond Gulf Group. The group was divided into a lower Pachi Formation and a similar upper Qingaaluk Formation, separated by a widespread subaerial basalt, the Persillon Formation.

Unlike some previous workers who correlated the Persillon Formation with the basaltic Eskimo Formation of the Belcher Islands to the west, Chandler and Schwarz (1980) suggested that the Eskimo Formation should be correlated with a basaltic unit in the overlying Nastapoka Group. One reason for the change was that these two units lie within carbonate sequences, whereas the Persillon Formation lies within a west-derived alluvial arkose sequence underlying the carbonates that would be unlikely to have had a granitic source area in the west at the same time as carbonates were being deposited there.

Chandler (1982) tested the aulacogen hypothesis of Chandler and Schwarz (1980) and described and interpreted lead-zinc and iron-manganese mineralization within the Nastapoka Group. Studies along the southern margin of the structure showed no connection between facies and the paleocurrent pattern in the arkosic alluvial sandstones of the Richmond Gulf Group and the structural evolution of the graben. This reinforced the view that graben formation followed deposition of the arkoses. Coincidence of major downwarp of the Richmond Gulf Group sediments, a concentration of east-trending mafic dykes and sills and an east-striking positive gravity anomaly (Gibb et al., 1983) in the axial zone of the graben suggested the location of a focus of rifting and mantle involvement.

Last, Chandler (1984) presented a fuller description of the Aphebian geology of the Richmond Gulf Graben in its regional setting, tentatively interpreting the geology within the framework of a Wilson Cycle. Occurrences of apatite in redbeds, disseminated copper sulphides, strata-bound lead-zinc and iron-manganese formation were placed at different stages (tectosomes) of the cycle. The body of this report consists of the detailed data that gave rise to the ideas already published by the writer, as well as previously unpublished data from the writer's studies in the area during the summers of 1978 and 1981. The discussion reflects more recent evolution of these ideas.

Fieldwork and acknowledgments

Studies in the area were carried out over the seasons of 1977 and 1978 and during August 1981. In the first season the writer mapped and studied the Aphebian rocks north of the central horst. Mapping assistance was given by A. Miller of the Geological Survey of Canada (Chandler, 1978; Miller, 1978). Richard Weber ably cooked and managed the camp. Ken Clark carried out paleomagnetic studies on the redbeds and volcanic rocks.

During 1978 the writer completed mapping of the supracrustal rocks south to the south shore of Lac Guillaume- Delisle. Christoph Weber competently performed camp duties. Travel during these two seasons was by float plane, rubber boat and foot. Uranerz-Canada kindly provided the writer with some helicopter transport in the region southeast of Lac Persillon (Chandler, 1979; Chandler and Schwarz, 1980).

During 1981 logistical support was cheerfully given by André Ciesielski of the Geological Survey of Canada from a base camp at the abandoned Mission. Travel was largely by helicopter and foot. Mapping of the supracrustals of the Richmond Gulf Group was completed and reconnaissance examination was made of the Nastapoka Group (Chandler, 1982). The writer was considerably aided in the mapping by A. Ciesielski and R. St. Michel (Chandler et al., 1982). S. Fogarasi, at the writer's request, carried out two gravity surveys across the graben to gather information for interpretation of a positive gravity anomaly beneath the gulf identified from a previous regional gravity survey. J. Maley of the Geological Survey of Canada performed the statistical processing of paleocurrent data for the moving averages of Figures 81-83.

During the first two seasons food was brought from Radisson at the Quebec hydroelectric

construction site on the La Grande-Rivière by La Sarre Air Services' beaver. Excellent air service during the third season was provided by Robert Pritchard of Les Hélicoptères Verreault.

REGIONAL TECTONIC FRAMEWORK

Testing the relevance of plate tectonic theory to Proterozoic fold belts of the Canadian Shield is an important part of understanding the Canadian landmass and of providing a predictive model for finding mineral resources.

The Lac Guillaume-Delisle area contains as its dominant structure a 75 km wide east-west graben that appears to die out eastward into the Superior Province and strikes westward into the Aphebian Circum-Superior Fold Belt, lying largely hidden farther west under the waters of Hudson Bay. A more practical attraction of the Aphebian rocks of the Lac Guillaume-Delisle area is the already known copper-lead-zinc and iron and manganese mineralization.

The eastern shore of Hudson Bay consists of granitoid rocks of the Archean Superior Structural Province that is largely surrounded by an Early Proterozoic supracrustal fold belt, the Circum-Superior Belt (Baragar and Scoates, 1981). The east shore of the bay forms a smooth, east-convex arc with a 500 km perimeter centred on the Richmond Gulf Graben at latitude 56°N. Preserved in the graben lie intricately faulted Aphebian arkose of the Richmond Gulf Group and minor mafic volcanic rocks, sills and dykes. Unconformably overlying these strata and the Archean craton north and south of the graben, the younger Aphebian Nastapoka Group of sediments and minor mafic volcanics forms a gently west-dipping, intermittently preserved coastal cuesta along the entire length of the arc (Eade, 1966; Stevenson, 1968; Lee, 1965). One hundred and twenty kilometres to the west of Lac Guillaume-Delisle, the Belcher Islands are composed of the Belcher Group, a much thicker probable correlative of the Nastapoka Group (Dimroth et al., 1970), that is arranged in a set of east-convex upright isoclinal folds (Jackson, 1960).

The first attempt at a comprehensive tectonic history of the geology of the region was that of Low (1902, p. 48D) who saw the Archean craton in northern Quebec as formed by a great outburst of granite which, not being "universal throughout this vast region" did not affect the Aphebian sediments along the east shore of Hudson Bay. These were, however, intruded by later granites. Contraction of the region on cooling after the first great phase of granite formation allowed outside pressure to thrust the Aphebian sediments eastward over the craton on surfaces at the base of the Nastapoka Group and between the mainland and the offshore islands. Apart from Kranck (1951) who explained regional topography by large curved faults, later writers (Leith, 1910; Woodcock, 1960; Eade, 1966 and Stevenson, 1968) have progressively discounted the existence of any granites later than the Aphebian sediments and of any major north-striking faults.

More recent opinion on the tectonics of the region, including the astrobleme hypothesis, is summarized by Chandler and Schwarz (1980). Explanation of the Circum- Superior Fold Belt as a continental suture started with Wilson (1968) who oriented it southward through Hudson Bay and James Bay. The collisional-suture model has received support from gravity studies of R.A. Gibb and co-workers. Gibb and Thomas (1976) noted similarities among gravity signatures of profiles across boundaries between structural provinces of the Canadian Shield. Their crustal model involved juxtaposition of a thinner, lighter, nonreactivated craton against a thicker, denser, reactivated (Dewey and Burke, 1973) craton. One of their examples was the boundary between the 2.5 Ga Superior Province and 1.75 Ga Churchill Province (Stockwell, 1982). Gibb and

Walcott (1971) realigned this suture to run southwest between the Cape Smith Belt and the Thompson Nickel Belt of Manitoba. Mukhopadhyay and Gibb (1981) placed the Superior-Churchill suture 150 km west of the Belcher Islands with an intervening zone of limited underthrusting by the Superior Province. Foreland effects of such a collision would be crustal shortening decreasing from 40% in the centre of the Belcher Islands to 25% in the eastern part of the islands as documented by Ricketts and Donaldson (1981).

Kranck (1951) was the first to note the structure of the Richmond Gulf Graben. From fold geometry in the Belcher Group he suggested that the graben might project beneath those islands. Woodcock (1960) thought the graben to be an eastward projection from the "Belcher Basin" in which the Pachi Formation was deposited, followed by the Richmond Gulf Formation after an intervening episode of block- faulting.

The Richmond Gulf Graben strikes at a high angle from the craton into the eastward-convex Belcher Fold Belt. Such arrangements can be explained by a family of high-angle rifts, the impactogen, the random rift and the aulacogen (Sengor et al., 1978). Features of the rift, including east- and southeast-directed fluvial and volcanic paleo-flow in the Pachi, Richmond Gulf and Persillon formations, arkosic, granite-derived nature of the graben-fill, absence of any significant amount of granitic conglomerate that could be related to pre- or syn-sedimentary faulting and position of the rift beneath unfaulted mioclinal carbonates prompted rejection of the impactogen and random rift models

and acceptance of the aulacogen model to explain Richmond Gulf Graben (Chandler and Schwarz, 1980). A local positive gravity anomaly associated with mafic intrusives and maximum downwarp of the graben could be evidence of mantle upwelling on the site of the graben (Chandler, 1982). Further, it was suggested that the sediments of the Richmond Gulf Group were eroded from a thermal dome formed on the granitic Superior Province some tens of kilometres to the west of the Belcher Islands (Chandler and Schwarz, 1980), a site fitting with the position of the suggested continental suture of Mukhopadhyay and Gibb (1981). Erosion of this dome could have concentrically thinned the western margin of the Superior Craton in Hudson Bay and contributed to the present arcuate shape of the east coast of Hudson Bay. During later collision the mioclinal sediments at the mouth of the failed arm, thickened by formation of a hypothetical delta from river capture by the failed arm (Burke and Dewey, 1973), would have been pressed eastward as an arcuate salient of the foldbelt (Belcher Islands?) into the re-entrant left at the edge of the Archean craton by the ocean-forming rift arms, perhaps analogous to the Mackenzie Mountains in northwest Canada (Burke and Dewey, 1973). Depression of the craton margin by the remnants of this salient also could have helped determine the arcuate shape of the east shore of Hudson Bay.

Ricketts and Donaldson (1981) concurred in the failed- arm interpretation of the Richmond Gulf Graben, but differed in details. Their interpretation of the Pachi Formation as a westward-prograding delta is difficult to reconcile with the formation's age relative to the graben and its mainly southeastward-flowing paleocurrent pattern. Also their placing of the Qingaaluk Formation at a stratigraphic level within their mioclinal sequence means that earlier mioclinal carbonates ought to have contributed source material to the west derived Qingaaluk Formation. No resistant rock types such as chertified stromatolitic material, for example, are present in the Qingaaluk.

Several interpretations of the Belcher Group are consistent with the Wilson Cycle model. Bell and Hofmann (1974) recognized in the Belcher Group several tectosomes, miogeosynclinal carbonate-sandstone; calc flysch; terrigenous platform; eugeosynclinal volcanics and sandstone, with paleoslope reversal to east-dipping and finally an exogeosynclinal molasse phase.

Ricketts and Donaldson (1981) viewed the Belcher Group as commencing with 2 km of peritidal carbonate-rich sediments, deposited as a west-facing miogeocline on the Archean continental margin. The upper part of the miogeocline contains continental-slope carbonate build-ups followed by deposition of widespread iron formation (Kipalu Formation) in a restricted basin.

A second major tectonic phase opened with reversal of paleoslope and extrusion of about 2 km of shallow water possibly island arc-related tholeiitic basalt (Flaherty Formation), dated at 1.8 Ga (Fryer, 1972; see Geochronology) followed by 2 km of northwest-derived volcanogenic turbidites (Omarolluk Formation) and craton- derived molasse (Loaf Formation).

Not all would interpret the Circum-Superior Orogen to have evolved through formation of a wide ocean. Baragar and Scoates (1981) envisaged annular rifting around the Superior craton to have formed the Circum-Superior Belt. Recognition of significant calc-alkali igneous rocks only in the Lake Superior region and paleomagnetic constraints (Irving and McGlynn, 1976), now not thought important (Irving and McGlynn, 1981) led them to postulate that ocean opening and subduction had occurred only along the present southern limit of the rift system. In their model major rifting-related volcanism followed immediately after miogeosynclinal sedimentation (see Discussion).

As mentioned above a problem with the plate tectonic interpretation of the Hudson Bay region is the voluminous basalt of ocean type (Baragar and Scoates, 1981) in a stratigraphic position where an actualistic model would place calc-alkali volcanics. Such rocks could be present under Hudson Bay 150 km west of the Belcher Group near the suture of Mukhopadhyay and Gibb (1981). Second, voluminous basaltic magmatism following shortly after the foundering of the continental terrace of the 2.1-1.8 Ga Wopmay Orogen was suggested by Hoffman (1981) to be related to a pronounced capacity of subducting lithosphere to release magma in trenches during the Early Proterozoic.

GENERAL GEOLOGY

Archean granitic basement

The basement to the Richmond Gulf Group and the Nastapoka Group, outside the graben, consists of granitic rocks giving uniform Kenoran K-Ar ages (Wanless, 1970). The basement was mapped at a scale of 1:1 000 000 by Eade (1966) and Stevenson (1968). Adjacent to the unconformity with the Richmond Gulf Group it consists of granitic gneiss (Fig. 2) with foliation oriented about 290° and widespread minor inclusions of mafic material (Chandler et al., 1982). At its contact with the Pachi Formation it appears unaltered apart from local white or green discoloration of feldspars. To the south Eade (1966) found the basal arkose to comprise a reconstituted granite, difficult to tell from the underlying granite. Certainly the writer found no reddening that might be expected from deep

weathering under an oxygeniferous atmosphere. This is in keeping with the lack of basement weathering found by Taylor (1982) beneath broadly similar supracrustals on the south margin of the Cape Smith Belt.

Aphebian supracrustal rocks

Richmond Gulf Group

Pachi Formation

Description of sandstones. The Pachi Formation if not fault- repeated could be over 500 m thick. In several cliffs around the graben over 200 m were measured. Locally the formation can be much thinner and is rarely missing. At the west end of the central horst (56°21'N, 76°19'18"W) it is 24 m thick and on the northern shoulder of the graben 0-15 m lie beneath the Persillon Formation.

In several places the base of the Pachi Formation is a pink arkosic grus separable from the underlying granite by faint stratification, heavy mineral layers and quartz pebbles. On the west end of the central horst, arkose and granite cobble conglomerate occur 0.5 km apart, along strike, but conglomerate is a very minor part of the formation, not everywhere present at the base. It is at most a few metres thick and certainly not spatially related to graben-bounding faults. Adjacent to a prominent basement inlier 3 km west of Lac Persillon, basal orthoconglomerate (Fig. 3) contains granite boulders 1-2 m across and white quartz cobbles. Elsewhere, quartz and granite pebble conglomerate was found on, or fills cracks in, the underlying granite. Attached to cliffs that in many cases lie along fault scarps, granitic breccia or paraconglomerate (Fig. 4) in patches usually less than a metre thick may be of fault gouge or mudflow origin.

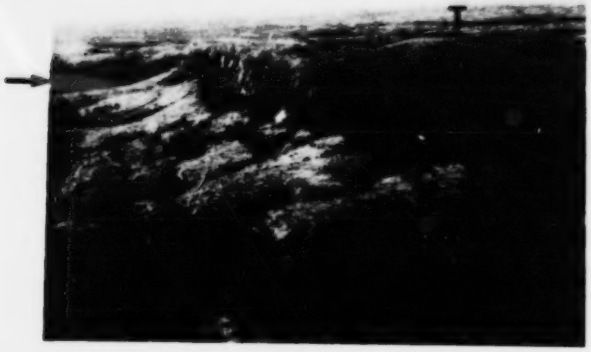

Figure 2. Southwest-looking view from altitude of 300 m toward southernmost southwest-dipping mafic sill(s) in the Richmond Gulf Group. Here the columnar-jointed body is separated from the Archean granitic basement (G) by about 15 m of feldspathic sandstone of the Pachi Formation which contains other sills. The peneplained Archean gneiss terrane (T) continues to the south beyond the margin of the graben (arrow; GSC 203897-G).

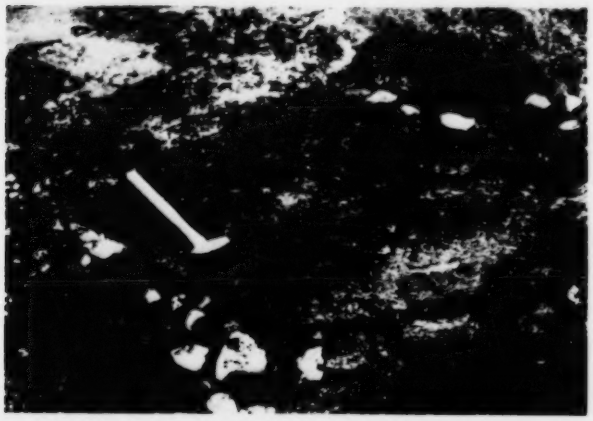

Figure 3. Granite-boulder conglomerate at base of the Pachi Formation, with interstitial granitic and white quartz cobbles and pebbles, south shore of lake 3 km west of Lac Persillon (56°28'18"N, 76°16'61"W; GSC 203263-X).

Figure 4. Matrix-supported granite breccia smeared on basement cliff at north end of Lac Guillaume-Delisle, likely of fault-gourge or mudflow origin (56°32'30"N, 76°24'36"W). 5 cm scale bar on photograph. (GSC 203263-V)

Thicknesses of redbeds up to 20 m, ranging from poorly sorted sandstone with dispersed quartz pebbles to thinly interbedded fine grained sandstone and rippled, mudcracked red mudstone occur locally near the base of the formation. In nearly all these rocks fine grained hematite is dispersed in the matrix or present as plates parallel to cleavage in altered biotite. Black sand grains are well rounded and little altered (Chandler, 1984, Fig. 4a). Hematite haloes around black sand grains and occurring as platelets lining pores provide good evidence of advanced oxidizing diagenesis from only one exposure of these redbeds (ibid, Fig. 4b).

Apart from several probable lacustrine units considered below, the rest of the formation consists of weakly upward- coarsening feldspathic sandstone (Fig. 5) to grit with scattered 1-8 cm quartz and 1-2 cm granite pebbles and rounded to very angular feldspar. The sandstone, light pink, green or grey, weathers pink, green, buff and rarely red and white. Siltstone and mudstone in layers up to a few centimetres thick or present as mudstone chips, comprise less than 1% of any exposure. These layers, coloured red, buff or green, are widely dispersed areally and stratigraphically. Black sand grains or layers are ubiquitous through the sandstone.

In the arkose, sedimentary structures include abundant planar and trough crossbeds (Fig. 6), with sets 5-20 m thick at the top of the formation. Parting lineations, linear wave ripples and linguoid current ripples are common. Measurement of trough crossbed orientations showed eastward and southeastward transport of sand occurred over the central and south parts of the graben. In the north a southward fan-shaped dispersal pattern occurs and may be related to local development at the northern margin of the graben of at least 10 m of quartz-pebble conglomerate near the top of the formation. At the outcrop level paleocurrents are strongly unimodal, unlike the bi- or polymodal patterns occurring in tidal marine sandstones (Klein, 1977). The above features suggest a braided fluvial mode of deposition for the arenaceous part of the formation.

Description of lacustrine units. Between Lac Guillaume- Delisle and Lac Persillon at least three very thin-bedded to laminated fine grained units (Fig. 7, 8, 9), up to 4 m thick, with sharp bases and gradational tops, occur in three cliff sections over an area of 14 km^2. Current lineations (azimuths, 065-110°) and dip of ripple and crossbed foresets indicate eastward current movement.

In the northward-facing first cliff (56°30'N, 76°15'W) lies mudcrack-free upward-coarsening laminated mudstone to rippled fine grained sandstone. It is 1.25 m thick and traceable for 200 m along strike within crossbedded sandstone and grit of the Pachi Formation. At its base the change from grit to mudstone occurs over a vertical distance of 10 cm. The lower half of the unit is varved red mudstone with isolated rare siltstone ripples (Fig. 9) and single-ripple beds less than 3 mm thick. Seven or eight laminae are present in the laminated mudstone. The upper half of the unit becomes increasingly rippled upward, with a scale of bedding and thickness of ripples increasing over a transition zone about 1 m thick to sandstone and grit of the Pachi Formation.

Eight kilometres southwest in the south-facing second cliff (56°28'30"N, 76°21'W) three red

Figure 5. Photomicrograph of feldspathic sand-stone, middle part of the Pachi Formation, typical also of the 3rd member of the Qingaaluk Formation. Grains of polycrystalline quartz, granite, microcline, orthoclase and microperthite rest in a matrix of quartz, feldspar and sericite. Nicols are crossed; grain "A" is 1 mm long.

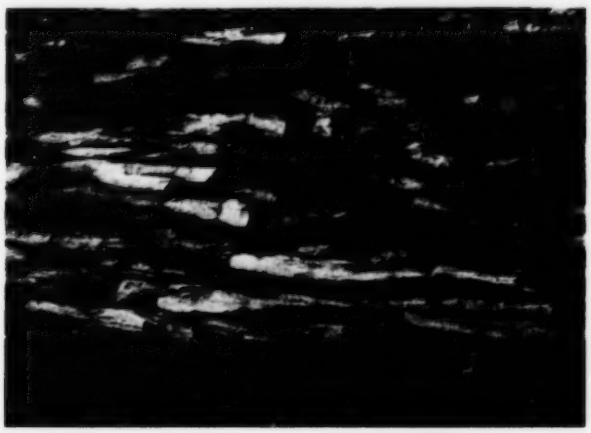

Figure 6. A 6 m high cliff section of trough-crossbedded arenite of the Pachi Formation, approximately normal to paleoflow direction. Lenticular bedding is caused by scour in front of advancing dunes and by bedform surface-topography (Harms et al., 1975, p. 46; GSC 203897-L).

laminated mudstone layers are exposed in crossbedded sandstone of the Pachi Formation sandstone. The sharply based lowest unit is 4 m thick and traceable for 1.5 km along strike. This unit is divisible into three members in ascending order; 1 m of parallel-laminated red siltstone, 1 m of laminated green graded mudstone with grey-green siltstone bases and some rippled silt layers and 2 m red, rippled, fine grained sandstone and siltstone coarsening up to pink coarse grained crossbedded sandstone above the unit. Although a heavy lichen cover prevented detailed study, the following features were seen in the lowest member; rippled siltstone, graded mudcracked layers 0.5-1 cm thick, 4-5 cm thick massive sand layers and load casts. Foresets of several sets of near symmetrical ripple foresets showed more or less eastward sediment transport. No mudcracks were seen in the green and the upper red members. Twenty-one metres above this unit was found a 0.5 m thick rippled and mudcracked red unit of fine grained sandstone to mudstone. Six metres higher in the crossbedded Pachi sandstone a further 0.5 m of similar material was found.

The third occurrence, 4 km southwest of the second cliff, lies in a south-facing cliff of coarse grained Pachi Formation sandstone (56°27'N, 76°19'W). It consists of a 4 m thick fine grained clastic unit with a red upper and lower member and a grey-green middle member, possibly a continuation

Figure 7. Four metre thick unit, probably of lacustrine origin, lying within pink feldspathic crossbedded grit of the Pachi Formation (P). It consists of hemicycles of fine grained laminated, rippled and graded fine sand to mud and is divided into a lower red member (L), a middle grey and green member (M), and an upper mudcracked red member (U). Unit boundaries are arrowed (56°27'N, 76°19'W; GSC 202909-O).

Figure 8. Detail of grey and green lacustrine member (M of Fig. 7), Pachi Formation, shows laminated grey sand beds, single ripple layers and isolated ripples (white) and thinner graded mud layers (dark grey; GSC 203264-K).

Figure 9. Detail of 1.25 m thick varved, red mudstone-rippled siltstone unit, possibly of lacustrine origin, Pachi Formation in north-facing cliff (56°30'N, 76°15'W; GSC 203897-U).

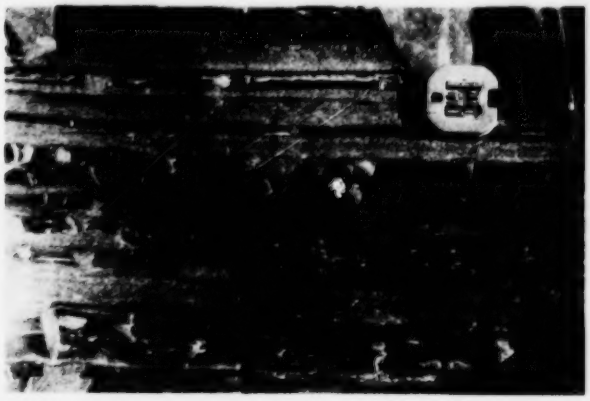

Figure 10. Interlayered graded volcanogenic red grit and desiccation-cracked mudstone from interflow sediments, Persillon Formation (56°14'N, 76°06'W; GSC 207265-V).

of the 4 m thick unit described from the second cliff. This third occurrence, traceable 150 m along strike, can be described in greater detail than the other two due to better exposure.

The lower red member lies abruptly on coarse grained crossbedded sandstone and ranges from 64-90 cm thick. The lower half of this member contains red graded, laminated beds up to 5 cm thick of fine grained sand, fining up to siltstone. The upper finer-grained half of the member is composed of graded siltstone laminae of centimetre to less than millimetre scale. Single ripple trains and isolated ripples with ripple symmetry index of F4 (Reineck and Singh, 1980, p. 35) show broadly eastward sediment transport (8 sampled). Because of few data a vertical facies sequence analysis was not attempted. It appeared however in the outcrop that the graded sandstone layers are overlain by the rippled layers, and that graded mud layers and rippled layers alternate.

The green member (Fig. 8) ranges in thickness from 0-8 cm. Discordance of the colour boundaries of this member suggests that although it may represent a less oxidized depositional environment than the upper and lower members its present thickness is diagenetically changed. This member contains three types of sedimentary unit. Pale green sand layers with parting lineations (azimuths 270°, 290°, 2 measurements) comprise 60% of the member and are evenly dispersed through it. Pale green fine grained rippled sand layers, usually one ripple thick, are distributed 5-10 cm apart through, and comprise 20% of, the member. Asymmetric ripples (ripple symmetry index less than 4, 6 data) suggest both eastward and westward transport. The third type of unit, dark green layers grading from silt to clay, comprises 20% of the member.

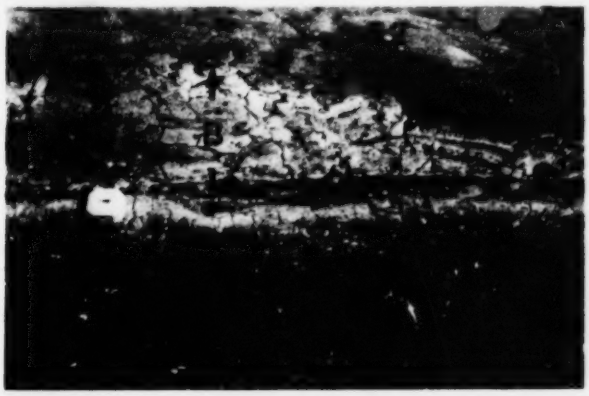

Figure 11. Flow-top breccia (B) consisting of rounded and angular fragments sandwiched between red vesicular flow top (F1) and overlying weakly reddened, sparsely vesicular flow base (F2), section normal to bedding, Persillon Formation (56°08'N, 76°22'W; GSC 203895-V).

The red upper member coarsens upward imperceptibly through 4 m to typical coarse *sandstone of the Pachi Formation*. The lower 40 cm of this unit contains sedimentary structures similar to the green unit, present in equal abundance, namely pink laminated very fine grained sand with parting lineations, pink rippled very fine grained sand ripples in 2-5 cm thick sets with no consistent orientation, and purple graded siltstone-mudstone layers up to 1 cm thick, with faint laminations and downward tapering V-shaped cracks, probably poorly developed mudcracks. The succeeding part of the upper red member consists of beds about 10 cm thick, of flaggy very fine grained sand with parting lineations (azimuth 245°, 1 datum), as well as planar crossbedded very fine grained sand. An oversteepened crossbed was noted 60 cm above the top of the green member. The transitional upper part of the upper red member consists of coarsening-upward medium grained planar and trough-crossbedded pink sandstone with red mud chips on some foresets.

Persillon Formation

Description. This unit is a sequence of up to 70m of basalt flows that, apart from local pinch-out, is present throughout the graben. Lying conformably between the lithologically similar Pachi and Qingaaluk formations it serves as a very valuable stratigraphic marker. Only a few kilometres north of the northern tip of Lac Guillaume-Delisle was the formation found to lie directly upon the granitic basement. It contains ubiquitous small amounts of vesicles and quartz, agate, zeolite and chlorite-filled amygdules less than 1 cm across. The unit consists of at least several flows separated in some places by several metres of interflow sandstone or red mudstone. At one location 14m of red and green

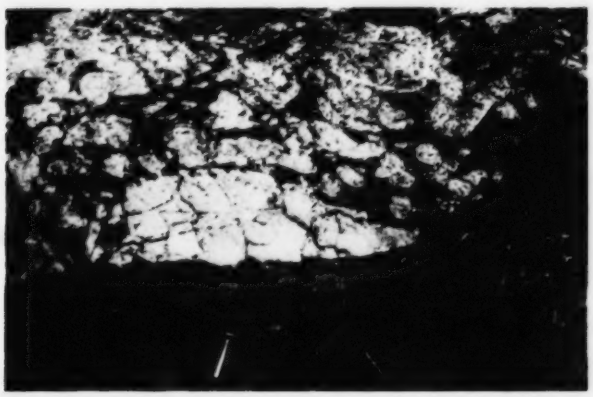

Figure 12. Vertical section of pillow-like bodies at base of lava flow overlying red laminated mudcracked interflow clastic sediments, Persillon Formation, at narrows (56°14'12"N, 76°06'W; GSC 203895-Q).

volcanogenic sandstone and red mudcracked mudstone (Fig. 10) separate a 9 m thick lower volcanic unit from a 16+ m thick upper volcanic unit. More commonly interflow sediments are absent and layers of volcanic interflow breccia (Fig. 11) or conglomerate may intervene with pipe amygdules present at flow bases.

The base of the flow unit is usually massive to weakly vesicular and rarely contains distorted bodies from the underlying Pachi Formation sandstone. Lava toes, volcanic breccia and pillow-like bodies (Fig. 12) usually less than 50 cm across can be present in a basal zone up to 6m thick. Locally pipe vesicles (Waters, 1960, p. 359) about 5 cm long and less than 1 cm across (Fig. 13) are present. Leaning mostly to the east they indicate a western source for the unit. Columnar jointing is rarely visible in cliff sections (Fig. 14) of the nearly flat-lying unit. An exception is shown in Figure 15, but it is seen almost everywhere in horizontal surfaces near the top of the unit (Fig. 16, 17). The joints are strongly exfoliated and adjacent basalt has been hematized or replaced by silica. Columnar jointing is further discussed under "Ellipsoidal structures" Local flow ropes (Fig. 18) and stretched vesicles on exhumed flow tops lack consistent orientation and probably reflect local flow-top relief.

Individual flows have green lower parts and red upper parts (Fig. 19) even where interflow sediments are not present. Reddening is much more marked at the top of the flow unit. . Measured at 6m thick, it penetrates below this level along joints. Dolomite

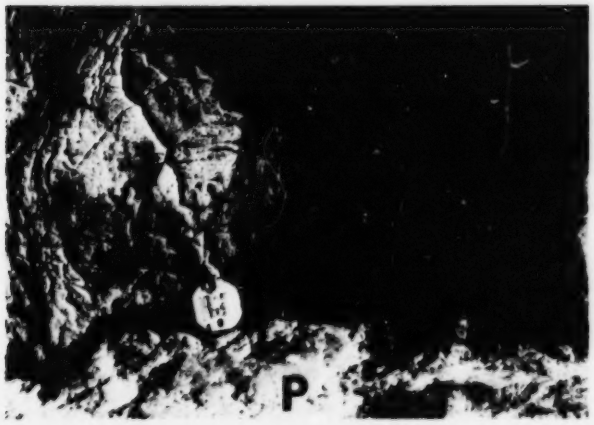

Figure 13. Eastward-leaning spiracles (arrowed, dark) indicating basalt flow direction, at base of Persillon Formation (56°08'N, 76°22'W). Sandstone of underlying Pachi Formation is marked (P; GSC 203989-A).

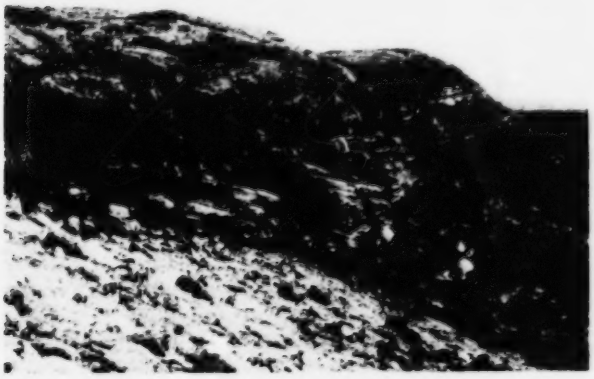

Figure 14. Typical scarp face of Persillon Formation, base arrowed (56°29'N, 76°16'W). The unit commonly caps cuestas of crossbedded sandstone of the Pachi Formation. Note rounding of cliff edge and usual apparent absence of columnar joints in foreground. Crossbed at centre is 5 m thick. (GSC 203263-W)

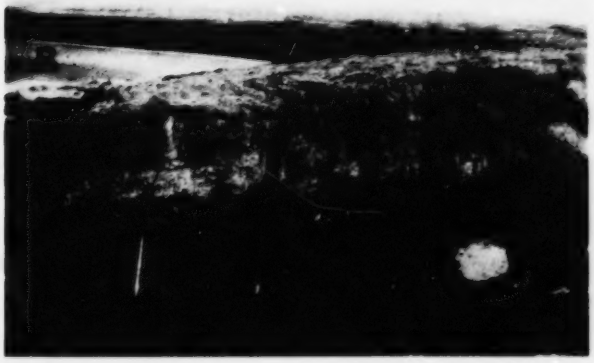

Figure 15. Aerial view of unusually well displayed columnar jointing (J), in the Persillon Formation, near Petite rivière de la Baleine (R). Volcanic unit caps cuestas of sandstone of the Pachi Formation (S). Looking northwest at 55°56'N, 76°35'W (GSC 203897-A)

Figure 16. Plan view of advanced hematitic alteration (weathering) of columnar joints, Persillon Formation. Unweathered cores of columns are pale. (56°24'21"N, 76°22'12"W; GSC 203263-B)

Figure 17. Detail of weathered joint column in Persillon Formation, "spheroidal structure" of Woodcock (1960). Similarity of vesicles in unweathered (pale) and weathered (dark) basalt shows alteration to be a post-crystallization event and therefore not connected with lava toe or pillow formation. (GSC 203263)

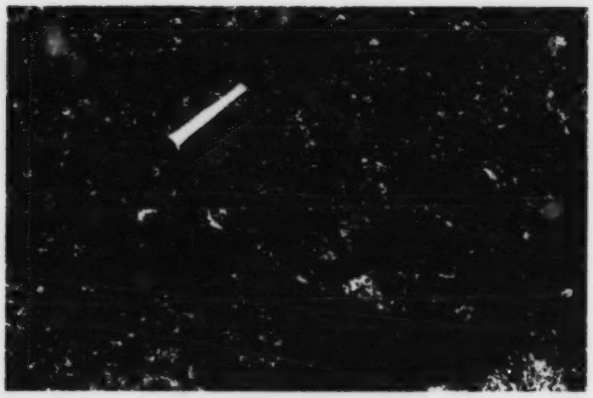

Figure 18. Ropy flow structure, upper surface of flow unit, Persillon Formation (56°30'10"N, 76°17'25"W; GSC 202909-V).

Figure 19. Highly oxidized set of basalt flows in the gently dipping Persillon Formation. Geologist, 180 cm high, stands at base of set, a basal remnant of which (R) is green (unweathered). The top of the set is marked by unoxidized (pale) base of a succeeding set (2). The lower set is interpreted to have been weathered before the extrusion of the overlying set. Within the lower set can be seen a white- bordered flow edge, pinching out to the left (E; 56°08'N, 76°22'W; GSC 203897).

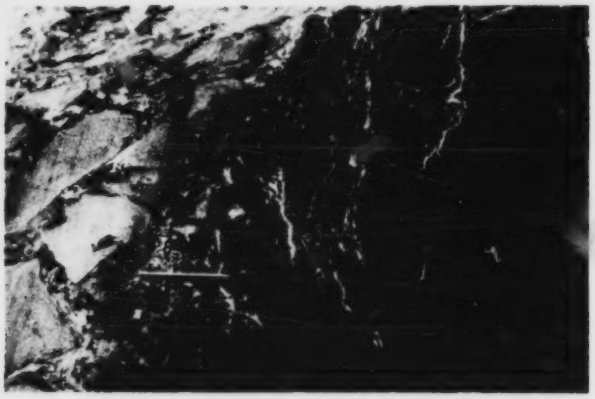

Figure 20. Contact between spheroidally weathered basalt "corestones" of the Persillon Formation (right) and overlying derived basalt-cobble conglomerate (left) at base of Qingaaluk Formation. Strata in horizontal outcrop surface dip to the left at 20° (56°07'N, 76°03'W; GSC 203895-U).

veining accompanies the reddening of the top of the unit. Reddening and exfoliation penetrating columnar and horizontal joints give rise to almost spherical cobbles which among angular blocks form a deceptively mature conglomerate at the top of the flow unit (Fig. 20).

Paucity of pillows, eastward leaning pipe amygdules at flow bases, mudcracked interflow sediments, abundant vesicles and a thick red-weathered surface together indicate eastward subaerial flow over locally damp sand under an oxygen-bearing atmosphere.

Ellipsoidal structures. Circular concentric banding is widespread in the Persillon Formation on sections parallel to flow surfaces (Fig. 16, 17). These structures are striking enough to have been employed as an illustration lining the front cover of the volume "Geology and Economic Minerals of Canada" by Douglas (1970).

The structure is of some paleoenvironmental significance because it was interpreted by Leith (1910, p. 239) as a "peculiar ellipsoidal or pillow structure often ascribed to subaqueous cooling". Woodcock (1960, p. 27) on the other hand described the banding as consisting of alternate bands of carbonate and hematite-chlorite rock, formed by carbonation along fractures in the basalt, and accompanied by iron enrichment.

At first sight these structures could be mistaken for pillows with altered margins or for lava toes. According to MacDonald (1953; 1972, p. 174), pillows commonly have a glassy skin, the result of rapid chilling, and have an internal radial structure arising from columnar jointing and collinear vesicle elongation. Clastic sediment fills the spaces between the pillows. On the other hand, with lava toes, both structure and arrangement of vesicles are concentric, being derived from the successive deposition of layers of lava on the walls of the toe. Both pillows and lava toes may have internal cavities resulting from partial draining of the structure before complete consolidation (MacDonald, 1972, p. 101).

For two reasons, the structures in the Persillon Formation are unlikely to be either pillows or lava toes. As Figure 17 shows, the form and distribution of the vesicles in the basalt is completely unrelated to the structures. Large vesicles would not be expected in a chilled margin of a pillow. Therefore the structures formed later than freezing of the basalt, and lack internal radial joints and cavities. Second, the circular structures are always exposed in exposures parallel to flow surfaces, an orientation unlikely to cut circular sections in lava toes. Rare associated vertical surfaces show that the structures continue downward as columnar joints (Fig. 21). Thus there is more truth in Woodcock's (1960) suggestion and the structures represent alteration of columnar jointing.

As Figures 16 and 21 show, the degree of reddening at the margins of columnar joints in the Persillon Formation basalt ranges from extreme to slight. On some exposures it is so advanced that the basalt is featureless, closely resembling a massive mudstone. Several observations lead to an interpretation of the reddening. It is not present at the contacts of any sills or dykes in the Richmond Gulf Group nor at the basal contact of the Persillon Formation. On the contrary, it affects only the upper surface of Persillon Formation flows (Fig. 19). In these flows reddening diminishes down vertical cracks. An 80 m thick red sandstone unit at the base of the non-red Qingaaluk Formation contains pebbles and sand grains from the basalt of the underlying Persillon Formation. At the base of this redbed unit a basalt conglomerate contains strongly exfoliated boulders that are also seen locally in place at the top of the Persillon Formation (Fig. 20). Where the Persillon Formation is missing, the base of the Qingaaluk Formation is marked by the presence of volcanic pebbles and a sharp upward change in colour from the light pink arkose of the Pachi Formation to dark red.

The reddening is therefore related only to the upper surface of the basalt flows of the Persillon Formation. Absence at margins of intrusive basalts, in the Richmond Gulf Group, at flow bases except where a flow is completely reddened, presence

Table 1. Chemical analyses of basalts.

	(1)	(2)	(3)	(3)	(4)	(4)	(4)	(5)	(6)	(7)
SiO_2	48.00	62.60	57.00	55.80	55.50	53.10	46.90	46.3	47.60	50.26
Al_2O_3	17.70	15.30	16.20	5.00	11.20	14.60	18.30	16.2	17.00	13.17
Fe_2O_3	4.70	1.60	7.60	5.60	12.60	10.50	2.80	2.52	2.34	3.29
FeO	4.70	3.10	1.30	3.50	5.10	3.30	6.40	4.78	2.96	8.23
MgO	8.71	0.38	3.44	7.71	4.37	6.62	11.50	5.7	6.85	8.63
CaO	2.81	0.00	0.13	4.87	1.58	0.33	0.56	10.9	8.12	9.24
Na_2O	5.10	0.00	0.50	0.30	0.90	0.80	1.40	1.70	2.20	2.13
K_2O	1.36	11.40	9.43	0.07	4.98	6.30	6.00	1.79	2.77	0.66
TiO_2	1.25	1.05	1.16	0.30	0.87	1.00		1.02	0.84	1.06
P_2O_5	0.12	0.00	0.13	0.05	0.18	0.18	0.17	0.06		0.12
MnO	0.12	0.00	0.02	0.11	0.07	0.03	0.12	0.14	0.14	0.17
S	0.00	1.60	0.00	0.03						
NiO	0.00	0.00	0.00							
Cr_2O_3	0.00	0.00	0.00							
CO_2	1.40	0.10	0.10	2.50	0.20		0.20	4.20	3.70	
H_2O	4.80	0.80	2.50	2.60	1.90	3.20	5.10	4.00	3.50	2.86
Total	100.77	98.33	99.51	99.50	99.50	100.10	100.90	99.31	98.06	99.53

(1) green-black, unweathered Persillon Formation
(2) pyritized Persillon Formation, 0.5 m below Nastapoka Group
(3) red (weathered) Persillon Formation
(4) Persillon Formation given by A.R. Miller
(5) local basalt unit, Qingaaluk Formation, 1 m above base of upper flow
(6) 5 m below top of lower flow
(7) average of 3 Karroo basalts from Carmichael et al. (1974, p. 432, no. 1-3, Table 9-2)

Figure 21. Rare vertical exposure of oxidized columnar oints in loose block of basalt from Persillon Formation on south shore of peninsula (56°28'36"N, 76°21'36"W; GSC 203264-E).

Figure 22. Colline Qingaaluk from the northeast. Typical homogeneous lenticularly bedded arkose of the Qingaaluk Formation in 300 m cliff is overlain by about 40 m of sediments (S) and basalt of the Nastapoka Group (56°28'N, 76°24'W; GSC 203263-Z).

of exfoliated boulders and restriction to the base of the Qingaaluk Formation where that formation directly overlies the lithologically similar but drab Pachi Formation all suggest strongly that the reddening is caused by surface oxidation of the Persillon Formation rather than by diagenesis after deposition of the Qingaaluk Formation. Oxidation of the upper parts of the basalt flows on extrusion is a common phenomenon affecting basalts extruded beneath oxygeniferous atmospheres. The redbeds at the base of the Qingaaluk Formation are evidence that such an atmosphere existed when the Persillon Formation was extruded. Occurrence of the thickest oxidized zone at the top of the flow unit immediately beneath the Qingaaluk Formation redbeds suggests that much of the oxidation postdates cooling of the lavas; i.e. is caused by weathering and that the redbeds acquired their colour from the weathered basalt.

Petrography and chemistry. Both the reddened and apparently unweathered green-black basalt at Lac Guillaume- Delisle have lost their original igneous minerals except for remnant sericitized feldspar. One green-black sample (Table 1, 78CGA361) is heavily sericitized and contains calcite-filled vesicles. Two reddened samples contain sericite, carbonate, quartz and the mafic minerals appear to have been replaced by hematite and sericite (Table 1, 78CGA339B, 77CGA70A).

Chemical analyses of red weathered basalt (Table 1, CGA77-70A, CGA78-141B, CGA78-339B) were compared with the average of three Karroo basalts, assumed to have been formed under a similar tectonic setting (Table 1). Chemical species concentrated in the weathered basalt are silica, and ferric iron. Those depleted include ferrous iron, Mg, Ca, Na and Mn. Species with no clear tendency, perhaps because of the small number of analyses, include Al and K.

Early in chemical weathering of mafic igneous rocks the relatively unstable Fe-Mg silicates, olivine, pyroxene and amphibole, and plagioclase, are removed, leading to losses of Mg, Ca and Na. Silica is released into the profile and can be concentrated in its lower parts (Loughnan, 1969). Field evidence of vertical silica movement occurs in the form of cherty silica laminae lining columnar joints in the basalt. Under reducing conditions iron is lost, but when conditions are oxidizing it is concentrated as ferric oxide and hydroxide minerals. Under advanced leaching of more extreme chemical weathering K is lost from phyllosilicates which are converted to kaolinite and gibbsite. But where chemical weathering is not rigorous K is retained with Al in minerals such as montmorillonite, illite and vermiculite (Loughnan, 1969). Thus the field observations and the chemistry of the reddened zone at the top of the Persillon Formation are consistent with oxidizing weathering.

Qingaaluk Formation

In cliffs on the west shore of Lac Guillaume-Delisle (Fig. 22) the Qingaaluk Formation (Chandler and Schwarz, 1980) reaches thicknesses of at least 500 m and consists of four sedimentary members and a volcanic member. A thin basal conglomerate (Fig. 23) composed mainly of cobbles from the Persillon Formation is nearly everywhere present. The conglomerate is followed by a redbed member (Fig. 24), generally fine grained and abundantly mudcracked (Fig. 25), then by an arkose member similar to that of Figure 5, consisting of sand to pebbly grit (Fig. 26). The arkosic member usually underlies the unconformable carbonates and sandstones of the Nastapoka Group on the west side of Lac Guillaume-Delisle. This member and other units upfaulted against the unconformity by block faulting of the Richmond Gulf Group are bleached and pyritized and locally mineralized with copper sulphides (Chandler, 1984). Two local basalt flow units occur high in the formation, one comprising a small island in the southwest part of Lac Guillaume-Delisle and the other forming a plateau in the coastal cuesta southwest of the gulf. In the axial part of the graben a higher, fifth member, 100 m of tidal marine sandstone, is preserved (Chandler, 1982).

Figure 23. Example of basal conglomerate (member 1), Qingaaluk Formation, with unusually angular basalt clasts. Vesicular and massive blocks lie within a fine grained red sandstone matrix. Photograph taken from area "1" in Figure 24 (see also Fig. 20; 56°08'N, 76°22'W; GSC 203895-Y).

Figure 24. View northward along bedding surface of gently north-dipping redbeds (member 2) of the Qingaaluk Formation, south shore Île Cairn, where redbed member is 80 m thick. Basal basalt conglomerate (member 1), derived from underlying Persillon Formation is overlain by fine grained redbeds (member 2) which grade up into medium- to coarse-grained pink arkose (member 3) of the Qingaaluk Formation (56°08'N, 76°22'W; GSC 203902-Q).

Description of members 1-3 (alluvial sedimentary rocks). Member 1 (basal, conglomerate). This is usually about 1 m thick and is composed of basalt cobble orthoconglomerate with a red sandstone or grit matrix. Clasts in the conglomerate may be very

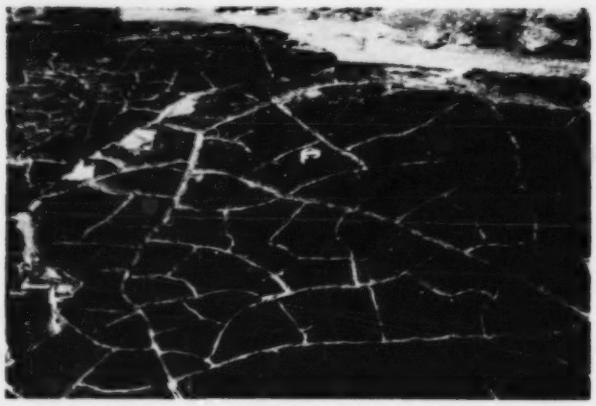

Figure 25. Mudcracked bedding surface of siltstone, very common in redbed member, Qingaaluk Formation (56°27'56"N, 76°21'W; GSC 203263-Q).

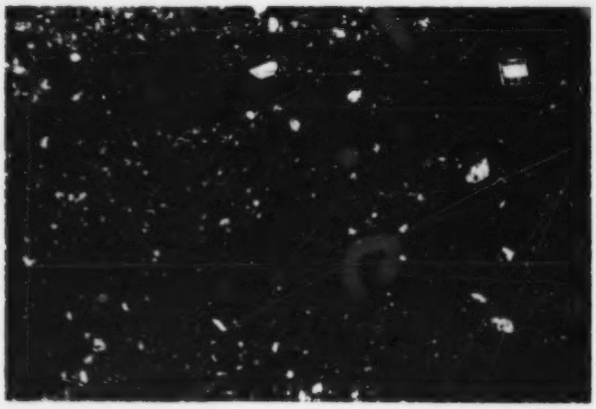

Figure 26. Typical coarse grained pebbly feldspathic sandstone of the upper part of the Qingaaluk Formation. Most pebbles are white quartz or pink granite (56°23'4"N, 76°21'W; GSC 203263-Y).

angular, or well rounded (Fig. 23); some are strongly exfoliated (Fig. 27) by Aphebian weathering. Locally, where the conglomerate is not present, crossbedded red grit, sandstone or very thinly interbedded red fine grained sandstone and suncracked mudstone overlie the Persillon Formation. In the rare cases where the Persillon Formation is absent a dark red sandstone with scattered basalt pebbles, probably derived from nearby basalt outcrop, abruptly overlies usually pale pink arkose of the Pachi Formation (Fig. 28).

Member 2 (redbed). About 80 m thick, this member ranges from dark red, thinly interbedded mudstone and fine- to medium-grained sandstone, to less common pink coarse grained sandstone and grit.

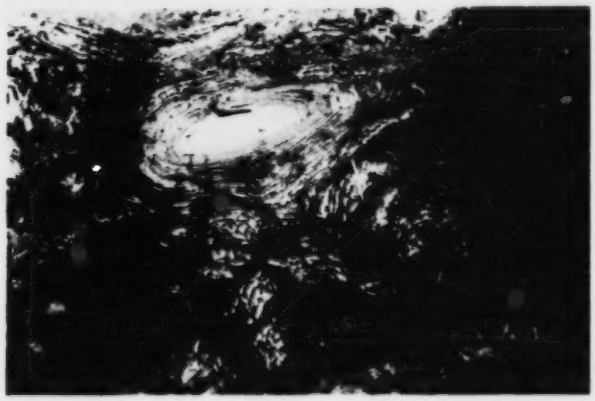

Figure 27. Strongly exfoliated boulder of basalt in basal conglomerate, Qingaaluk Formation. White striping is carbonate crack-fillings (56°07'N, 76°03'W; GSC 203265-F).

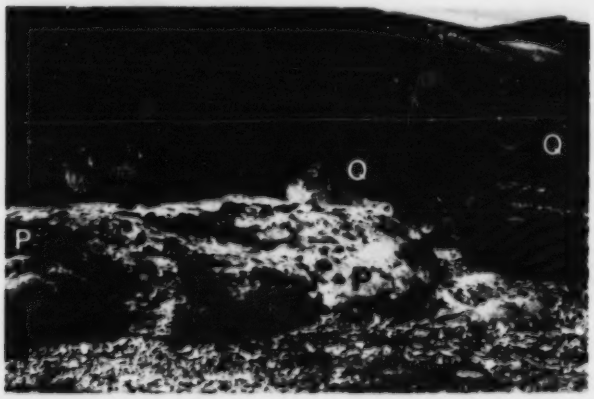

Figure 28. Contact between grey feldspathic grit of the Pachi Formation (P) and red coarse grained sandstone of the Qingaaluk Formation (Q). Here, a rare occurrence, the normally intervening Persillon Formation is missing and its stratigraphic position is marked by a basalt-pebble conglomerate up to 1.5 m thick. Location is at triangular island 800 m long (56°11'N, 76°03'W; GSC 203895-S).

Scattered pink granite, red weathered basalt and white quartz clasts up to 5 cm across occur. Common, particularly in finer grained parts of the member, are dark red mud chips (rip-ups; Fig. 29). In some outcrops angular pebbles of fine grained dolomite also occur. In two outcrops yellow micritic carbonate layers (Fig. 30), up to 5 cm thick, were found. At one outcrop the carbonate, traceable 2 or 3 m, is draped over rippled sandstone.

The finer grained facies is abundantly mudcracked (Fig. 25) and rippled. It contains linear, occasionally bifurcated and undulose wave ripples, linguoid and rhombic current ripples, small scale trough-crossbeds, well developed black sand laminae, and parallel lamination with parting lineations. Complete waning-current cycles about

Figure 29. Red mud-chips in pink medium- to coarse- grained trough-crossbedded sandstone at the top of the redbed member, Qingaaluk Formation, probably derived from desiccation-cracked mud layers ("M" in Fig. 31) of preceding waning-current alluvial flood cycles (56°14'55"N, 76°14'42W"; GSC 203902-K).

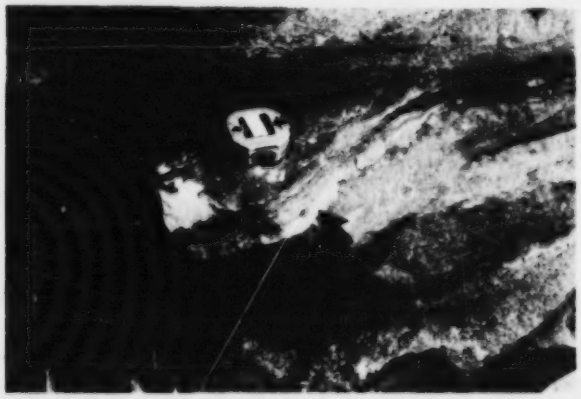

Figure 30. Yellow (pale) carbonate layer, arrowed, within desiccation-cracked current-lineated and rippled maroon siltstone, redbed member, Qingaaluk Formation, north shore of east-west oriented, 1.5 km long island (56°26'36"N, 76°18'12"W; GSC 202909-Y)

10 cm thick (Fig. 31, 32) passing through trough and planar crossbeds, parallel lamination, ripples and suncracked mud layers, indicate eastward transport. The coarser facies is composed of stacked crossbeds with minor amounts of mudcracked and rippled fine grained material.

Paleocurrents measured from trough-crossbeds and from ripples are strongly unimodal at the outcrop level and demonstrate uniform eastward transport over the graben. Trough-crossbeds were measured from this and the succeeding pink arkose member at several locations at the base of cliffs of granitic basement that lie along major graben forming faults. Current directions toward the cliffs without facies change indicate faulting after deposition of the sandstone.

Member 3 (the overlying bulk of the Qingaaluk Formation). This member (see Fig. 21) is composed of pink, grey, green or puce, crossbedded coarse grained sandstone and grit that weathers pink and buff. Pebbles, 1.5-4 cm in size, of white quartz and pink granite are common (Fig. 26). Basalt clasts are rare. A large part of this member is composed of beds, alternating on 1 m scale, of pink and chloritic, green pebbly sandstone-grit (Fig. 33, 34). Black heavy minerals are common in coarse- and fine-grained rocks. Waning-current cycles are composed of stacked crossbedded coarse sand locally capped by less than 10% of remnants of flaggy, mudcracked cream, red-green or black siltstone with wave ripples, linguoid current ripples and current lineations (Fig. 35). As with the underlying redbed member paleocurrents measured from trough-crossbeds flowed eastward to southeastward over the graben and are strongly unimodal at the outcrop level.

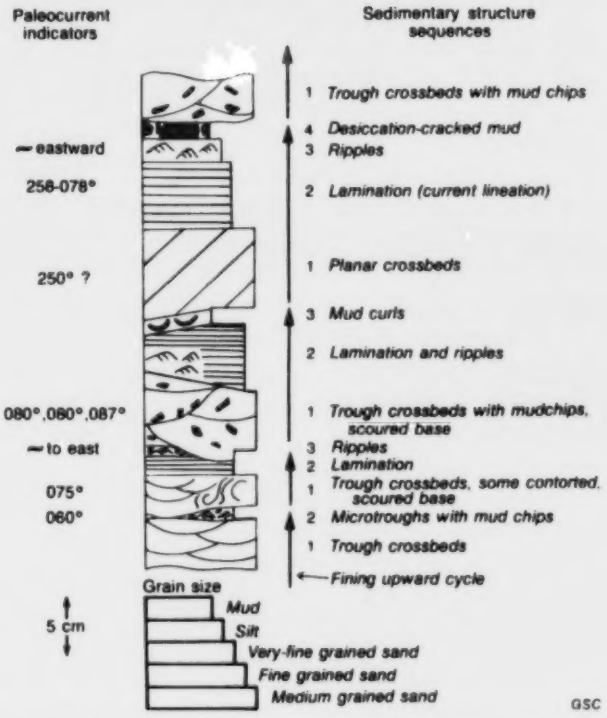

Figure 32. Parts of five fining-upward alluvial cycles from the redbed member, Qingaaluk Formation (56°27'N, 76°20'18"W. For details see Appendix 1, first facies sequence.

Figure 31. Fining-upward waning-current cycle in medium grained sandstone to mudstone, redbed member, Qingaaluk Formation. Cycle starts with planar crossbeds (C) that overlie mud curl layer (M) of previous cycle, passes up through current-lineated and rippled siltstone (L) to desiccation-cracked mud layer (D) that terminates cycle. Local sand transport was to azimuth 080°. See Figure 32 for a sketch of a sequence of several such cycles (56°27'15"N, 76°20'29"W; GSC 203263-T).

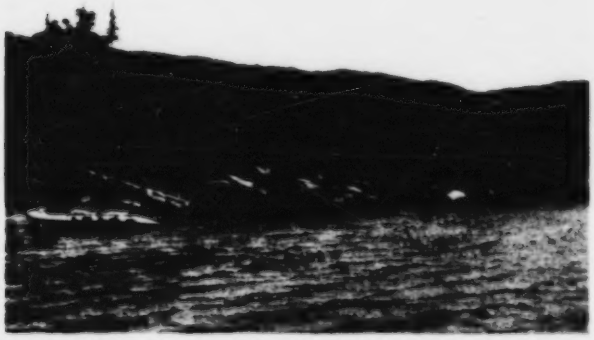

Figure 33. Thick- and wavy- to planar-bedded, crossbedded feldspathic sandstone typical of the third member of the Qingaaluk Formation (56°8'36"N, 6°33'36"W). For details of sedimentology see Figure 35 and Appendix 1, second facies sequence (GSC 203902-C)

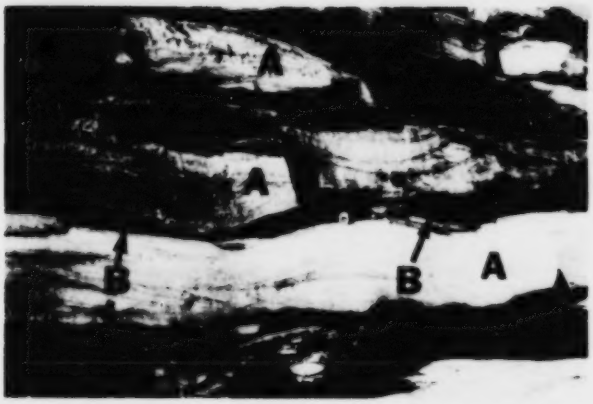

Figure 34. Trough-crossbedded coarse grained arkose with basal scours (facies A) and interbedded lesser amounts of darker rippled, current-lineated and mudcracked finer grained arkose (facies B), Qingaaluk Formation (56°24'30"N, 76°27"W). For details of sedimentology see Appendix 1, third facies sequence (GSC 202909-U).

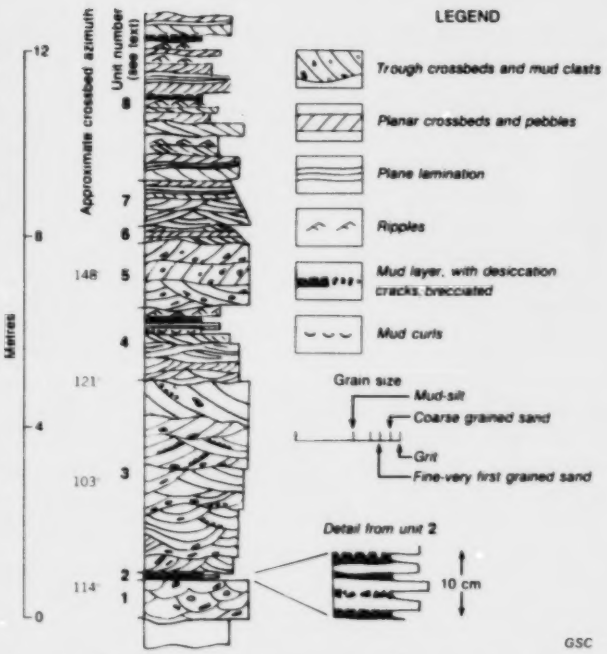

Figure 35. Stratigraphic section, 12.75 m thick, of typical braided fluvial sandstone of the third member of the Qingaaluk Formation (56°N, 76°33'36"W). The exposure is shown in Figure 33 and details of the sedimentology are given in Appendix 1, second facies sequence.

Description of member 4 (local basalt flows). Two volcanic units of limited extent occur high in the Qingaaluk Formation. One consists of two light grey weathering, green- grey flows with well developed columnar jointing. It forms an island 15 km northeast of the outlet of Lac Guillaume- Delisle. The other, similar in appearance to the Persillon Formation, forms a plateau in the east-facing coastal cuesta 14 km south of the outlet.

The former basalt (Fig. 36) is texturally very altered. Two samples were classified according to Irvine and Baragar (1971), as follows, one sample from 1 m above the base of the upper flow (Table 1, 78CGA477 A) is a tholeiitic basalt of the K-rich series. The second from 5 m beneath the top of the lower flow (Table 1, 78CGA477 B) is a K-rich series calc-alkaline basalt.

Only a thickness of 10 m of the lower flow is exposed. The lower 5 m are massive and the upper part becomes increasingly vesicular upward, finally grading into a 60-100 cm thick flow-top breccia composed of massive to scoriaceous basalt fragments up to boulder size and of twisted bodies of red sandstone. The breccia grades upward into a continuous layer 15-30 cm thick of laminated fine grained red sandstone (Fig. 37).

At the base of the upper flow there is some brecciation and formation of small cavities (steam bubbles?) in the underlying red sandstone. Measurement of the inclination of a limited number of pipe amygdules with white fillings, from two sites, suggests that the upper flow moved toward azimuth 087° and 213°.

The upper flow has a basal zone about 50 cm thick in which columnar joints are 20-30 cm across and an upper part at least 15 m thick in which joints are up to 2 m across. Higher parts of the flow are eroded. Inclusion of the two flows in the Qingaaluk Formation, a unit interpreted as alluvial, and the features discussed above fit with their subaerial extrusion, but, bearing in mind the marked reddening of the top of the Persillon Formation, lack of reddening at the top of the lower flow suggests that it was quickly buried.

The second local basalt unit, not chemically analyzed, outcrops as the surface of a plateau traceable at least 5 km northeast along strike. The unit is at least 21 m thick in the centre, pinches out at its northeast limit, and is probably lenticular in northeast-southwest vertical section. Its field appearance is similar to the Persillon Formation that underlies the Qingaaluk Formation. Similar features include columnar joints with altered margins (ellipsoidal structures, see Persillon Formation), white phenocrysts and hematite- rich vein-fillings. At one place a 2 m thick breccia layer overlies the unit. A bright green (malachite?) stain 20 x 20 cm in area was found 2 m beneath the top of the unit.

The unit overlies pink crossbedded feldspathic sand- stone common to the Pachi and Qingaaluk formations, but the basalt cobble conglomerate (Fig. 23) that typically overlies the Persillon

Formation is absent. Instead the plateau- forming basalt is overlain by facies not seen elsewhere, generally by several metres of quartz-pebble-rich conglomerate in a white arenaceous matrix. At one locality pebbles include red siltstone, pink sandstone and minor red granite in a matrix of red sandstone, but basalt pebbles are not present. At another locality the basalt is directly overlain by 2 m of dark grey weathering arkose with both microcline (granitic or arkosic source) and basalt grains and abundant chlorite in the matrix. The arkose passes up into 30 m of white arkose with similar framework grains but no chlorite. The sandstone appears to be overlain without angular unconformity by carbonates of the Nastapoka Group.

The orientation of 7 trough-crossbeds from the sandstone overlying the basalt indicates sediment transport to azimuths between 112° and 126°. Crossbeds in sandstones in the upper part of the Nastapoka Group (see below) are usually of planar type and indicate transport to the west, whereas those of the Richmond Gulf Group indicate transport to the southeast in this part of the graben and are of both trough and planar type. Thus the crossbed data from the sandstone above the basalt suggests that the sandstone belongs to the Richmond Gulf Group rather than the Nastapoka Group. Stratigraphic relations from mapping shown on the accompanying 1:100 000 scale map (Fig. 1), as well as the unique conglomerate and sandstone overlying the basalt

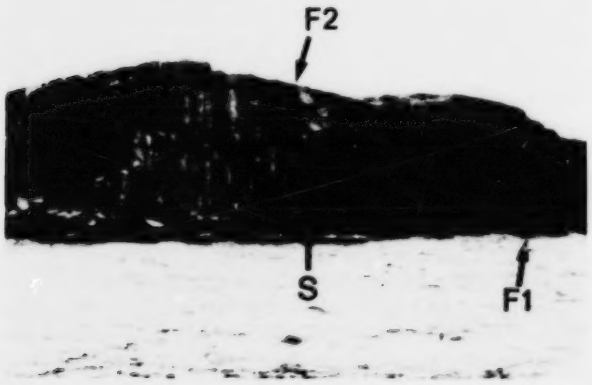

Figure 36. Two basalt flows (F1, F2) separated by flow-top breccia and red sandstone (S; see Fig. 43) comprising island 400 m across (56°14'N, 76°27'W), member 4, Qingaaluk Formation. See Table 1 for chemical analyses. (GSC 203897-B)

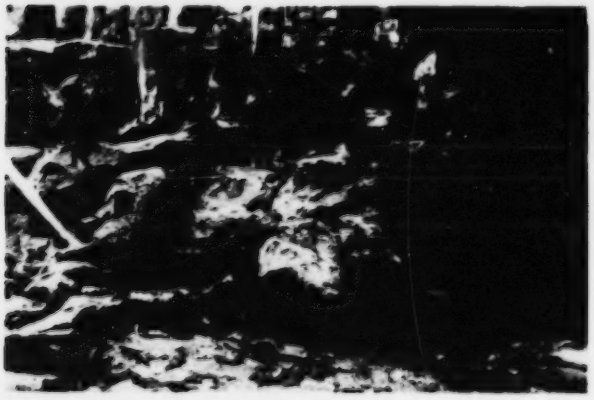

Figure 37. Flow-top breccia on lower basalt flow (F1) from near letter "S" in Figure 42, member 4, Qingaaluk Formation. Breccia, 1-2 m thick, contains scoriaceous blocks (B) in a massive red sandstone matrix and is overlain by a 0.6-1.0 m laminated, fine grained red sandstone (R) and columnar- jointed basalt (F2) of the upper flow of member 4. (GSC 203897-E)

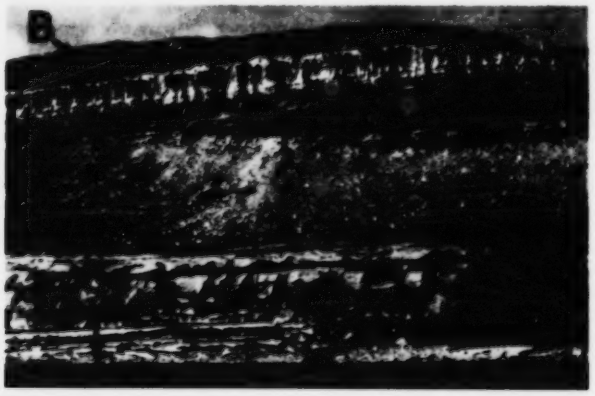

Figure 38. Tidal marine sandstone (member 5; G and S), Qingaaluk Formation, comprising 30 m of flat-bedded texturally mature grit overlying planar-crossbedded sandstone with opposed crossbeds (G; see Fig. 39). This unit is overlain by 70 m of interbedded herringbone-crossbedded sandstone and rippled siltstone (S; see Fig. 40, 41). Carbonates (C) and basalt (B) of the Nastapoka Group disconformably overlie these units (56°13'N, 76°32'W; GSC 203902-F).

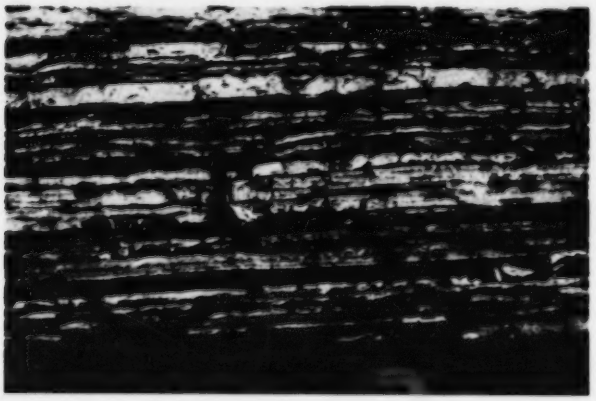

Figure 39. Herringbone-crossbedded feldspathic sandstone (pale) and interbedded lenticular, flaser and wavy-bedded siltstone (dark), tidal (5th) member, Qingaaluk Formation (56°12'N, 76°33'W; GSC 203902-E).

unit, make it likely that the basalt is not the Persillon Formation and that the unit lies high in the Qingaaluk Formation.

Description of member 5 (marine sandstone). The top member of the Qingaaluk Formation (Fig. 38, 39) is restricted to a north-south strike length of 11 km in a very gently west- plunging open syncline at the southwest corner of Lac Guillaume-Delisle. It was removed to the north and south by truncation of the fold at the unconformity beneath the overlying Nastapoka Group. It contains a lower grit-sandstone unit 30 m thick and an upper sandstone-siltstone unit 70 m thick.

The grit-sandstone unit consists of texturally mature bimodal feldspathic flat-bedded grit (Fig. 40) and coarse grained sandstone. Planar crossbeds about 10-15 cm thick from one large outcrop of the latter gave a bimodal paleocurrent pattern (Fig. 41). These rocks are conformably overlain by about 70 m of parallel-interbedded feldspathic sandstone (Fig. 39) and lenticular, wavy and flaser-bedded siltstone-fine grained sandstone (Fig. 42). Herringbone crossbeddng was visible in the feldspathic sandstone of the 70 m section in several places (Fig. 43). Examination of the faces of a loose block showed that the herringbone crossbedding was opposed at 180 degrees.

Interpretation of the sedimentary rocks of the Richmond Gulf Group

Sandstones. The Pachi and Qingaaluk formations are comprised essentially of feldspathic sandstone, in many places coarse grained and pebbly (Fig. 26) with well developed lenticular (Fig. 6) to parallel (Fig. 33) bedding. Silty and shaly facies are very sparse and in general represented by angular pebbles (Fig. 29) or present as rippled and mudcracked units truncated by the basal scours of trough-crossbedded sandstone units (Fig. 6). Both trough and planar crossbeds are abundant. Wave and current ripples are present in the finer grained sands and in the coarse mudstones where, significantly, they are accompanied by a widespread occurrence of mudcracks (Fig. 25, 31). Other structures in the finer grained clastics include current lineations and one occurrence of current crescents (see Fig. 86, in Appendix 1). Paleocurrents form crossbeds, and current ripples are unimodal at the outcrop level. Carbonate units are almost absent as are dark shale units. Texture and mineralogy are immature.

In general outcrop was not suitable for analysis of vertical facies sequence because of gentle dips and lichen cover away from the shores of Lac Guillaume-Delisle. However detailed observations were possible on three exposures of the Qingaaluk Formation. Facies sequences were examined, one from the redbed member at the base of the formation (Fig. 32) and two others from coarse arkoses higher in the formation (Fig. 33-35).

These formations are composed overwhelmingly of sand and grit sized material. Excluding the tidal member of the Qingaaluk Formation, abundance of wavy-bedded and trough- crossbedded sets on scoured bases and presence of planar- crossbedded sets without scoured bases indicate deposition of much of the sand in dunes and waves (terminology of Harms et al., 1975). Textural immaturity, unimodal

Figure 40. Photomicrograph of beach grit, upper part of unit 'G' in Figure 36, tidal member Qingaaluk Formation. Grains of granite, polycrystalline quartz, microcline, microperthite and orthoclase, generally well rounded, rest in a matrix of finer grained similar material and of euhedral carbonate rhombs, Nicols crossed. Grain 'A' is 1.7 mm long.

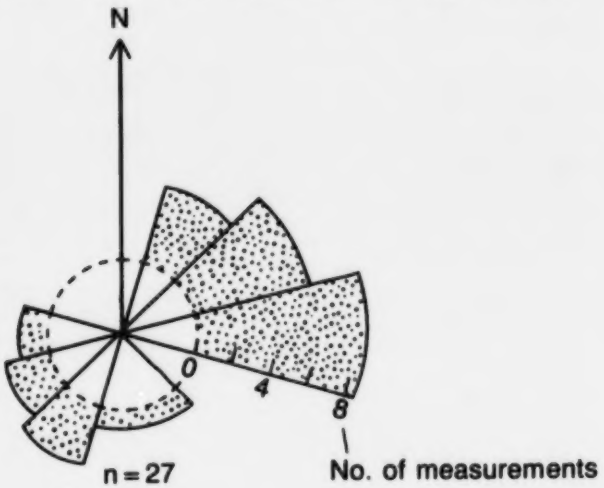

Figure 41. Sediment transport directions from trough and planar crossbeds in sandstone at base of unit 'G', Figure 36, tidal marine sandstone member, Qingaaluk Formation.

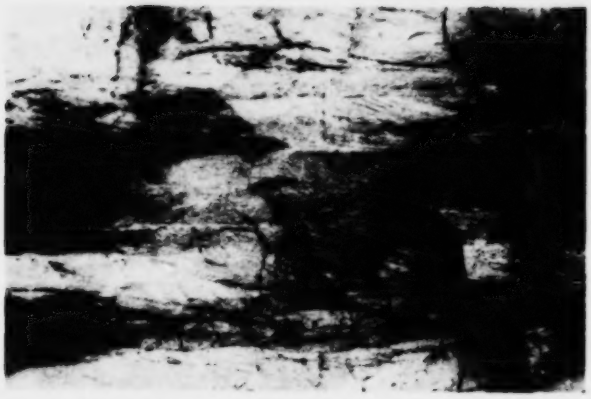

Figure 42. Ripple-topped sandstone beds and wavy to lenticular-bedded siltstone, upper part of tidal member (member 5) Qingaaluk Formation (in unit 'S' of Fig. 36; 56°12'N, 76°33'W; GSC 203902-G).

Figure 43. Herringbone crossbedding in sandstone bed of unit 'S' Figure 36, tidal member, Qingaaluk Formation (56°12'N, 76°33'W; GSC 203902-D).

paleocurrents at the outcrop level and across the gulf, presence of abundant desiccation cracks throughout the two formations, absence of tidally-bedded fines, and of lithologies suggestive of marine deposition together point to repeated emergence in an alluvial rather than a tidal marine environment. The thick red weathered zone on the Persillon Formation, which intervenes between the Pachi and Qingaaluk formations is evidence of emergence also.

Fining upward cycles, in many cases nested, passing up from crossbedded sandstone and grit that contains angular mudstone clasts through finer grained rippled facies to terminate in much thinner desiccation-cracked mud layers, mud curl layers, or layers of angular mud clasts, are suggestive of alluvial flood cycles and indeed resemble in facies and proportion of lithologies some of the fining-upward cycles of Proterozoic alluvial stream deposits illustrated by Long (1978, p. 330).

The paucity of thick extensive mudstone units is consistent with the absence of clearly-defined vegetation- stabilized flood plains under the braided fluvial regime. Thin (several centimetre) mud layers are traceable laterally in these sandstones at best a few metres until truncated by scour surfaces. Such deposits very likely were deposited from suspension as floods waned and were later brecciated by desiccation on emergence (Fig. 31, layers D,M). They were easily incorporated as sun-hardened angular mud clasts into the migrating dunes of the sandy bedload of a later flood and eventually preserved in the resultant crossbedded sandstone.

Several features of the locally preserved uppermost member of the Qingaaluk Formation indicate a shallow marine tide-influenced mode of deposition. The grit at its base (Fig. 40) is well sorted and rounded and composed of a grain size notably deficient in fluvial or shallow marine deposits and because of its high mobility concentrated mainly in beaches by currents mainly of wave origin (Russell, 1968). But much of the Pachi and Qingaaluk formations interpreted as alluvial is also coarse grained. Important differences between this grit, interpreted as of beach origin and the above alluvial sandstones are the dolomite cement, the degree of sorting and roundness, and the opposed herringbone crossbedding of the sandstone associated with the grit and of the sandstone overlying it, a structure characteristic of shallow subtidal sand bodies (Klein, 1977, p. 71). Further, low angle crossbedding and flat bedding, the only sedimentary structures in the grit unit, are common in high energy beach environments (Collinson and Thompson, 1982). Lenticular, wavy and flaser bedding in siltstones interbedded with this sandstone are commonly developed by alternating traction and suspension deposition in tidal marine environments (Reineck and Singh, 1980, p. 112 et seq.).

In conclusion, superimposition of facies independently interpreted from their sedimentary structures as alluvial (redbed and arkose members), beach (grit) and tidal marine (local upper sandstone) is evidence of a marine transgression during the deposition of the upper part of the Qingaaluk Formation.

Lacustrine unit of the Pachi Formation. Using the three facies, current-lineated sandstone, rippled sandstone and graded mud, exploratory vertical facies analyses to test for cyclic deposition were carried out on the upper red and the green members of the fine grained unit in the third cliff. The data are admittedly too few for firm conclusions but the 27 measured transitions seem to point to a cyclic

mode of deposition that is capable of hydrodynamic interpretation (Middleton, 1965).

To search for cyclicity, the method of Harms et al. (1975, p. 69) was used. The number of transitions between the various facies was recorded on a tally matrix. From this number was subtracted the number of transitions which ought to have occurred randomly. The random transitions were got by multiplying the row and column numbers of transitions that involve a particular transition and dividing it by the total number of transitions recorded. The non-random transitions for the upper red member suggest a sedimentary cycle passing from current-lineated sandstone, through rippled sandstone to graded mudstone. Current lineations (Allen, 1982, p. 264) occur chiefly in waterlaid, relatively fine grained sands on plane beds at relatively large shear stresses, that is at higher energy than the fields of ripples and dunes. Graded mud layers with mudcracks are interpreted to have been deposited from suspension in slack water that eventually dries up.

The cycles can therefore be interpreted on bedform phase diagrams such as that of Leeder (1980, p. 424) and Harms et al. (1975, p. 23) as waning flood cycles. The thinness of the deposits, small lateral extent and mudcracks suggest local shallow dry basins, periodically inundated by shallow, high velocity floods carrying small amounts of fine grained clastic sediment.

In this context the words of Collinson (1978, p. 38) are instructive. In describing alluvial sedimentation he wrote that overbank sedimentation rates are rather low owing to the rather high velocity of flood plain currents and the low concentration of suspended sediments at the flood peak. Most sedimentation is from suspension. Only major floods deposit a centimetre or so of sediment, and then only patchily. Flood plain deposits dry out between floods and desiccation cracks may develop. In humid settings the flood plain may never fully dry out and remains a backswamp or even a lake.

Inclusion of the fine grained sediments at Lac Guillaume-Delisle in sandstones interpreted as of braided fluvial origin suggests that a situation like that described by Collinson (1978) might be appropriate. Twelve facies transitions from the green member of the unit in the third cliff tend to support a waning flood-cycle model. The colour of the member and absence of mudcracks suggest that during its deposition a shallow lake existed – evidence of a humid climate. Further, if the three exposures represent sediments from the same lake, the lake would have been at least 8 km long and 14 km^2 in area.

Intrusive rocks

Wiachuan Sills. Altered mafic sills occur in the Richmond Gulf Group, along the east shore of Lac Guillaume-Delisle, between the Rivière Caribou valley at latitude 56°20'N and a syncline 6 km south of Contact lake at latitude 55°58'N. Woodcock (1960) recognized them as one sill, the "Wiachuan Sill" though he reported branching of the sill. Here the name is altered to "Wiachuan Sills" to reflect the discovery of several other sills at separate stratigraphic levels.

The sills are up to 30 m thick. Two lie in the Pachi Formation, in some exposures between 2 and 100 m above its base. Extensive exposure of sills in the Pachi Formation, not reported by Woodcock (1960) is present on the mainland immediately south of Île Cairn. Three sills probably mapped by Woodcock as Persillon Formation, though it is hard to be sure from his small sketch map, lie within the Qingaaluk Formation, some way above the Persillon, and are clearly different sills from those in the Pachi Formation.

Because of grain size and composition (plagioclase, An_{54}) Woodcock (1960) classified the sills as gabbros. However many of the thinner sills found by the writer have the grain size of diabase or basalt.

At the outcrop level the sills are homogeneous, of even grain size, undifferentiated and contain varied amounts of match-head to pea-sized vesicles. They branch to enclose rafts of sandstone up to 50 m long and 10 m thick. Well developed columnar jointing (Fig. 2) is useful in distinguishing the sills from the Persillon Formation from a distance in nearly all cliff exposures.

Being absent from the nearly unfaulted Nastapoka Group rocks and dislocated by the abundant faults cutting the Richmond Gulf Group, the sills are connected with or predate graben formation.

Dykes, igneous and sedimentary. Only thirteen mafic dykes or sets of dykes (6 or less parallel individuals) up to 35 m across were found in the Lac Guillaume-Delisle area. These are mainly concentrated in the central part of the graben and 7 of 13 examples are oriented east-west (Chandler, 1982, p. 2). They cut all formations of the Richmond Gulf Group and the granitic basement but not the Nastapoka Group which is excellently exposed all along the west side of Lac Guillaume-Delisle in often sheer cliffs.

Because the dykes are in general traceable only short distances and were not seen to cross faults or cut the Nastapoka Group they are unlikely to postdate graben formation. One northeast-trending dyke, traceable discontinuously across the southeast corner of the gulf does not appear to have been offset by faulting and may be younger than the other dykes.

On a frying pan-shaped island 400 m long (56°12'18"N, 76°13'36"W) lie two 2-3 m across nonvesicular mafic dykes (the handle of the frying pan is caused by resistance to erosion of the dykes) separated by 5 m of sandy conglomerate (Fig. 44) against which the igneous dykes appear to have been chilled. The country rock outside the dykes, composed of Qingaaluk Formation sandstone, has been brecciated (Fig. 45). The material between the dykes is rich in cobbles and pebbles of pink and green massive and laminated fine grained sandstone with a grey sand matrix. The larger clasts are concentrated in an axial conglomerate zone, are poorly sorted and have a wide range of shape and angularity. Pebbles near the igneous dykes are oriented parallel to them. The brecciated country rock, Qingaaluk Formation sandstone, also contains well rounded clasts.

Alignment of clasts parallel to dyke margins is not uncommon in clastic dykes (Chandler, 1973; Allen, 1982). A central coarse zone in the Lac Guillaume-Delisle dyke is reminiscent of flowage differentiation, a process postulated to operate in the intrusion of some igneous dykes (Bhattacharji and Smith, 1964). If the pebbly sandstone between the mafic dykes at Lac Guillaume-Delisle is a clastic dyke it was probably intruded forcefully by laminar flow (Eisbacher, 1970; Allen, 1982, p. 555). Apparent absence of igneous material in the pebbly sandstone and in the breccia outside the igneous dykes, chilled margins of the igneous dykes against the enclosed pebbly sandstone, and similarity of these two conglomeratic zones and the host rock as well as other points made above, suggest that these coarse sedimentary rocks may be a complex large clastic dyke along which mafic igneous dykes were later emplaced. Similar sedimentary rocks were found in the Rivière Caribou valley (56°18'N) by Uranerz Exploration and Mining Ltd. (personal communication, 1978).

Similar breccias occur in zones within and parallelling the trend of the East Arm of Great Slave Lake, at the southern boundary of the Slave Structural Province. Reinhardt (1972) considered them due to diatreme activity. It is significant that Hoffman (1973, p. 551) interpreted the East Arm as an aulacogen.

Nastapoka Group

Introduction

The Nastapoka Group is a thin (0-160 m), and by far the most complicated, sequence in the Aphebian succession at Lac Guillaume-Delisle. At the present level of study it is divisible into ten mappable informal members (A-J, Fig. 46, 47 in pocket).

The discussion in the following pages should be regarded as a reconnaissance account. It starts with an outline of earlier work on the group, followed by a description of the sub-Nastapoka Group basement, a description of the unconformity immediately underlying the group, and the immediately overlying local conglomeratic and sandy facies (member A) seen at scattered locations to overlie the unconformity. Then follow summary descriptions of

Figure 44. Five metre-wide sandstone conglomerate zone separating two nonvesicular basalt dykes in the Qingaaluk Formation, on island in axial zone of Richmond Gulf Graben (56°12'18"N, 76°13'36"W; GSC 203897-C).

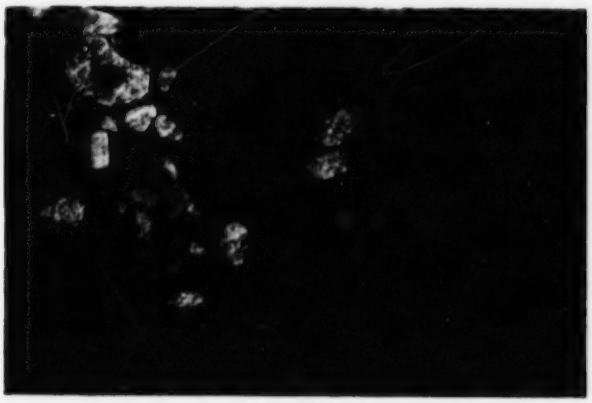

Figure 45. Brecciated sandstone of the third member of the Qingaaluk Formation adjacent basalt and sandstone conglomerate dykes of Figure 44. (GSC 203897-F)

members B to J. Next follow interpretations of the members of the group with some background notes on stromatolites and environmentally sensitive sedimentary structures useful in interpreting carbonate members D, F and G.

An illustrated appendix (Appendix 2) contains the bulk of the raw data from which the chapter has been compiled. This is in the form of descriptions of twelve stratigraphic sections summarized graphically in Figure 47. These sections extend over a north-south strike-distance of 110 km (Fig. 48).

The biostratigraphy of the carbonates of the Nastapoka Group is currently (1983) being studied

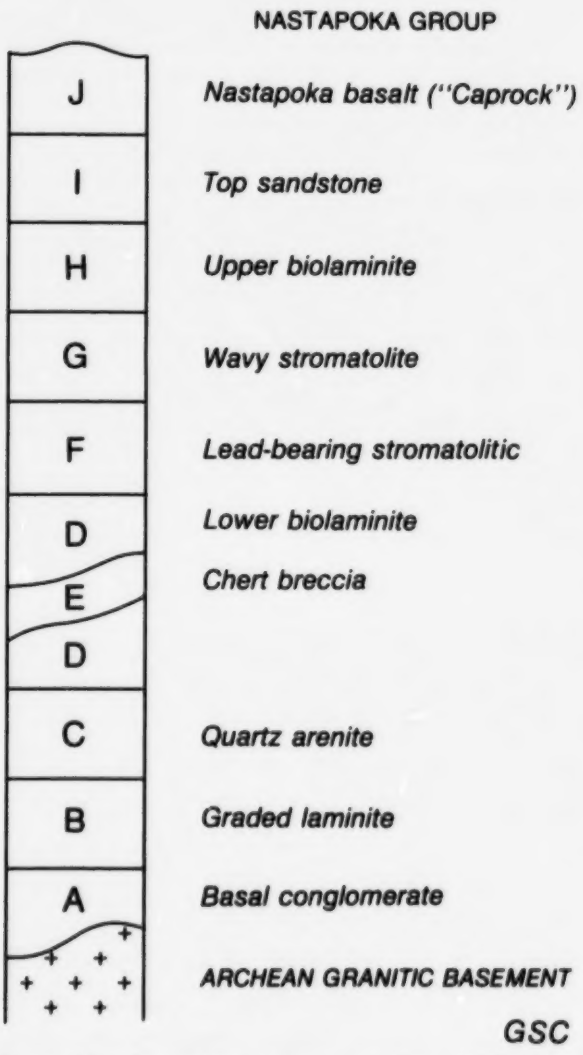

Figure 46. Generalized column to show stratigraphic subdivision into informal members of Nastapoka Group, Lac Guillaume-Delisle area. Not to scale. For details see Figure 47.

for an M.Sc. thesis by Catherine Hamel at the University of Montreal under Dr. Hans Hofmann.

Geological investigation of the Nastapoka Group started with Bell's (1879) report of its distribution along the east shore of Hudson Bay from Long Island near the mouth of James Bay, to the Hopewell Islands near Port Harrison (Inoucdjouac) 400 km to the north. He excluded the clearly unconformable Qingaaluk Formation in Lac Guillaume-Delisle but included it near Petite rivière de la Baleine where the units are disconformable.

At the latitude of Lac Guillaume-Delisle the Nastapoka Group dips gently west and is composed of a lower part, mainly of carbonate and quartz-rich and feldspathic sandstone, overlain by subaerial basalt flows (Ciesielski et al., 1983) that cap the coastal cuesta of Hudson Bay, and were named the "basaltic caprock" by Woodcock (1960). Several kilometres offshore to the west in Hudson Bay a west-dipping cuesta forms the Manitounuk and Nastapoka islands and the Hopewell Islands that lie to the north near Inoucdjouac. In these islands quartzites, siltstones and thin iron- and manganese-rich units form the upper part of the Nastapoka Group and are dealt with in reports by Low (1903), Lee (1965) and others. The only recent work on these overlying rocks is included in a sedimentological interpretation of a stratigraphic section from Belanger Island near the outlet of Lac Guillaume-Delisle by Chandler (1982).

Low (1902) measuring sections of the group on the cliffs on the west shore of Lac Guillaume-Delisle noted stromatolites, "concretionary forms", within the carbonates. Observing the southward thickening of the sedimentary rocks (Fig. 47) he felt that it resulted from truncation of the strata by eastward thrusting of the sediments.

It was Leith (1910) who introduced the name Nastapoka Group for these supracrustal rocks and who recognized the basal contact of the carbonate-quartzite sequence to be unconformable rather than the result of thrusting as Low (1902) thought. He also named the underlying arenaceous sequence (Richmond Gulf Group of this report), the Richmond Group, a term soon changed to Richmond Gulf Group by Young (1922) on account of the prior use of the former term for Ordovician rocks. The evolution of stratigraphic nomenclature of these rocks was discussed more fully by Stevenson (1968) and changes were made by Chandler and Schwarz (1980).

Parks (1949) published a detailed general stratigraphic section based on diamond drilling associated with exploration for lead and zinc. He observed oolites, mudcracks, laminite- breccia and concretionary structures, that is stromatolites. Harwood (1949), also engaged in mineral exploration, remarked on the occurrence of "shale ripples" and mudcracks in the Nastapoka Group,

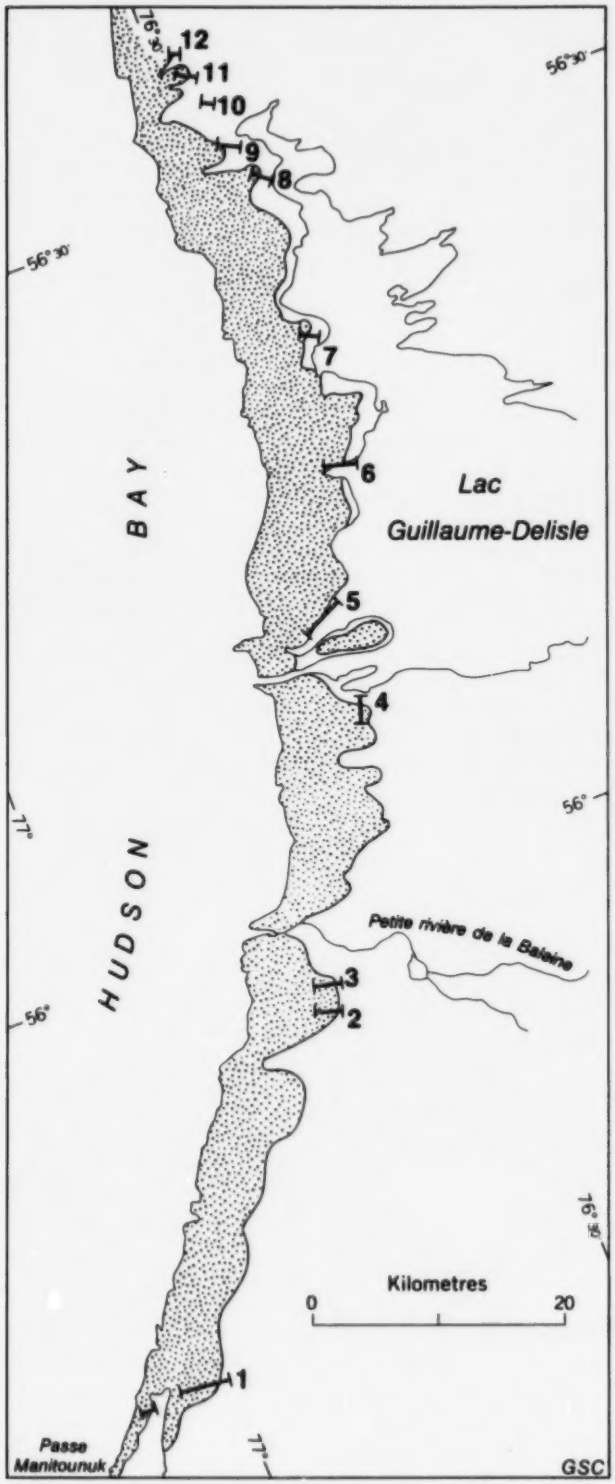

Figure 48. Location of stratigraphic sections (1-12) of the Nastapoka Group (stippled) shown on Figure 47.

believing them to indicate a shallow water or subaerial environment. Finding that the lead-zinc mineralization in the carbonate occurs in jointed silicified carbonate, he hypothesized that the host carbonates were thrust eastward against coeval granite plugs. The thrusting was thought to have caused brecciation of the silicified beds and the granites and localized the jointing, both of which provided access of mineralizing fluids from the granites. Chandler (1984) and some other writers (see text) do not accept the existence of the thrusting or of post-Archean granites.

Eade (1966) and Stevenson (1968) who mapped the region at 1:1 000 000 scale commented on oolites and stromatolites in the Nastapoka Group, which they included in their Manitounuk Group and Eade suggested a marine shelf environment for the group. Lastly, Chandler (1982) presented a sedimentological interpretation of a detailed stratigraphic section of both the rocks of the mainland and of Belanger Island (not considered here), one of the Nastapoka chain, regarding both to be tidal-marine, in origin.

In the vicinity of Lac Guillaume-Delisle the group can be broken at the present level of study into ten members as shown in Figures 46 and 47. On the west coast of Lac Guillaume-Delisle where a rugged unconformity has been cut into the feldspathic sandstone of the Qingaaluk Formation (Fig. 49) local thin conglomerate and sandstone (member A) drape the slopes of the unconformity surface and form talus pockets at the base of the slopes (column 5, Fig. 47). In cliffs on the west side of Lac Guillaume-Delisle a graded carbonate laminite (member B) overlies the conglomerate. This is overlain by (member C) a mature crossbedded arenite of quartz and micritic carbonate grains. Members A-C comprise the basal clastic part of the group.

The next member (D), the lower biolaminite, is termed a biolaminite because of its distinctive laminated appearance and its very likely biological origin. The unit is full of evidence of micro-organisms such as oncolites and stromatolites, but as the affinity of the organisms is as yet unknown the prefix bio- rather than the term algal is used. Although member D is internally complex, containing numerous thin zones of low domal stromatolites usually less than 1 m thick and some thicker stromatolite biostromes and numerous environmentally sensitive sedimentary structures, the unit was not divisible at the present level of study. Within member D lies a slightly discordant widespread chert breccia member (E) probably representing an erosional lag.

The thickest stromatolitic biostrome (member F), is significant because it is traceable over much of the strike length of the group and because it is mineralized with lead and zinc. Following the

mineralized unit is a distinctive unit, the "wavy stromatolite unit" (member G), that consists of small scale undulose stromatolites. It can be used as a stratigraphic marker to find the mineralized unit. This unit is followed by a second biolaminite (member H), the upper biolaminite, that cannot be distinguished from the lower biolaminite (member D). The upper biolaminite passes up into a white weathering feldspathic crossbedded sandstone (member I) and finally into basalt flows (member J).

In the extreme north of the area, section 8 and those farther north, the northward thinning group is markedly condensed, many of the above members being unrecognizable, and finally in the extreme north it is represented by only a few metres of feldspathic crossbedded sandstone.

Sub-Nastapoka Group basement. The rocks beneath the unconformity are invariably bleached and pyritized to varied degrees and depths. In the granitic basement this effect was seen in the basement knob on the north shore of Le Goulet (entrance from Lac Guillaume-Delisle to Hudson Bay) as well as outside the graben south of Petite rivière de la Baleine (55°54'N, 76°3'W) and near the mouth of Passe Manitounuk (55°44'N, 77°00'12"W). In the granite it takes the form of local pyrite patches and fracture coatings found down to 4 m beneath the unconformity.

On the south bank of Le Goulet the Persillon Formation basalts are heavily rust stained and pyritized where the formation underlies the carbonates (Table 1, sample 78CGA340 E). Both the pink arkoses and the basal redbed member of the Qingaaluk Formation are bleached up to 15 m beneath the unconformity on the south side of Le Goulet within 2 km south of Le Goulet, although bleaching associated with reduction at the unconformity can occur up to 200 m beneath the unconformity (Chandler, 1982, p. 9), as on the scarp slope of the coastal cuesta 4 km north of Colline Qingaaluk.

In a west-trending gully in the coastal cliff (56°27'N, 76°25'W) the Qingaaluk Formation is pyritized and very rusty for 10 m beneath the unconformity.

Similarly on the west shore of the gulf at latitude 56°24'42", longitude 76°27'30", an east-trending canyon 75 m across has been eroded into the Qingaaluk Formation (Fig. 50). Continuity of bedding in this formation beneath the canyon shows that faulting has played no part in its development. For several metres beneath the floor of the canyon the arkose of the Qingaaluk Formation carries scattered nodular patches of disseminated pyrite, in some cases comprising up to 40% of the material of the nodule. The vertical south wall of the canyon, 25 m high, and the more gently sloping north wall are partly lined with carbonate-sandstone conglomerate. Laminated carbonate is draped over these rocks and fills the canyon. Recently tumbled blocks of the laminated carbonate yield grab samples rich in pyrite, chalcopyrite and erythrite.

The relief of the sub-Nastapoka unconformity is varied. In some places, due to the similarity in the attitudes of the beds beneath and above it and the absence of relief at the break, it is not readily

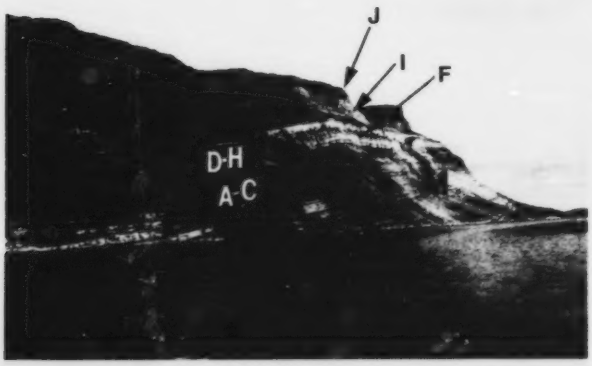

Figure 49. General view of the Nastapoka Group in a 400 m high cliff. The group overlies the tidal (fifth) member of the Qingaaluk Formation (M) with gentle angular unconformity (arrowed). Clastic members A-C of the Nastapoka Group are draped in depressions on the agged unconformity surface and are followed by members D-H (mainly carbonate) containing a widespread, rusty lead-zinc bearing zone (member 'F') and, sandstone of member 'I' capped by basalt of member 'J' (56°12'N, 76°32'W; GSC 203895-M).

Figure 50. Looking west toward 75 m wide paleocanyon eroded into Qingaaluk Formation at the base of the Nastapoka Group. Grey arkose of the Qingaaluk Formation (Q) defined 25 m high vertical south wall and gently sloping north wall (N). The canyon is filled with cupriferous, pyritic, dolomitic graded laminite (member B) at the base of the Nastapoka Group. (GSC 202909-R)

discernible, as in some east-facing cliffs (56°14'N, 76°31'W), and is best termed a disconformity. Elsewhere it is obvious (Chandler, 1982 Fig. 1.6; Fig. 49) and in many cases it is mantled by a few metres of conglomerate formed from carbonate debris and material up to block-size (Chandler, 1982, Fig. 1.9) derived from the underlying Qingaaluk Formation.

The usual appearance of the basal conglomerate is shown in Figure 51 (56°22'30"N, 76°26'30"W), taken from an east-facing slope. South of Copper cove at the foot of a north-facing cliff (56°20'6"N, 76°28'30"W) buff-weathering sandstone of the Qingaaluk Formation is successively overlain by 6 m of quartzite-pebble conglomerate, crossbedded carbonate-cemented arkose with granite clasts and laminated dolomite.

Basal unconformity and basal clastics (member A). On the west shore of Lac Guillaume-Delisle the basal units of the Nastapoka Group consist of thin sandstone and conglomerate (member A) overlying a rugged unconformity cut into units of the Richmond Gulf Group. In sections 5 to 7 these units are overlain in turn by a laminated, graded carbonate (member B), and a crossbedded quartz arenite (member C). This is in contrast to the attenuated section in the north, all crossbedded feldspathic sandstone, and that to the south where stromatolitic laminated carbonate appears to overlie the granitic basement in exposure of varied quality. The nature of the sub-Nastapoka unconformity is described from the stratigraphic columns of Figure 47, but also was examined at many other locations.

Graded, laminated carbonate (member B). Overlying the local coarse clastic facies at the base of the Nastapoka Group in sections 5 to 9 along the west shore of Lac Guillaume-Delisle lies an even parallel-laminated, graded, micritic, carbonate unit of varied thickness (Fig. 52; unit T in Fig. 53). In contrast to stromatolite bearing bio- laminite members D and H this unit is chert free.

In section 5 the unit occupies depressions on the unconformity surface and coarsens upward to grade into a quartz arenite. Mass flow conglomerates, fallen blocks, recumbent intraformational folds, and sedimentary structures similar to those of sandy turbidites, indicate deposition by a variety of mass flow mechanisms.

Figure 52. Cliff of graded laminite of member B of the Nastapoka Group. The laminite unconformably overlies bleached pyritized poorly sorted arkose of the Qingaaluk Formation (Q). Vertical hammer above 'Q' gives scale. (GSC 203263-S)

Figure 51. Vertical section of base of the Nastapoka Group. Massive carbonate and sandstone clast conglomerate of member A (C) overlies gently west-dipping arkose of the Qingaaluk Formation (Q) on an unconformity surface inclined to the left at about 30°. The local relief of the unconformity is 15 m. Vertical hammer, arrowed, gives scale. (GSC 202909-S)

Figure 53. Lenticular turbidite (T) of member B and quartz arenite (Q) of member C (units 1 and 2, stratigraphic section 5, Fig. 47) filling depression on unconformity surface beneath carbonates (C) of Nastapoka Group (see A-C, in Fig. 49; GSC 203265-Y).

Quartz arenite (member C). In section 5 (unit 2) the transitional contact of members B and C and the abundant trough crossbedding of member C (Fig. 53, unit Q) indicate a gradual conversion from the mass flow transport of member B to transport by dune-migration in the quartz arenite (Harms et al., 1975, p. 46). In sections 5 and 6 (unit 2) abundant dolomicrite clasts with included siliciclastic silt grains are evidence of erosion of previously deposited or coeval carbonate, possibly unit B. Absence of feldspar clasts in this arenite unit, that overlies feldspathic sandstone of the Richmond Gulf Group or Archean granitic gneisses, could have been caused by winnowing in the tidal marine environment as suggested by Klein (1977, p. 109), a suggestion supported by the textural maturity described above and by their association with carbonates. Removal of feldspar by tropical weathering of the feldspathic basement is unlikely because of lack of evidence of a weathering profile on the unconformity beneath the Nastapoka Group.

Lower biolaminite (member D). This unit thins northward and is traceable north to section 7 (Fig. 48). In the south it forms the basal unit of the Nastapoka Group but west of Lac Guillaume-Delisle it overlies other units (A,B,C). Although the member contains common clearly defined layers of stromatolites, it was not possible at this level of study to subdivide member D into smaller mappable units. One potential member is unit 8, column 5, that may be equivalent to unit 5 section, column 6 (see Appendix 2).

The unit is characterized by its almost universal lamination except where interrupted by features such as stromatolite zones or laminite breccia beds (Fig. 54). Also characteristic of the biolaminite is several per cent of generally black, in some cases grey, usually tabular, sometimes nodular, replacement chert. Several samples of the black chert have been examined, without success, by the writer and by Hans Hofmann of the University of Montreal for microfossils. Other very common features are layers several centimetres thick of edgewise laminite breccia and zones, usually less than 1 m thick, of linked low domal stromatolites or isolated examples of the same.

Among the less common structures in the member (see Figures in Appendix 2) are spherical, columnar, club-shaped and rare conical stromatolites, oncolites and tepee structures. Some domal and spherical stromatolites are separated by adjacent pockets of laminite breccia. Others are interlayered with mudcracked siltstone. Other less common structures include oolitic sand waves, ripples, truncation of laminae, mudcracks and syneresis cracks.

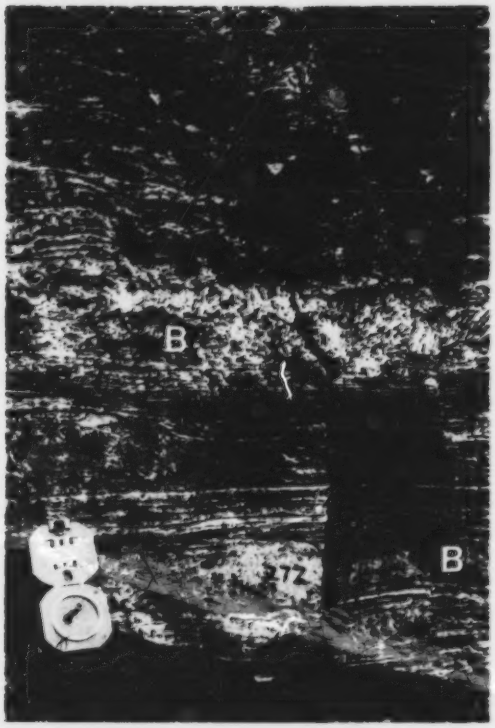

Figure 54. Vertical section of straight and crinkly laminated biolaminite with edgewise laminite breccia layers (B), section 7, Figure 47, Nastapoka Group (56°22'50"N, 76°0'52"W; GSC 202909-P).

Chert breccia (member E). A unit of massive breccia, 4-6 m thick, formed of black chert fragments in a light grey quartz- rich coarse grained arenite matrix was recognized in three sections over a strike length of over 30 km (stratigraphic sections 9,2, unit 2 and section 5, unit 3c). Continuity of the unit over the 30 km is suggested by the presence of a massive pale grey cliff-forming unit of similar thickness, and at a similar stratigraphic position (not examined closely) over a strike distance of 6 km above the local volcanic unit in the Qingaaluk Formation at latitude 56°N.

The chert fragments in the breccia are in many cases tabular and very angular and up to 10 cm thick (Fig. 55). In outcrop they appear identical to the tabular black chert occurring in the enclosing carbonates, being mostly massive and in some cases laminated. In thin section (2 examples) the chert is microcrystalline and appears in some places to ghost poorly sorted granular material (ooids?). The arenite of the matrix is composed mostly (75%) of monocrystalline quartz grains, moderately sorted and rounded, and indistinguishable from the form of quartz derived from granitic gneiss terranes. The rest of the matrix is composed of sand-sized chert grains similar in internal texture to the larger

tabular black fragments. Rare pebble-sized fragments of buff dolomite occur in the breccia in stratigraphic section 2.

In stratigraphic sections 1 and 2 the breccia is underlain by poorly exposed laminated dolomite with tabular black chert layers 2-10 cm thick and overlain by talus for several metres of section. In section 5 (Fig. 56) it overlies a laminated carbonate with laminite breccia zones, stromatolites and black chert layers. The upper metre of the carbonate has been brecciated and the base of the chert breccia describes a topography that unconformably cuts 3 m into the underlying carbonate unit.

In section 5 the succeeding 7 m of section contains laminite breccia zones with chert fragments and a 2 m thick crossbedded quartz arenite unit, and siltstone with mudcracks filled by quartz grains. Some of the siltstone interlayered with quartz arenite beds, is draped over stromatolites. These features indicate that vigorous traction currents, deposition of sandstone and emergence interrupted the carbonate depositing regime immediately after formation of the unconformable chert breccia. The vigorous currents would be inimical to the establishment of widespread algal mats, and the emergence suggests that part of the carbonate section was removed by karstification. Insoluble black chert from the carbonate formed a lag deposit that was infiltrated by craton-derived quartz sand probably under beach conditions.

Figure 55. Detail of chert-breccia zone, 6m thick, unit 2 stratigraphic section 3 (member E) Nastapoka Group (see also Fig. 56; GSC 203895-A).

Figure 56. Four metre-thick black-chert breccia (B), (member E) of unit 5 section 5, Figure 47. Note unconformable top and base of unit. (GSC 203265-Z)

Lead-zinc-bearing stromatolitic biostrome (member F). No stromatolitic bioherms were found in the Nastapoka Group. However one or two zones, better termed biostromal and up to several metres thick, occur in all sections south from section 6 inclusive. They are packed with a variety of stromatolites, are generally markedly pyritic

Figure 57. Irregular mass of pyrite (black) 45 cm across in lead-bearing zone (member F) Nastapoka Group (unit 12 of section 5, Fig. 47; GSC 203902-U)

Figure 58. Cavity, largely in shade, 60 cm across in dolomite of member F (unit 12, section 5) Nastapoka Group. Quartz (Q) and calcite (C) are arrowed. Abundant pyrite (black) is in shadow. Note pitted weathering, top left, due to selective solution of pyrite nodules. (GSC 203902-V)

(Fig. 57; see Fig. 90, in Appendix 2), and the best developed of these zones contains lead and zinc mineralization.

Other characteristics of the lead-bearing zone include quartz geodes, large euhedral calcite crystals (Fig. 58), brecciation with disorientation of the blocks, cavernous weathering (Fig. 59, 60) and heavy limonite-staining, presumably due to weathering of pyrite. Stromatolites include various types of branched (Fig. 61) and single columns and club-shaped stromatolites as well as domes and spheres.

According to Chandler (1984) heavy sulphur isotope values from various pyrites in the Nastapoka Group and underlying rocks suggest biological sulphur fractionation in a closed basin.

Due to disturbance of the lead-bearing zone and heavy limonite staining, confident assessment of its depositional environment could not be made. However mudcracks in the upper part of the zone are evidence of emergence.

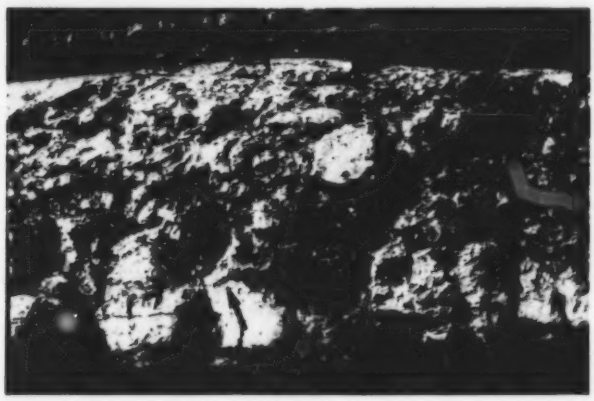

Figure 59. Cliff of strongly brecciated, cavernous, limonite-stained, galena-bearing member F (unit 12, section 5, Fig. 47) Nastapoka Group. (GSC 203265-Q)

Figure 60. Disoriented stromatolites in pyritic transitional zone (zone 13 section 5, Fig. 47) immediately above member F, Nastapoka Group. (GSC 203895-N)

Wavy stromatolite zone (member G). Distinctive laterally- linked low domal stromatolites form a stratigraphic unit several metres above the lead-bearing zone. The unit is up to 10 m thick and extends over at least 110 km in stratigraphic sections (Fig. 47, see section 4, unit 2 and correlatives). At first sight the unit in vertical section appears to be crammed with climbing ripples and few other structures (Fig. 62) but bedding surface exposure shows that it consists of concentric domal structures (Fig. 63).

In east- and southeast-facing sections the unit weathers white and can be traced by eye along the cliffs west of Lac Guillaume-Delisle. It is the white layer immediately above the lead-bearing zone marked "F" in Fig. 49. The unit is packed with little

Figure 61. Branched columnar stromatolites peculiar to member F of the Nastapoka Group (section 6, Fig. 47). The left side of the figure represents 45 cm of vertical section. (GSC 203264-W)

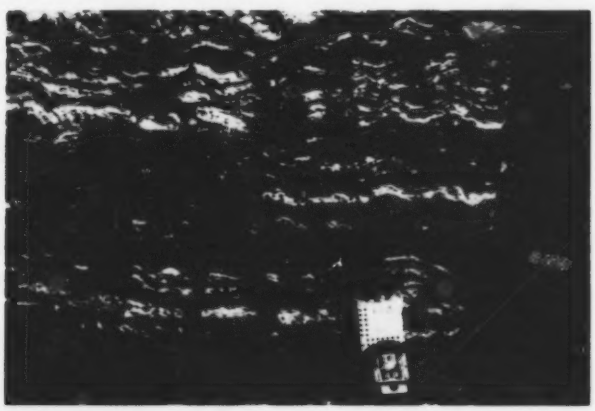

Figure 62. Vertical section of member G, (wavy stromatolite zone), Nastapoka Group (unit 13, section 3), see Figure 63. (GSC 203895)

Figure 63. Plan view of member G (wavy stromatolite zone; unit 13, section 3, Fig. 47) Nastapoka Group. (GSC 203895-G)

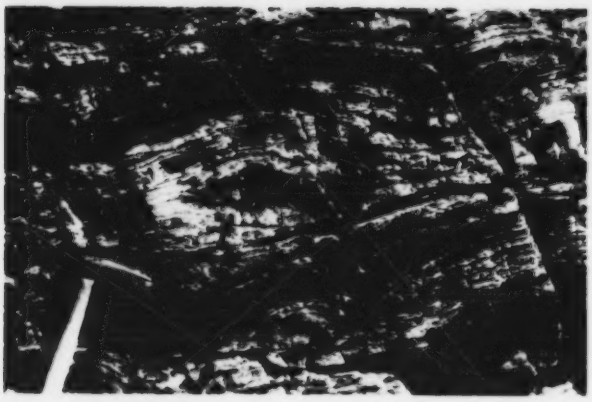

Figure 64. Vertical section of low domal stromatolites in laminated dolomite, one formed on pocket of edgewide laminite breccia (arrowed), upper biolaminite (member H) section 6 Figure 47, Nastapoka Group. (GSC 203895-P)

else but undulating domical laminae with an amplitude of 1-3 cm and a wavelength of about 5-9 cm. Associated sedimentary structures include abundant (10%) grey chert layers and nodules, minor oncolites and at the base and top of the unit, rare oolite sand waves and edgewise laminite breccia layers. Hand specimens of the rock show that oolite and granular laminated carbonate form lenticular fillings of interdome depressions, occur as laminae several millimetres thick on the top and flank of the domes, and are evidence of vigorous shallow water clastic sedimentation.

Truncation of laminae in these lenticles, as well as disposition of sigmoidal laminated lenticles of granular dolomite on the flanks of domes, are reminiscent of climbing ripples with erosion on the stoss side. In plan view, as noted above (Fig. 63), the structures are domical-concentric rather than linear as in many ripple fields. It is suggested that mats, possibly of algal origin, struggled for survival on a substrate of moving rippled sand with significant intrabasinal clastic sediment input. The low concentration of other structures, the nature of the associated structures, presence of oolites and the absence of mudcracks suggest a subtidal to intertidal environment.

Upper biolaminite (member H). The carbonate section overlying the wavy stromatolite zone thins northward from about 30 m in the region of sections 1 and 2, to pinch out at section 7. The following interpretation is drawn from sections 4, 6 and 7 in which exposure is very good. This unit is mudcrack-free, generally laminated (Fig. 64) and has a weak development of usually isolated low domal stromatolites. It is chert-bearing, contains oncolites, edgewise laminite breccia upon which isolated stromatolite domes have grown (Fig. 64), tepee structures, and overthrust laminae, all features of a protected subtidal to intertidal environment that was periodically disturbed by storms. Conophyton-like stromatolites at the base of the unit (section 6) may be further evidence of a subtidal environment. Rippled dolomite and sandstone beds occur in the top 6 m at section 6, the latter a harbinger of the influx of siliciclastic sediments. Sedimentary structures are shown with Appendix 2.

Top sandstone (member I). The sandstone unit at the top of the Nastapoka Group (Fig. 65) immediately beneath the basalt thins northward from about 30 m until it is 0-3 m thick in the northernmost section (section 12, Fig. 44). In all sections south of, and including, section 9 it is a well-defined unit overlying clearly separable carbonates. To the north of these sections the entire sedimentary part of the Nastapoka Group consists of 0-10 m of red, buff or grey texturally immature microcline-bearing arkose with small amounts of mudcracked maroon shale (section 10).

In the southern nine sections the sandstone is a texturally rather mature white-weathering, sometimes bimodal, arkose to subarkose, evenly parallel-bedded on a 10-15 cm scale (Fig. 65). The top 12 m appear in the field to be texturally very mature. The unit is mainly quartz- cemented. Some layers are carbonate-cemented, especially at the base near the underlying carbonates. Abundant planar crossbedding in 10 cm thick sets shows, in 3 stratigraphic sections, that sand transport is more or less to the west. Subordinate black, grey and rusty shale and siltstone contains wavy bedding, symmetrical ripples and mudcracks.

Figure 65. Well parallel-bedded light grey- to buff-weathering sandstone of member I (boundaries arrowed; unit 10, section 6, Fig. 47), overlain by basalt of member J, Nastapoka Group. (GSC 203895-B)

Bearing in mind the very cursory nature of the writer's examination, a tidal marine environment with intermittent exposure is suggested for this sandstone unit. Supporting data include even parallel bedding (Fig. 49), uniform small- scale crossbedding, paucity of evidence of emergence, and occurrence between tidal marine sandstone (Chandler 1982) and peritidal carbonates of the Nastapoka Group.

Nastapoka basalt ("Caprock"; member J). Detailed sections of the Nastapoka Group basalts were examined from drill core by Parks (1949) at the Nancy Island drilling camp in the coastal cliffs at latitude 55°57'30"N. The basalts, 107 m thick (regionally up to 230 m, Dimroth et al., 1970), are conformable on the underlying sediments of the Nastapoka Group (Fig. 38). The section consists of 3 columnar-jointed flows of similar structure, 15-40 m thick, underlain by a mafic sill and separated by thin pyroclastic units. The base of a typical flow is fine grained and contains few amygdules. The flow is coarsest in its central part, passes up to a 3 m amygdaloidal zone, and finally to a 1.5-3 m flow breccia with angular amygdaloidal or vesicular fragments in a fine grained matrix. The sill contains abundant 5 cm across feldspar crystals in its upper two thirds.

More recent work south from the area considered in this report to Grande rivière de la Baleine, a distance of 90 km, by Ciesielski et al. (1983) indicated at least 4 flows in the volcanic unit, one possibly the sill of Parks (1949) and a greater number of flows to the north, west of Lac Guillaume-Delisle. These latter writers found the flows to be macroscopically homogeneous along the Manitounuk Islands, separated by thin horizons of detrital sediments. Flow-top breccias, vesicles, agates and reddening occur at interflow contacts. On the north side of Petite rivière de la Baleine phenocrysts were seen in the basal flow (sill of Parks, 1949).

Paucity of interflow shales, almost complete absence of pillows and other features indicated to A. Ciesielski (personal communication, 1983) that extrusion was subaerial with local flow over shallow water.

Summary of sedimentology

The carbonate-rich part of the Nastapoka Group exposed in the cliffs on the west shore of Lac Guillaume- Delisle can be traced south to the Long Island area near the mouth of James Bay over which distance an approximately similar thickness is maintained (Eade, 1966). To the west, in the Belcher Islands, the carbonates are considerably thicker (Ricketts, 1979) although problems with details of correlation make an exact comparison impossible at present. At the north end of Lac Guillaume-Delisle, as shown in this report, carbonates are absent in the thin arkosic section. Further to the north, in the Nastapoka Islands, where a stratigraphically higher part of the group is represented, carbonates are also absent (Low, 1903). In the Hopewell Islands, about 250 km to the north of Lac Guillaume-Delisle, carbonates are absent from a 50 m thick clastic section of the Nastapoka Group (Kranck, 1951, Fig. 35; Lee, 1965).

Low (1902, p. 72d) explained the northward thinning of the Nastapoka Group at Lac Guillaume-Delisle (Fig. 48) by thrusting of the Aphebian strata from the west. Later writers from Leith (1910) to Stevenson (1968) were unable to support this view. Facies change from a carbonate- dominated sequence to a few metres of crossbedded arkose with local red mudcracked mudstone at the northern end of Lac Guillaume-Delisle, coupled with continuity of stratigraphic units within the limits set by the facies changes, suggest that the northward thinning of the group at Lac Guillaume-Delisle is the result of

synsedimentary processes rather than of later deformation as was suggested by Low (1902).

Regional considerations (see Implications of Richmond Gulf Graben for the Archean tectonics of northern Quebec) and the probability of a southeastern paleoslope during the deposition of the Richmond Gulf Group suggest the possibility that during the deposition of the carbonates a source area may have lain to the north and that the facies change across Figure 47 may represent a section from alluvial deposits in the north to shallow marine deposits in the south.

The surface of the sub-Nastapoka unconformity within Lac Guillaume-Delisle is unweathered and rugged on the scale of tens of metres (Fig. 49) and flanked by thin massive conglomerates of sedimentary derivation. Depressions on the unconformity surface are filled with turbidite-like laminated carbonates (member B) that contain mass-flow conglomerate beds and blocks of sandstone from the underlying Qingaaluk Formation that have tumbled down the sides of paleohills (Chandler, 1982, Fig. 1.9). These data suggest rapid marine transgression over rough topography within the gulf and the filling of local depressions with mass flow sediments.

Several exposures of the contact between the Nastapoka Group and the Archean paleosurface (Kranck, 1951) suggest slight weathering (temperate climate) and a smooth basement surface. A. Ciesielski (personal communication, 1983) regards this surface as quite flat, an idea supported by the absence of turbidite-like basal sediments. The Richmond Gulf Group within the graben is at present more easily eroded than the granitic shoulders of the graben. Evidence of this is the irregular depression which is at present filled by Lac Guillaume-Delisle itself. A similar shallow paleovalley that may have existed on the site of the graben at the beginning of Nastapoka time would have allowed such local mass flow sedimentation.

Evidence of a marine rather than a lacustrine depositional environment for the Nastapoka Group carbonates is not abundant in the Gulf. It is limited to tidally bedded siltstones (see Fig. 92, in Appendix 2), mature quartz arenites and a wide range of sedimentary structures particularly in the biolaminites, which are common in Recent and other Phanerozoic marine carbonates. Moulding of stromatolites into linear ridges (Chandler, 1982, Fig. 1.13) and herringbone- crossbedded quartz arenites, both evidence of tidal activity, were only found higher in the section on Belanger Island.

Member C, a bimodal quartz arenite that completes the filling of some depressions on the unconformity surface, may be of tidal marine deposition. Carbonate sedimentation recommenced with the biolaminites (members D,H) many features of which are consistent with intertidal and subtidal deposition. Such structures as bird's eye fabric (Shinn, 1968) and calcrete (Read, 1976) both indicative of supratidal exposure are absent. Linear ridged stromatolites may not have been found because this feature is best seen in plan view and nearly all the exposures of the carbonates at Lac Guillaume-Delisle were examined in vertical cliff section.

Stromatolites and environment-sensitive sedimentary structures. The following section consists of a short review of aspects of stromatolite geology and of the environmentally sensitive sedimentary structures both useful in interpreting unit D as well as units F and G, both stromatolitic, followed by a summary interpretation of unit D.

Stromatolites are laminated structures formed generally in carbonate rocks by the agency of filamentous organisms including blue-green algae and bacteria. Layered structures with little relief are known as algal laminites or laminites and their modern counterparts as algal mats. Various forms of the modern counterpart exist (Kinsman and Park, 1976; Logan et al., 1974). In this paper structures with higher relief have been given names such as dome, column and club depending on individual shape.

Monty (1977) who traced the evolution of opinion on the subject of stromatolites stated that by the 1960s a threefold dogma had crystallized in the Western literature: that stromatolites form only on intertidal flats, that they form by the trapping and binding of detrital particles (e.g. Gebelein, 1969), and that their overall morphology is determined by environmental factors (e.g. Logan, 1961). Although these criteria encompass many examples, they are not all embracing. For example, in the Proterozoic at least (e.g. Hoffman, 1976b) a wide range of environments were colonized. Further, blue-green algae have been found at marine depths of 1 km and bacteria are implicated in the formation of deep oceanic laminated Fe-Mn nodules (Monty, 1977). There is also evidence that stromatolites can form by the precipitation of carbonate (Hoffman, 1976b, p. 611). Thirdly, there is the Russian view that stromatolite form has some evolutionary basis (Cloud and Semikhatov, 1969). Thus there is a divergence of views on the relative significance of environmental and biological factors in determining stromatolite form (Haslett, 1976, p. 580), and some authors cautiously consider both factors important (Serebryakov, 1976; Golubic, 1976), the latter suggesting that the influence of the biological factor can be influenced by climate and local ecology.

For the above reasons, in interpreting the sedimentary environments of the Nastapoka Group carbonates in the Lac Guillaume-Delisle area,

although comparisons are made with structures of modern stromatolites, more weight is given to sedimentary structures of less controversial origin.

One of the classical areas in which recent intertidal stromatolites are forming is Shark Bay, Australia. The structures are forming possibly because the high salinity inhibits predation by metazoans. Logan (1961) suggested two important ideas; that by analogy with the intertidal stromatolites he described at Shark Bay, stromatolites are an intertidal phenomenon and that the form of the stromatolites in the intertidal zone of Shark Bay is determined largely by the environment. Club shaped bodies, analogous to the fossil **Cryptozoon**, grow on headlands exposed to maximum wave action, with their height determined by tidal range. The structures tend to become confluent inland and farther inland, protected behind them, grow as a sinuous low domal form, analogous to the fossil **Collenia**. In the most protected parts of Shark Bay grow wide areas of flat-lying algal mat, interspersed with low domes. In the supratidal zone where wetting is rare, desiccation breaks the mat and its adhered laminae formed of carbonate particles into laminite breccia.

Gebelein (1969) also noted that current velocity and rate of sediment movement determined stromatolite form in Bermuda. Interestingly, algal mat was found forming at depths down to 10 m where it was being broken into laminite breccia by currents that also rippled sand. Further, Playford and Cockbain (1976) found conical, parallel sided and club- shaped columnar stromatolites growing in the subtidal zone of Shark Bay.

Thus, even among the "environmentalists" there is considerable divergence of views upon the environmental significance of stromatolite form.

A large part of the carbonate section of the Nastapoka Group at Lac Guillaume-Delisle consists of straight-parallel laminated dolomite, the biolaminites of members D and H of Figures 49, 54 and 64. Associated with this biolaminite facies are occurrences of low domal stromatolites, ooids, and derived oncolites, edgewise laminite breccia and tepee structures, and other sedimentary structures all listed in numerous publications as commonly occurring in very shallow marine waters.

Gebelein (1969), Logan (1961) and Hardie and Ginsburg (1977) have demonstrated how modern subtidal to supratidal blue-green algal mats bind fine grained detrital carbonate particles to form laminated carbonate rock. Restrictions on the environments of growth and preservation of modern algal mats include desiccation and evaporite mineral-formation in arid supratidal zones (Kinsman and Park, 1976; Gebelein, 1976), physical disturbance of high energy sandy shores (Gebelein, 1976), and bioturbation and grazing by metazoa in the lower intertidal zone and below (Gebelein, 1976). Therefore in modern environments algal laminite development should reach its acme in the upper intertidal zone unless some factor such as salinity restricts the metazoa (Kinsman and Park, 1976), as in Shark Bay, Australia, where high salinity restricts metazoan grazing and algal mats are well developed on low-energy upper and lower intertidal mudflats (Logan, 1961) and subtidal zone (Playford and Cockbain, 1976).

Kinsman and Park's (1976) studies on the algal mats of the Persian Gulf coast indicate that a wide variety of morphotypes of algal mat occurs and that these are bathymetrically zoned (see also Hoffman, 1976, Shark Bay), but according to Kinsman and Park only the smooth mat that grows between 40 cm below and 3 m above spring low tide has a high preservation potential. Nevertheless Eriksson and Truswell (1974) believe that other morphologies of mat such as blister, crinkled and pustular mat have been preserved in the early Proterozoic Transvaal Dolomite of South Africa.

But in the Early Proterozoic metazoa were very likely absent. Also contrary to some opinion, blue-green algae, although photosynthetic, are not restricted to the photic zone. Some planktonic forms have been recovered from oceanic depths of 100 m (Monty, 1977).

Thus studies of modern algal mats, a possible precursor of the biolaminite of the Nastapoka Group, indicate that widespread development of algal mat occurs only when weak agitation of the environment permits extensive colonization of loose substrate and only when predation by metazoa is prevented as in the hypersaline Shark Bay. It seems that because of the probable absence of such grazers in the Early Proterozoic, algal mats might well have colonized both intertidal and subtidal environments of low mechanical energy.

The low domal stromatolites in the biolaminites of the Nastapoka Group are similar in appearance to the laterally linked hemispheroid type (**Collenia**-type) of Logan et al. (1964) which in modern environments result from enhanced growth of continuous algal mat over substrate irregularities such as erosion surfaces, mudcracks and breccia fragments. Their growth mechanism involves trapping of fine grained sediment preferentially on the dome crests and inhibition by current scour in the low interdome areas. In Shark Bay the linked domal structures are believed to develop characteristically from continuous algal mat in re-entrant bays or behind such structures as barrier islands where wave action is slight.

Many of the stromatolites in the Nastapoka Group biolaminites at Lac Guillaume-Delisle are low domal (see Fig. 98, in Appendix 2) to spherical structures (see Fig. 94, in Appendix 2) either linked

or isolated. There is a common association of edgewise laminite breccia with the low domal stromatolites. The breccia can fill interdome spaces (see Fig. 89, in Appendix 2). In one such layer, in units 6 and 8 of section 5, the stromatolites are interlayered with rippled and mudcracked siltstone-shale. Some have developed on elevations on the underlying laminite such as mounds or ridges of laminite breccia (Fig. 64) or appear to be perturbations of unknown cause of the generally otherwise straight parallel lamination of the carbonates.

Edgewise laminite breccia is a very common feature of the biolaminites. Apart from the occurrences associated with domal stromatolites listed above it is even more common as discrete beds (Fig. 54 and 66) at all stratigraphic levels in the biolaminites.

Gebelein (1969) reported flat-pebble conglomerate formed from disrupted algal mat associated with rippled sands in the subtidal zone of the Bahamas, but did not state that the fragments had an edgewise orientation. Logan (1961) found that laminated carbonate sediments of algal origin in the supratidal zone of Shark Bay are normally broken, by desiccation and by the influence of storm waves and abnormally high tides, into flat polygonal fragments that simulate the flat pebble conglomerate so often found with stromatolites in the rock record. Logan (Logan et al., 1974) went on to say that laminated flat-pebble breccias and conglomerates are common in this zone. Logan (1961) felt that the intertidal algal mats, because of the frequent wetting, remain moist and coherent and resist brecciation. Gebelein (1976) suggested that thick algal mat does not characterize the supratidal zone and that breccia so formed would be liable to be blown away; thus laminite breccia development is not likely in that environment.

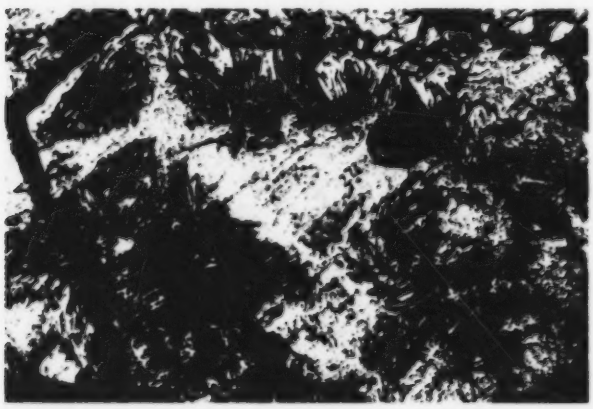

Figure 66. Plan view of edgewise laminite breccia replaced by white chert in wavy stromatolite zone (member G), Nastapoka Group (unit 6, section 7, Fig. 47; GSC 203263-L)

In discussing the environmental significance of edgewise flat-pebble conglomerate of any composition Ricketts and Donaldson (1979) pointed out that recent studies have demonstrated that there are two principal requirements for the formation of edgewise flat-pebble conglomerate, an ample supply of thin tabular clasts and the swash-backwash conditions provided by breaking waves on a shoreline.

The weight of the evidence briefly presented above suggests that edgewise laminite breccia may be formed by wave action in the high intertidal zone. The domal stromatolites associated with much edgewise laminite breccia, especially those interlayered with mudcracked siltstone-mudstone, may well have been formed in a similar environment. Other features associated with the many occurrences of domal stromatolites mentioned above include replacement chert, tepee structures, oncolites, oolites and rippled quartz arenite layers. These together are common in marine tidal carbonates (see discussion below of tepee structures, oncolite, oolites and chert).

Columnar stromatolites grow in the intertidal zone in Shark Bay on headlands where activity is maximized. Low domal forms and mats grow in more protected areas (Logan, 1961). More recent work (Playford and Cockbain, 1976) has shown that column, dome shaped, cylindrical and club shaped, are also characteristic of the subtidal zone of the Shark Bay area, where they grow to a height of up to 0.75 m, though usually less than 0.5 m, and to a depth of at least 3.5 m. The example illustrated by the latter authors appears to be growing on rippled sand.

In the biolaminites of the Nastapoka Group few sedimentary structures were seen to accompany the columnar stromatolites. At one locality (section 4, unit 3) tepee structures, crinkled mat- and bun-shaped stromatolites occur. At two other localities columnar stromatolites characterize the lead-bearing unit (Fig. 61). All that can be said from the field data is that, bearing in mind the abundant sulphide and the abundance of domal and spherical stromatolites in the transition zones above and beneath the lead-bearing zone, the columnar forms probably represent the acme of stromatolite growth in the section.

Conophyton is a distinctive form of columnar stromatolite in which vertical sections of the laminae have the form of a Gothic arch. Donaldson (1976) interpreted sedimentary structures associated with two Proterozoic **Conophyton** occurrences to indicate a turbulent shallow subtidal to intertidal environment in one case and a subtidal environment in the other. Hoffman (1976) believed conophyton to be sublittoral in the Proterozoic McLean Formation and perhaps in general to be exclusively subaqueous.

Conophyton-like forms are rare in the Lac Guillaume-Delisle area and are restricted to unit 9 of section 6 (see Fig. 97, in Appendix 2) where they change upward to a columnar form with low domal laminae, and unit 9, section 3, where the upper part of the structure is conophyton-like.

Oncolites are detached stromatolites (Milliman, 1974). Like stromatolites they are laminated bodies but, due to having been rolled in agitated water during growth, are more or less concentrically encircled by the laminae. According to Logan et al. (1964) they are formed permanently submerged in shoal water. Gebelein (1976) noted that in the Bahamas modern examples are most prominent in depths of less than 1 m. Logan et al. (1974, p. 76) illustrated a series from biconvex-lenticular to spheroidal forms relating increase in sphericity and concentricity of the laminae to decreasing importance of periods of rest between the phases of agitation.

Unlike the forms illustrated by Logan et al. (1974) and some other authors, that grew from detached more or less equant stromatolite heads, those of the Lac Guillaume- Delisle area (see Fig. 96, in Appendix 2) are more like some shown by Eriksson and Truswell (1974) from the South African Early Proterozoic and probably formed on detached slabs of laminite. If oncolites are indeed subtidal this is evidence of laminite formation from smooth algal mat in the subtidal zone.

Viewed in the context of the apparently energy-sensitive oncolite types of Logan et al. (1974) the encapsulated slab form of the oncolites at Lac Guillaume- Delisle coupled with the thickened laminite formation on one side of the body (see Fig. 96, in Appendix 2) suggests that these are lower energy forms that have spent significant periods of their development at rest.

Tepee structures are sections through pressure ridges that are formed at the edges of polygons of layered carbonate sediment. They were probably caused by syndepositional crystallization of interstitial aragonite in carbonates (Assereto and Kendall, 1977; Smith, 1974). Slip between algally bound layers and interbedded sediment permitted movement of the layers. Assereto and Kendall (1977) and Smith (1974) believed that the structure forms in the supratidal to intertidal environment, though Shinn (1969) reported similar structures to have formed in shallow subaqueous environment.

Smith (1974) found them almost completely restricted to rocks inferred from their lamination to be algally bound, and with size ranged from a few centimetres in height to 2 m. Typical tepees have a roughly symmetrical chevron-like structure with a subvertical axial fracture zone, interdigitation of beds lying on opposite sides of the fracture, wedging of contemporaneous beds on the sides of the anticline and erosion of tepees crests. Tepee structures also appear to be forming by pore-water pressure and post- disruption carbonate crystallization at the margins of modern South Australian salinas (Warren 1983).

Tepee structures are not uncommon in the laminites of the Lac Guillaume-Delisle area ranging from heights of several centimetres (Fig. 67) to one of at least 1 m (see Fig. 93, in Appendix 2). Several features of the structures listed above are apparent on those of Lac Guillaume-Delisle. Overlap of the edges of the carbonate, as well as absence of an axial cavity and infrequent observations of overthrust carbonate laminae not associated with tepee structures, are strong evidence that lateral expansion of the laminae was involved in forming the tepees. Onlap of laminae sedimented on the flanks of the tepees, absence of any folding in any laminae immediately above and beneath the tepees, and truncation of the apical part of some tepees are evidence of a synsedimentary origin of the structures.

According to Simone's (1981) review ooids are spherical to subspherical carbonate grains usually averaging 0.25-1 mm across that nowadays seem to form in warm water less than 5 m in depth. Tangential arrangement of crystals in the ooids seems to be related to turbulent environments and radial disposition to quiet environments. Milliman (1974) found that although modern oolites are found as deep as 160 m on modern shelves they are relict after low Pleistocene sea levels. Modern oolites form in tropical to subtropical waters generally shallower than 2 m although they can form as deep as 15 m. Milliman felt that they form most rapidly in agitated environments and that deeper water ooliths can be distinguished by their thin uneven concentric lamination and irregular surface texture. Among

Figure 67. Tepee structure in unit 1, section 4, Figure 476 (member H), Nastapoka Group. Note onlap of succeeding carbonate laminae over structure. For discusison see text. (GSC 203902-T)

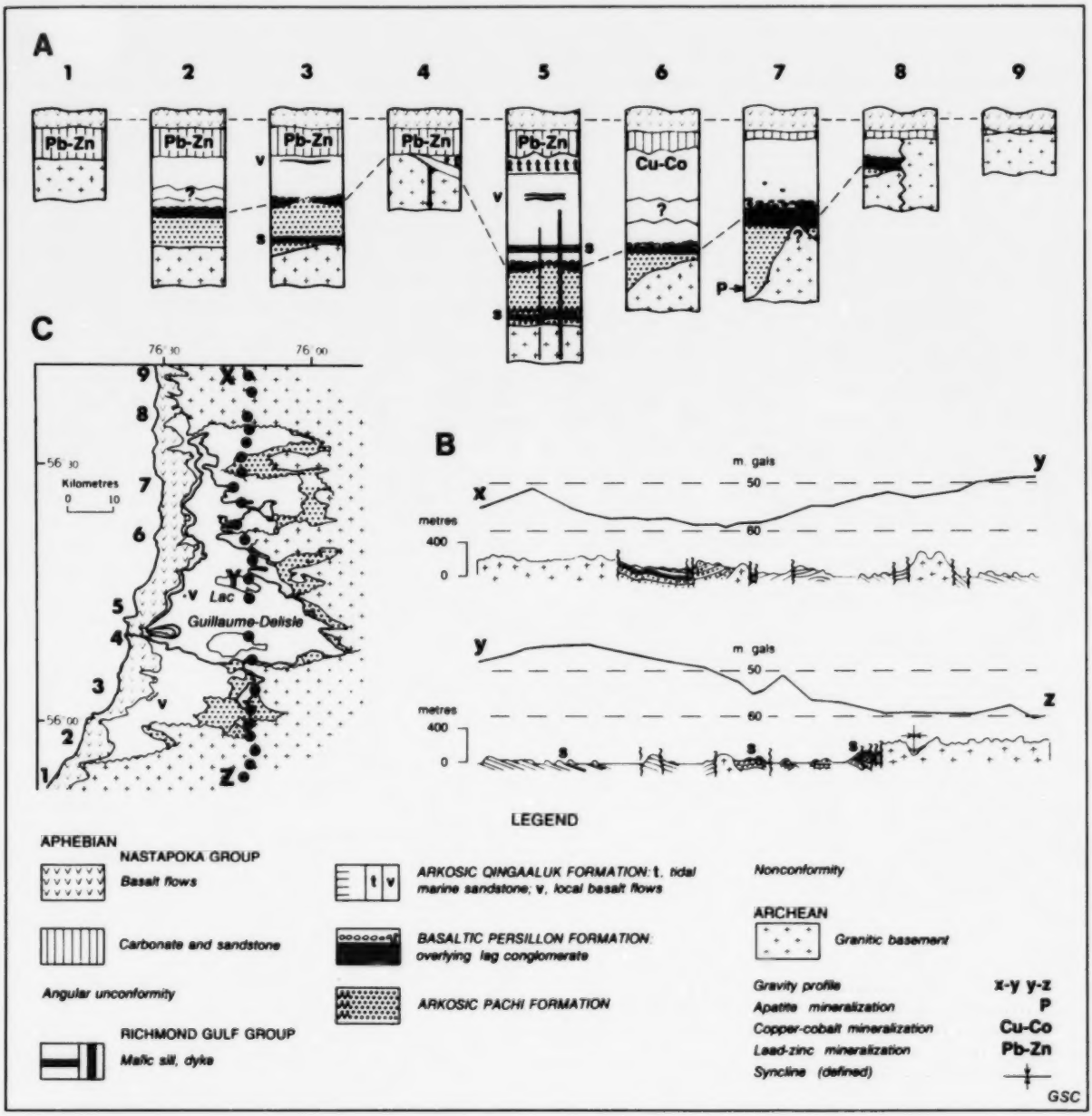

Figure 68. Geological and gravity profile across the Richmond Gulf Graben. (a) Stratigraphic variation across the graben. Each column summarizes the geology in an east-west strip. (b) Geological section and collinear Bouguer anomaly profile after Gibb et al. (1983) along the line X-Y-Z . (c) Map showing location (latitude) of stratigraphic sections (1-9), geological cross-sections and Bouguer anomaly profiles (X-Y-Z).

the varied theories of origin, that of some unknown mechanism of inorganic precipitation is currently in fashion.

Ooliths were hard to recognize in the carbonates of the Nastapoka Group, very likely because of the advanced textural alteration. They were found in three places. Very altered spheroidal grains occur in the wavy stromatolite zone (member G) section 5, unit 13 and section 6, unit 8). In section 6, unit 6 where they form a 15 cm thick bed interlayered with low stromatolite domes and rippled dolomite they are

well enough preserved to show fine even concentric laminations, subordinate weakly developed radial structure, high sphericity and a smooth outline. This last example may have been deposited in very shallow warm agitated water.

Nodular and layered replacement chert is common in Phanerozoic carbonates. It also occurs in the Proterozoic (Sathyanarayan and Muller, 1980). The silica may be of inorganic, possibly volcanic origin or of organic origin. Silica-secreting organisms, such as diatoms, sponges and radiolaria, are thought to be silica sources for much Phanerozoic replacement chert in limestones but the existence of such organisms in the Precambrian is not certain (Blatt et al., 1972). Thus the origin of the chert in the Nastapoka Group carbonates is unknown.

Eley and Jull (1982) considered replacement chert in a Silurian biostromal carbonate to be of early diagenetic replacement origin and to have been localized by pH decrease at the site of decaying organisms. Association of much nodular chert in the Nastapoka Group with stromatolites (see Fig. 95, in Appendix 2) and occurrence of concordant layered chert in the biolaminite members (D and H) in contrast to its absence from the graded laminite (member B) suggests that decaying algal mats could have caused pH reduction in this case.

A widespread slightly unconformable chert breccia (member D) within the lower biolaminite is evidence of local emergence and erosion of the carbonates. Some stromatolite zones have produced enough organic material to allow sulphate-reducing bacteria to generate considerable pyrite and in the case of member F, the acme of stromatolite development, to fix sphalerite and galena. The presence of these sulphides is indirect evidence of marine sulphate.

The carbonates are overlain by a texturally mature tabular crossbedded sandstone interpreted as marine. The overlying basalt was probably extruded subaerially and locally over very shallow water (A. Ciesielski, personal communication, 1983).

Structure and age of the graben

Crustal studies of the Lac Guillaume-Delisle area started at least a hundred years ago (see References). Although Low (1902, p. D46-D48) recognized that the arkosic Richmond Gulf Group has a granitic source area, he did not consider the immediately surrounding granitic rocks to be older than the supracrustal rocks. Rather, in correlating the supracrustals and the Nastapoka Group with the metamorphosed rocks of the Hastings Group of eastern Ontario and the Labrador Trough, he regarded them as a stratigraphic equivalent that had escaped the effects of a great burst of granite almost universal over the Archean shield east and southeast of Hudson Bay. At Lac Guillaume- Delisle local presumed intrusive contacts with and contact-metamorphic effects in the supracrustals were taken as evidence of a later phase of granite formation.

Leith (1910) was not impressed by Low's (1902) stratigraphic correlation between the supracrustal rocks at Lac Guillaume-Delisle and the above metamorphosed sequences elsewhere on the eastern shield. Further, re-examining Low's (1902) evidence, he was less than convinced that granites intruded the sediments.

Later writers have stressed the existence of an unconformable relation between the supracrustals and the granitic rocks. Eade (1966) mentioned a regolith of reconstituted granite at the contact. Woodcock (1960) and Stevenson (1968) were unable to find any evidence of an intrusive contact.

The first reference to the Richmond Gulf Graben as such was that of Kranck (1951) who related its orientation to a presumed east-west axial depression beneath the Belcher Islands, the latter deduced from the plunge of north-south striking fold axes in the islands toward the centre of the islands. Later Woodcock (1960) regarded the Richmond Gulf Group as deposited in a small depression that projected eastward from the main Proterozoic basin of Hudson Bay.

Faulting and folding

The geological structure and geometry of the fill of the graben is shown in Figure 68. Figure 68a is a set of generalized sections that attempts to summarize important stratigraphic relations of east-west strips at the latitudes shown on the inset sketch map. Figure 68b is a topographic and geological section that shows an example of the detailed structure and relief across the graben and its relation to a positive gravity anomaly that occurs in the centre of the graben and is interpreted by Gibb et al. (1983) as due to a mafic intrusive.

Figure 68a shows that the Richmond Gulf Group is restricted to the graben and that the northward-thinning Nastapoka Group postdates the graben (see also Fig. 69). As argued in this report, the Richmond Gulf Group pre-dates graben formation but the intricate faulting related to graben formation that cuts the group is not shown in the columns of Figure 68a to preserve clarity. Figure 68a also shows that there are marked thickness variations in the Pachi Group (Fig. 70) and that mafic sills and east-trending mafic dykes are concentrated in the axial region of the graben, a relationship shown in the form of a map by Chandler (1982). Some assymetry in the distribution of the sills may indicate that the central horst was active at the time of their intrusion so blocking their access to layered strata on its north side. The sections also show in a

general way the stratigraphic position of the various types of mineral occurrences in the Richmond Gulf and Nastapoka groups.

Figure 68b shows the depression of the graben and its contents below the level of the granitic basement horsts and shoulders of the graben (Fig. 71, 72). It also shows the abundant faults and minor gentle folds affecting the Richmond Gulf Group.

The writer's studies (Chandler, 1978, 1979, 1982; Chandler and Schwarz, 1980; Chandler et al., 1982) show Lac Guillaume-Delisle to be an east-striking, west-plunging graben (Richmond Gulf Graben) about 75 km across. Bott (1981) suggested, on theoretical grounds, a correlation between graben width and the thickness of the rifted brittle crust. A

Figure 69. Graben-margining fault north of Lac Guillaume-Delisle. Qingaaluk Formation (Q) is downthrown against granitic basement (G) in south-facing cliff by fault marked (-------). Unfaulted basalt, underlain by 10 m of grey arkose, both of the Nastapoka Group (N) overlie the faulted rocks and therefore probably postdate graben-formation. (GSC 203899-W)

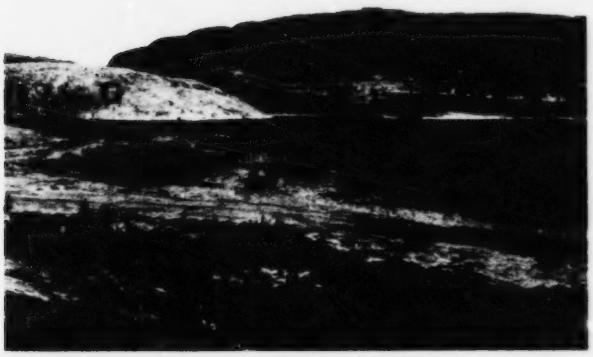

Figure 70. View northwest across Le Goulet (outlet of Lac Guillaume-Delisle) towards paleohill (inlier) of Archean granitic basement (G) upon which rest, in sequence; sandstone of the Qingaaluk Formation (Q), carbonates (N) and basalt flows of the Nastapoka Group (B). The exposure in the foreground is of the Qingaaluk Formation. (GSC 203899-Z)

Figure 71. Looking north at an altitude of 500 m toward the central horst (H), a west-plunging 300 m high hogsback of Archean basement. Here the horst is upthrown against the Qingaaluk Formation (Q). The coastal cuesta, beyond which lies Hudson Bay, is composed of the upper part of the Qingaaluk Formation overlain by the Nastapoka Group and forms the horizon at latitude 56°20'N, longitude 76°15'W. (GSC 203899-O)

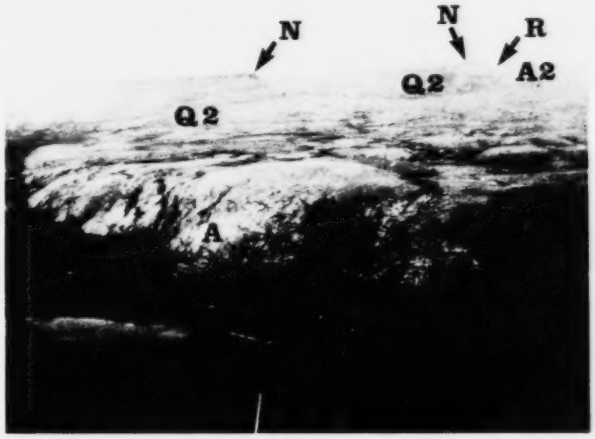

Figure 72. Looking northwest at the northern tip of Lac Guillaume-Delisle from an altitude of 500 m. Cliff-forming Archean granite basement (A) is upthrown against the Qingaaluk Formation (Q). This relationship is repeated 6 km to the northwest (at R) where the Qingaaluk Formation (Q 2) 2 is downthrown against the basement (A2). The faulted rocks are all overlain by the unfaulted Nastapoka Group. Details of the faulting at 'R' are shown in Figure 69. (GSC 203897-V)

width of 65 km is predicted (Vening Meinesz, in Bott, 1981) for a 35 km thick crust, close to the 40 km suggested for the Superior craton of northern Quebec (Mukhopadhyay and Gibb, 1981). According to Bott, a thick upper brittle layer (low heat flow far from main rift zone?) would give a wider graben.

In the graben apart from the coastal cuesta, the Aphebian Richmond Gulf Group lies about 100-300 m topographically below the Archean granitic shoulders (Fig. 72) and horsts (Fig. 71). The graben is cut by, and bordered by, clearly visible listric normal faults that have a strong statistical east strike (Fig. 73). This is contrary to Woodcock's (1960) finding that there are two dominant fault strike directions, one east-west and the other, northwest- southeast.

Within the graben several basement horsts also occur as inliers (see Fig. 1, in pocket) Apparent draping of the Nastapoka Group, as west-plunging synclines over the westward subsurface extension of these horsts, may occur in the offshore Nastapoka Islands (Chandler and Schwarz, 1980, p. 63).

Faults in the Aphebian sequence cut only the Richmond Gulf Group (see Fig. 1, in pocket). There is no sign of a pre- Qingaaluk Formation phase of faulting that cuts the Pachi and Persillon formations, as was suggested by Woodcock (1960). Faults within the Richmond Gulf Group generally have displacements of tens of metres or less, as measured from offsets of the Persillon Formation, although some faults that downthrow the group against the Archean basement have larger throws, in the order of a few hundred metres, as seen from the present heights of basement cliffs at these faults.

The faults clearly offsetting geological units were marked with solid lines on maps by Chandler (1979) and Chandler et al. (1982). These were put on a histogram with segments of zig-zag faults plotted separately. The graph (Fig. 73) shows a clear east-striking mode with a large number of data within 45° of the modal class. The separate class of northwest-striking faults reported by Woodcock (1960) was not found.

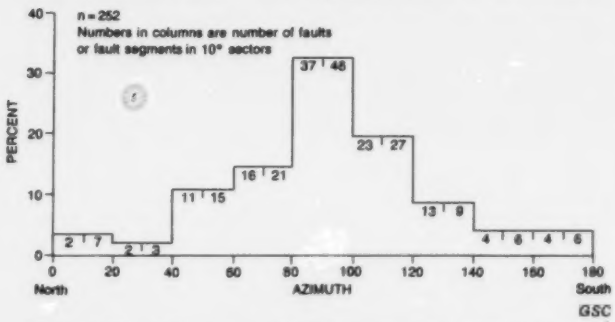

Figure 73. Orientation of faults cutting the Richmond Gulf Group, Richmond Gulf Graben. Data from Chandler (1979) and Chandler et al. (1982).

Some major graben-bounding faults have an irregular trace. Where examples are exposed, as along the south shore of the gulf between Île Cairn and the abandoned Hudson Bay Post to the east (see Fig. 1, in pocket), they have a zig-zag pattern with segments not diverging greatly from an east-west orientation. This is similar to the 'gridded' fault-pattern of some major rifts of the world that Ramberg and Smithson (1975) attributed to local structural grain. Figure 73 as well as earlier geological mapping of the basement (Eade, 1966; Stevenson, 1968) indicates that this effect is subordinate to east-west fractures in the Lac Guillaume-Delisle area.

No faults other than normal were found. They seem to have stepped progressively downward from graben margins or horsts, with the strata on the downthrown side often dipping toward the fault surface (Fig. 68b). In some cases the direction of the dip reverses close to the fault forming a drag-syncline (Fig. 74). This overall geometry is an attribute of listric faults, the class of faults formed on a concave-up surface.

East-striking faulting has tilted the Richmond Gulf Group strata to dips of generally less than 20°, but many fault-blocks dip to the southwest (see Fig. 1, in pocket). The unconformably overlying

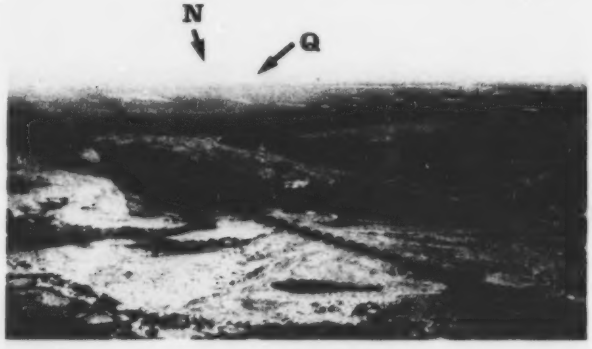

Figure 74. West-plunging drag syncline in Pachi (P) and Persillon (E) formations, formed on downthrow side of normal fault (dotted line) at south margin of Richmond Gulf Graben. Upthrown, drift-mantled Archean basement (A) is in foreground, and cliffs in distance are formed from west- dipping strata of Qingaaluk Formation (Q) overlain by the Nastapoka Group, 56°N, 76°25'W. (GSC 203265-E)

Nastapoka Group dips west at about 5° (Fig. 74, 75). Thus the southwest dip of the Richmond Gulf Group probably reflects a post-Nastapoka Group westward tilt superimposed on an earlier pre-Nastapoka southward dip acquired during graben formation. Visual inspection of the map in the pocket (Fig. 1) suggests that southwest-dipping blocks of Richmond Gulf Group strata are much more common than northwest-dipping ones. This may indicate that a large proportion of the faults affecting the group are downthrown to the north.

Folding is not a prominent feature of the Aphebian rocks of the region. In the Richmond Gulf Group it is restricted to gentle open synclines developed as a result of drag on fault surfaces (Fig. 74), draping over basement elevations (Fig. 70) or possibly a combination of the two causes as north of Persillon Lake. In the Nastapoka Group it is restricted to local outcrop-scale wrinkles and west-plunging anticlines formed over presumed extensions of basement horsts beneath the Nastapoka Islands (Chandler and Schwarz, 1980 p. 63).

Evidence from paleocurrents

Despite Woodcock's (1960, p. 27,29) claim that very little "false bedding" is present in the Pachi Formation but is characteristic of the Qingaaluk Formation, the writer found both trough and planar crossbeds to be abundant in both formations, particularly on the wave-washed bedding-surface exposures along the rocky shores of Lac Guillaume-Delisle. The trough crossbeds were used for the paleocurrent study (Fig. 76-78) because of ease of measurement (Fig. 79) and because of their generally observed low variance (High and Picard, 1974).

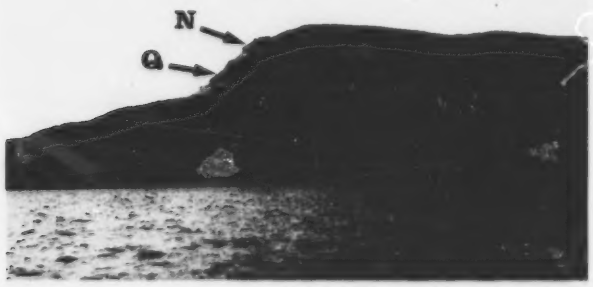

Figure 75. Gentle angular unconformity separating Qingaaluk Formation (Q) from gently west-dipping Nastapoka Group (N); looking south from Point Tikiraujaq toward 444 m high Collines Tursujuup Qaraalukgik. (GSC 203902-B)

In this study several dozen crossbeds could have been measured in many large outcrops, but it was found that after measurement of 5 or 6 examples no decrease in variance was gained by further measurement. In some cases a quick glance at the outcrop showed that all trough crossbeds had an orientation similar to within 10° or 20°. Therefore it was judged adequate to measure 5 or 6 crossbeds to have an adequate estimate of the flow pattern over a vertical stratigraphic distance of several metres.

The crossbed data were collected to discover direction of source areas, to help in paleoenvironmental analysis, i.e. to test for bimodality, a sign of marine tidal influence, and to aid in reconstruction of structural and tectonic

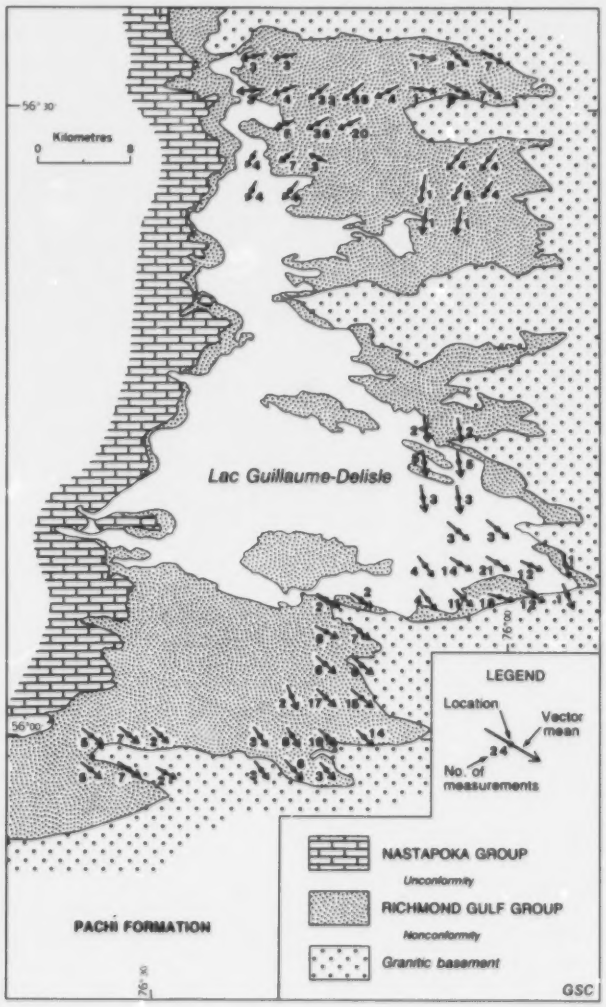

Figure 76. Paleocurrents, Pachi Formation, moving average compiled from trough crossbeds, based on 36 km² squares.

history, including the relative age of sedimentation and graben formation.

The transport directions of the sandstones were divided according to stratigraphic unit and summarized statistically by J. Maley using a computer program after Curray (1956). A moving average based on a grid of squares each 36 sq. km in area was constructed for each unit (Fig. 76-78). The flow directions based on leaning pipe amygdules (Fig. 13, 80) were measured at the base of the basaltic Persillon Formation.

The pattern from the Pachi Formation suggests a southeast-dipping paleoslope in the central and southern parts of the graben. In the north a more or less south-dipping fan-shaped pattern could have been caused by irregular topography. This view is supported by the marked thickness variation and lacustrine units in the north, both of which could be related to irregular topography.

Deposition of the Persillon Formation over almost the whole of the graben indicates that depressions in the topography had been largely filled at the end of Pachi time, although rare absence of the basalt unit suggests the presence of a few hills with elevations of at least 70 m, the thickness of the Persillon Formation.

The suggested smoothing of the topography is supported by the much more uniform paleocurrent pattern in the redbeds at the base of the Qingaaluk Formation (Fig. 77). Thickness variation of the basalt unit, 0-70 m, suggests that the volcanic unit may have also been instrumental in smoothing the

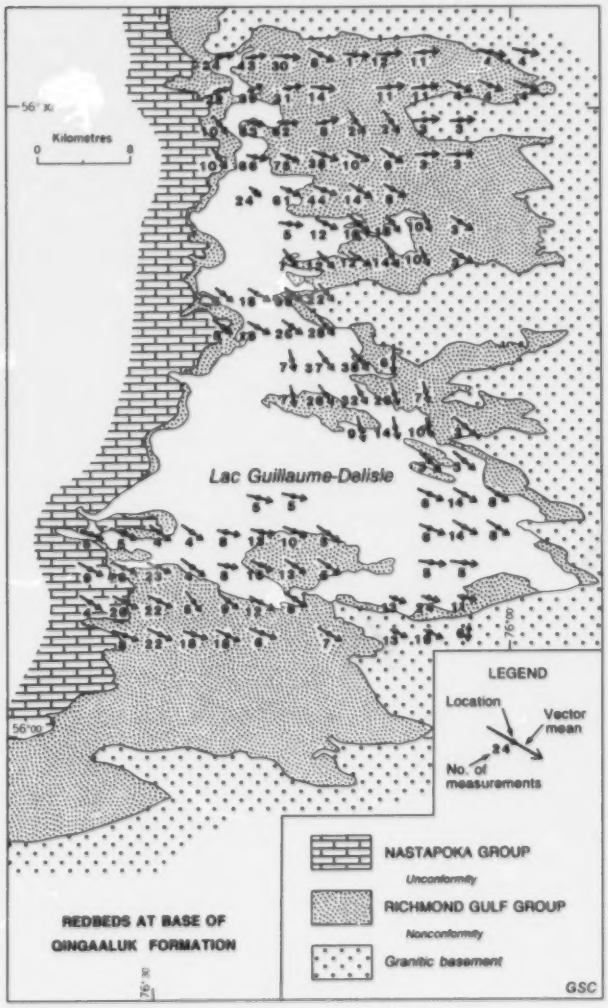

Figure 77. Paleocurrents redbed (2nd) member Qingaaluk Formation, moving averages compiled from trough crossbeds, based in 36 km^2 squares.

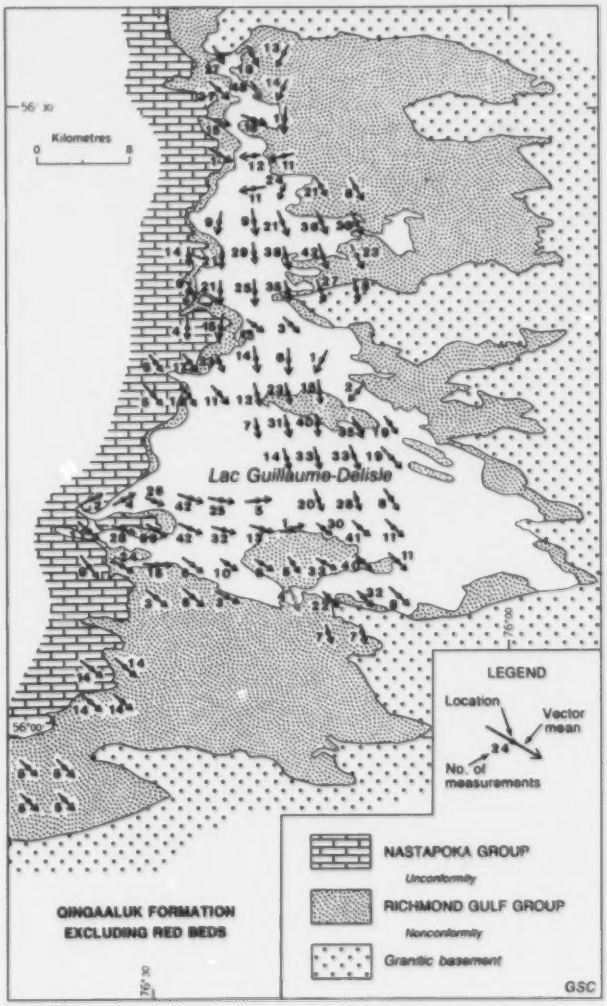

Figure 78. Paleocurrents arkosic 3rd member, Qingaaluk Formation, moving average compiled from trough crossbeds, based on 36 km^2 squares.

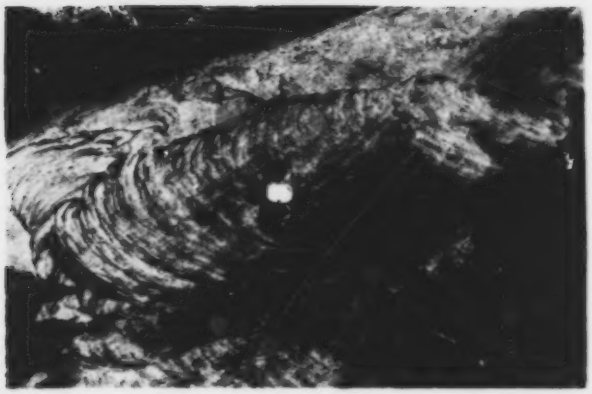

Figure 79. Trough crossbed in pink arkose of the 3rd member of the Qingaaluk Formation to show excellent preservation of these paleocurrent indicators. Laminae of oxide heavy mineral grains accentuate foresets and margins of troughs (56°24'24"N, 76°12'47"W; GSC 203263-U).

topography. The paleocurrent pattern of the redbeds at the base of the Qingaaluk Formation clearly shows a source area in the west. A similar pattern for the Persillon Formation, coupled with the composition of the Qingaaluk Formation redbeds, suggests that a granitic terrane was being elevated and was undergoing enough tension for basalt to have been extruded.

The paleocurrent pattern for the overlying bulk of the Qingaaluk Formation shows superimposition of southward flow in the northern half of the area. This may have regional significance (see Discussion) because of the northward thinning and pinch-out of the carbonates of the Nastapoka Group. Both of these data point to an elevation in the north.

Unimodality of the crossbeds coupled with mudcracked mudstone wisps throughout the two sandstone formations of the Richmond Gulf Group is an argument in favour of an alluvial mode of deposition rather than a tidal marine one. In a search for tidal influence in the mudcracked siltstone-rich redbed member of the Qingaaluk Formation paleocurrent measurements were made from current ripples (Fig. 81) with a ripple symmetry index greater than 4 (Reineck and Singh, 1980, p. 23,35) in three areas of outcrop at the north end of Lac Guillaume-Delisle. The measurements were compared with trough crossbeds from the same outcrops. Both troughs and ripples yielded similarly oriented strongly unimodal data as shown in a summary sketch (Fig. 82). Unexpectedly the spread of the ripple data is no greater than that of the troughs. The test shows that bimodality, a test of tidal influence appears lacking in these rocks. The importance of the paleocurrent patterns in establishing the time relation between graben

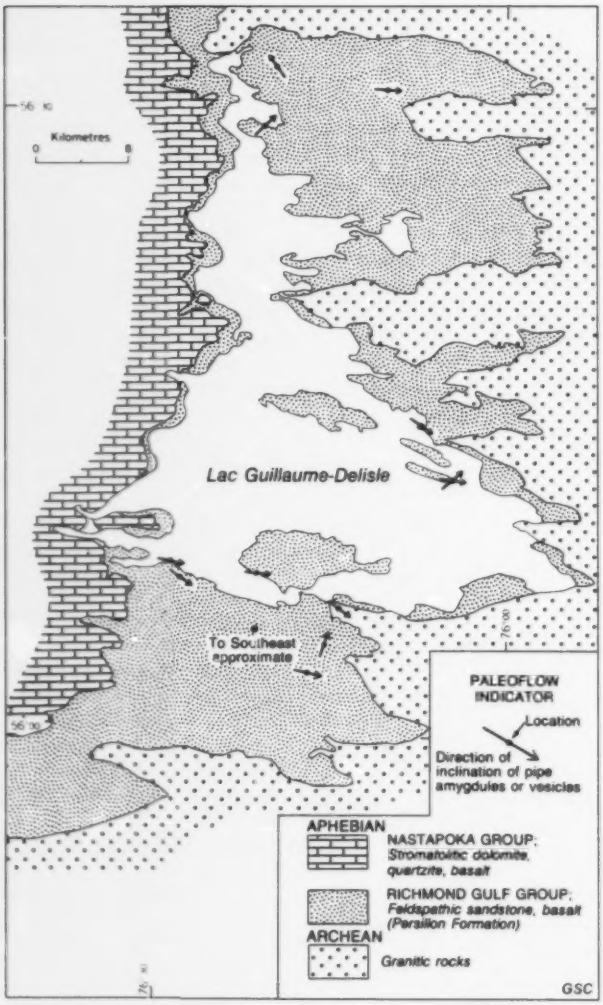

Figure 80. Flow directions of Persillon Formation, from leaning pipe amygdules and vesicles at base of flow unit (see Fig. 13).

formation and deposition of the Pachi and Qingaaluk formations is treated below under structure.

Using trough crossbeds the paleocurrent pattern of the Qingaaluk Formation was measured to within 100 m of the fault bounding the northern side of the central horst (Fig. 83), a west-plunging basement granite ridge that now rises to the south of the fault to an elevation of 200-300 m above the arkose of the Qingaaluk Formation. Figure 83 shows that paleoslope in these alluvial sands is to the south even to the foot of the present granite bluff, an unlikely orientation if the bluff were present during Qingaaluk sedimentation. As stated earlier, there is no granitic breccia or conglomerate facies either in the Pachi or in the Qingaaluk Formation of any

significance, certainly none is developed adjacent to any fault. This general statement holds for this locality also. In the area shown on Figure 83 conglomerate-free Pachi arkose, and overlying Persillon Formation basalt, show that the horst was not being eroded locally during deposition of the Qingaaluk Formation. These data from paleocurrents, facies and stratigraphy together indicate strongly that the horst was not a source area, nor even elevated during deposition of the adjacent Qingaaluk Formation sand.

A similar relation between the downfaulted Richmond Gulf Group and elevated granitic basement exists at a major graben-bounding fault along the south shore east of Ile Cairn (see Fig. 1, in pocket). Here also there are no conglomerate or breccia facies but the paleocurrent data are less convincing because of the east and southeastward flow (Fig. 76, 77, 82).

One concludes from the above that the present elevation of the granitic shoulders of the graben and of the granitic horsts did not exist during deposition of the Richmond Gulf Group.

Chandler and Schwarz (1980) noting, first, that the Richmond Gulf Graben strikes at a high angle into the Archean craton on the convex side of a salient on the Circum-Superior Foldbelt and, second, that the graben is earlier than associated mioclinal sediments (Nastapoka Group) proposed that the graben is an aulacogen related to the development of the foldbelt. Because of its west-derived arkosic composition and age the Richmond Gulf Group was interpreted as shed from a thermal dome to the west of the Belcher Islands. Absent from the sequence, however, is the alluvial sandstone that the aulacogen model (Burke and Dewey, 1973, p. 428) predicts would occur in the graben as it captures major continental drainage on sinking of the trailing edge continental margin, e.g. the modern Niger River or the Proterozoic Odjick Formation of the Athapuscow Aulacogen (Hoffman et al., 1974). But as mentioned earlier a section of unknown thickness overlying the Richmond Gulf Group was eroded before deposition of the mioclinal Nastapoka Group. Another deviation from the model is the absence of the bilateral symmetry of the mioclinal lens that forms during post-rifting downwarp (see Hoffman et al., 1974, p. 53). At Lac Guillaume-Delisle the Nastapoka Group thins northward, as seen both on the scale of a section across the gulf and on the scale of a section from Passe Manitounuk to the Hopewell Islands, a distance of 300 km (Ciesielski et al., 1983; Lee, 1965). In this connection should be remembered the southward component in some of the paleocurrent patterns of the Richmond Gulf group (Fig. 76, 78). Interestingly also Ricketts and Donaldson (1981) suggested a northern cratonic source on paleocurrent grounds for the arkosic Loaf Formation, the uppermost formation of the Belcher Group and one that some (Ricketts and Donaldson, 1981) feel is a molasse resulting from termination of the Wilson Cycle that formed the Belcher Foldbelt, the western side of the Circum- Superior Foldbelt.

If the Richmond Gulf Graben (Chandler and Schwarz, 1980) is an aulacogen, and the continental suture resulting from the relevant ocean closing lies about 150 km west of the Belcher Islands

Figure 81. Microtrough-crosslamination (rib and furrow marks), a section of current ripples in the bedding surface, second (redbed) member of the Qingaaluk Formation. As in Figure 79 foreset laminae and trough margins are accentuated by oxide heavy mineral grains. (56°41'47"N, 76°13'28"W; GSC 203902-O)

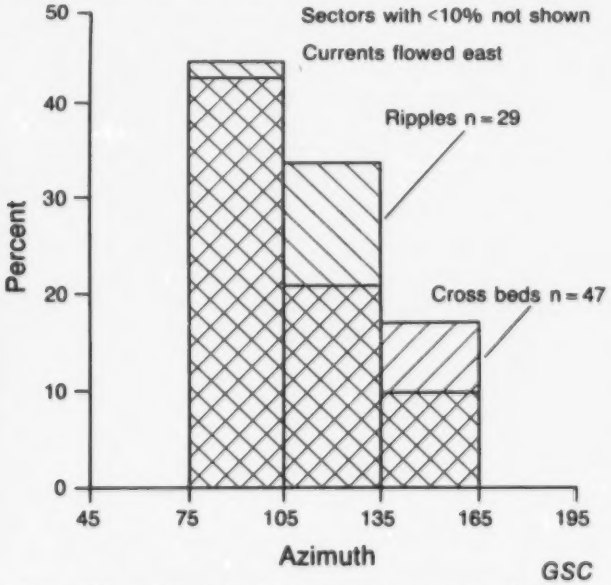

Figure 82. Comparison of some paleocurrent data from trough crossbeds and current ripples from the second (redbed) member of the Qingaaluk Formation, to show reliability of ripples as a paleocurrent indicator in this formation. See discussion in text.

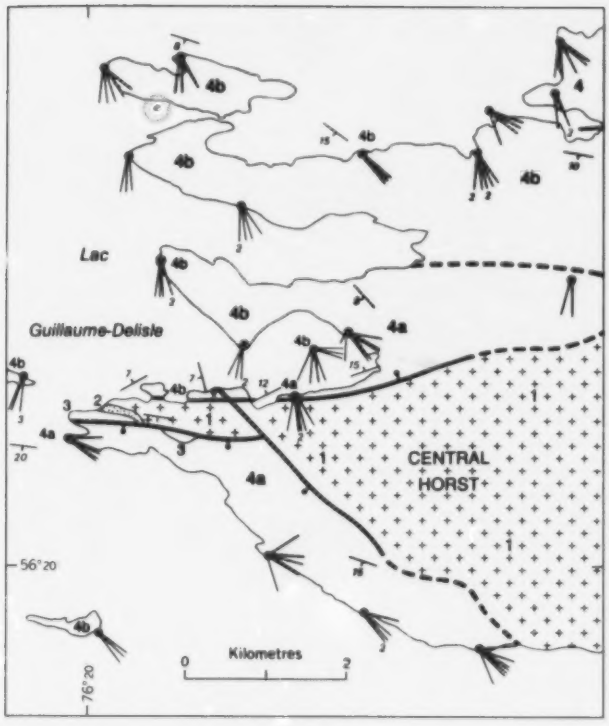

LEGEND

4 — 4b, pink arkose, (member 3) Qingaaluk formation; 4a, basal redbeds, (member 1, 2) Qingaaluk formation

2 — PACHI FORMATION

3 — PERSILLON FORMATION

Granitic basement

Bedding, tops known (inclined)

Fault (solid circle indicates downthrow side; defined, assumed)

Trough crossbed sampling point. Lines show individual measurement with eastward flow. "2" indicates two measurements with same direction

GSC

Figure 83. Detail from geological map (Fig. 1, in pocket) with added paleocurrent data to show lack of effect of present granitic basement horst on fluvial paleocurrent trend of Qingaaluk Formation. Data indicate absence of horst at time of sedimentation of Qingaaluk Formation.

(Mukhopadhyay and Gibb, 1981), the simplest thermal doming model would have alluvial debris shed eastward from the updomed Archean craton centred west of the Belcher Islands before and during rifting. Some recent reconstructions of the Circum-Superior Foldbelt (Baragar and Scoates, 1981; Mukhophadhyay and Gibb, 1981) would have the belt pass from a point 150 km west of the Belcher Islands (site of the triple junction?) both west to the Thompson Nickel Belt and north to the west end of the east-striking Cape Smith Foldbelt via the Ottawa Islands (see Fig. 85).

Elevation of the Archean crust along this line of future rifting would impose a generally southeastward component of paleoslope. The segment of the line running from the Belcher Islands, north, then east through the Cape Smith Belt is closer than that part to the west of the Belcher Islands and ought to have had a dominant effect on the Richmond Gulf Group paleoslope. The eastward curvature of this segment of the belt through the Cape Smith Belt should have added a strong southeastward component to the paleoslope of the time. Thus the south-dipping component of the Richmond Gulf Group paleocurrent pattern can be reconciled with placing a thermal dome due west of the Belcher Islands.

Geochronology

Previous attempts to date igneous and sedimentary rocks from the Lac Guillaume-Delisle region (Hews, 1976) and the Belcher foldbelt (adjacent part of the Circum- Superior Foldbelt) by both the K-Ar and Rb-Sr methods (Jackson, 1967; Fryer, 1972) have yielded results in the range 1620-1800 Ma as well as a more diffuse group of ages in the range 830-1300 Ma, the latter very likely the result of resetting.

It has been suggested (Ricketts and Donaldson, 1981) that the Belcher Foldbelt formed by a Wilson Cycle, an event that in this case might have a duration of three hundred million years (Chandler, 1984). Some of the 1800 Ma ages (Fryer, 1972) are from rocks which have been interpreted to have formed during later parts of the Wilson Cycle (Ricketts and Donaldson, 1981), an idea with opponents (Baragar and Scoates, 1981). The Richmond Gulf Graben is a structure that could have formed during an early tensional phase of this Wilson Cycle (Chandler and Schwarz, 1980) and therefore ought to be somewhat older. It is significant that the oldest dates obtained from the rocks at Lac Guillaume- Delisle (Hews, 1976; Esquevin and Menendez, 1973) are also about 1650-1800 Ma and that this age broadly coincides with the so-called Hudsonian Orogeny, a widespread event that affected the adjacent Churchill Structural Province (Stockwell, 1982). On this basis it was thought likely that the rocks of Lac Guillaume-Delisle were updated. This thought supports Burke and Dewey (1973) who pointed out assumedly rift-related mafic dykes in the Archean Superior craton adjacent to the possible junction of the Cape Smith Belt and the Labrador Trough that have a K-Ar age of about 2.1 Ga and is supported by the 2.15 Ga (Rb-Sr) age of mafic volcanic rocks at the southern

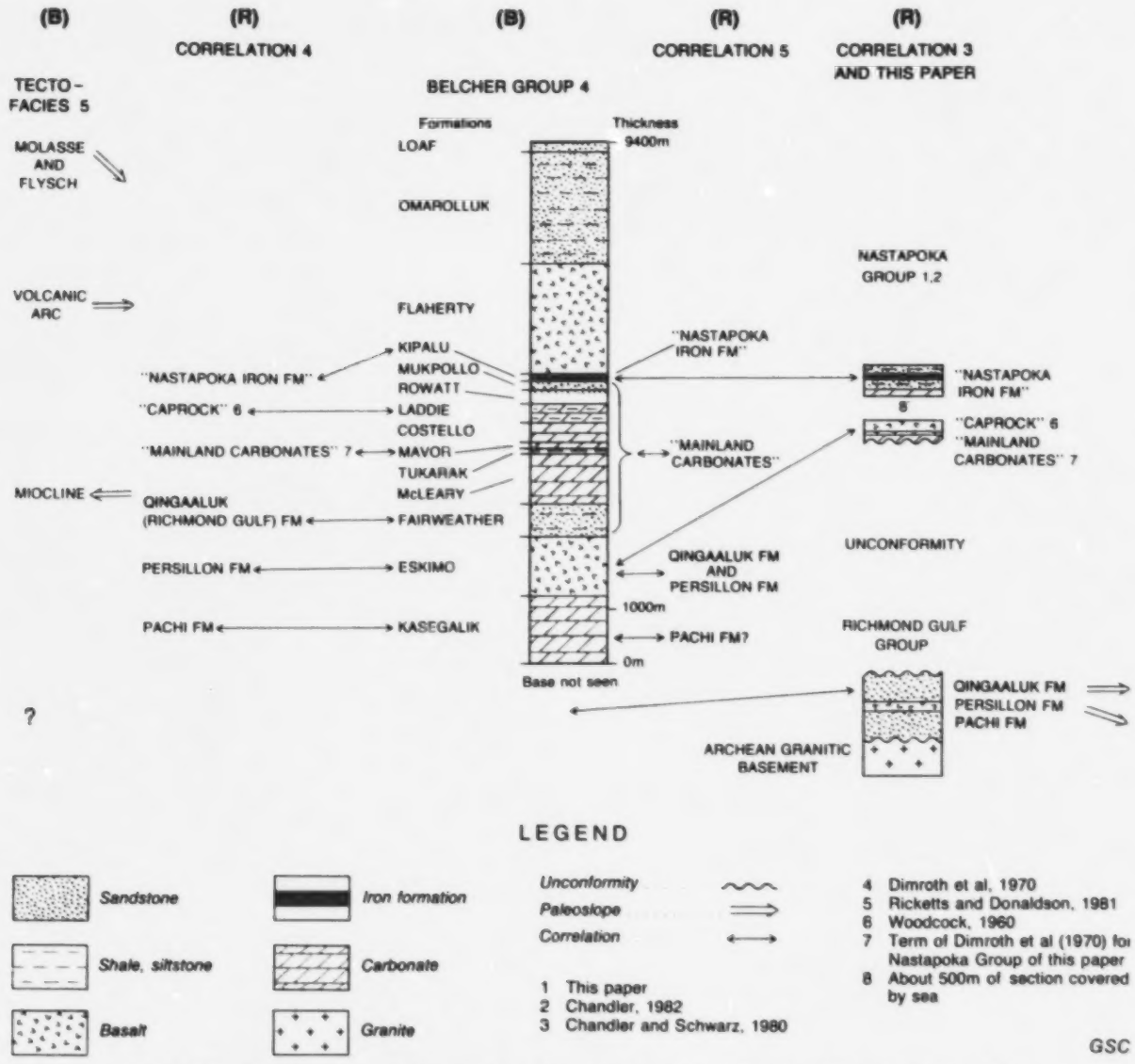

Figure 84. Stratigraphic correlations of the Aphebian supracrustal rocks of the east Hudson Bay region, Richmond Gulf Graben (R) and Belcher Islands (B).

edge of the Cape Smith Belt (Schimann, in Baragar and Scoates, 1981).

With this in mind the writer sought older Aphebian ages from the igneous and sedimentary rocks of the Richmond Gulf Graben (see map, Fig. 1, in pocket). An attempt to date fine grained clastic sediments of the Pachi and Qingaaluk formations (Rb-Sr, whole-rock) gave ages of 1610 ± 208 Ma and 1748 ± 52 Ma respectively, similar to those obtained by Esquevin and Menendez (1973) and Hews (1976) respectively from argillites in the Lac Guillaume-Delisle area. Because the greater of Chandler and Schwarz' (1980) two ages comes from the overlying unit of the two dated it is likely that one of these ages at least is not original.

By the K-Ar whole-rock method, igneous rocks of Lac Guillaume-Delisle gave the following K-Ar ages. The Wiachuan Sill gave 1711 ± 42 Ma and 1787 ± 101 Ma and mafic dykes cutting the Richmond Gulf Group yielded 1548 ± 60, 1654 ± 46 and 1801 ± 55 Ma. Thus the writer has been unable to penetrate the presumed Hudsonian overprint that has affected the rocks of the area.

In conclusion, the timing of tectonic events around the Circum-Superior Belt is poorly

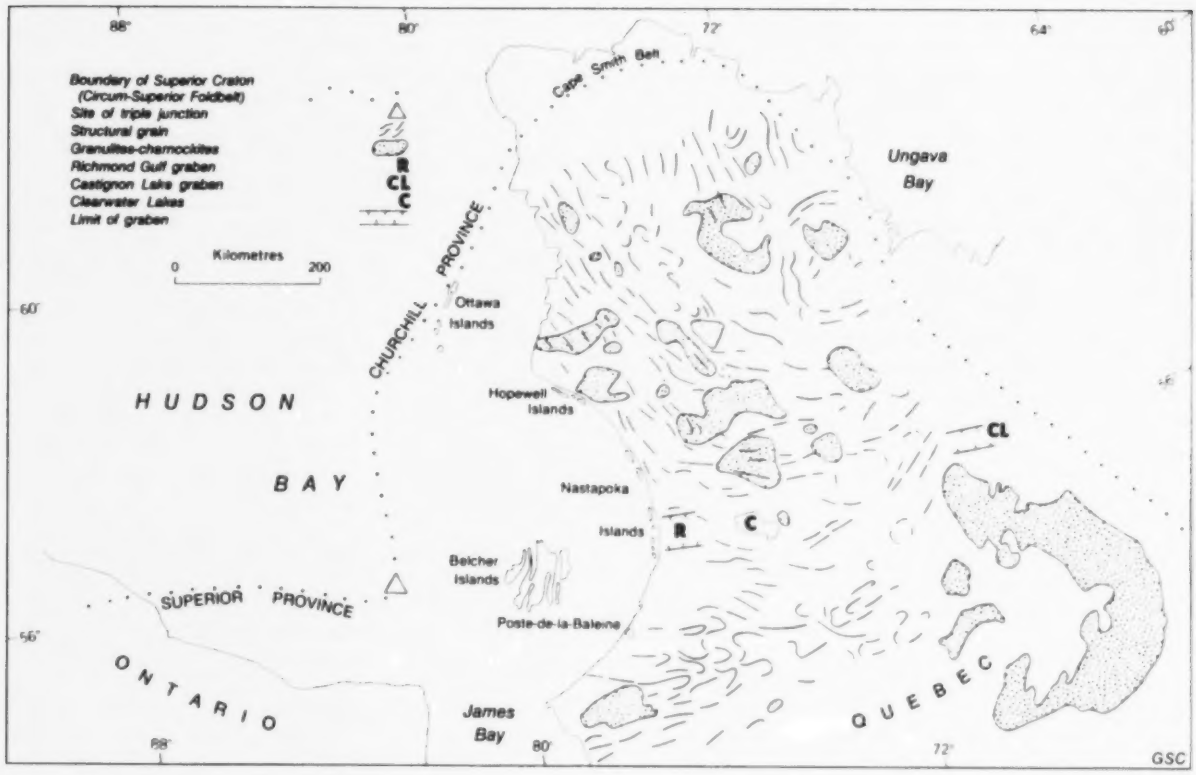

Figure 85. Some major structural elements of the northeast Superior Structural Province and adjacent areas, after: (1) Baragar and Scoates (1981), Mukhopadhyay and Gibb, (1981), (2) Stockwell (1969) and (3) Douglas (1969).

understood. A situation that hampers greatly understanding of these rocks. Hudsonian ages around the belt (Fryer, 1972) probably fix the end of these events at about 1.8 Ga. However the commencement of these events is not yet dated. Both Burke and Dewey (1973) and the writer (Chandler, 1984) have suggested that initial rifting might have occurred about 2.1 Ga. That such an event is at least this old is suggested by the 2.15 Ga date from the Cape Smith Belt and by a zircon age of 2.142 +4, -2 Ga (personal communication, T. Krogh, 1984) from rhyolite in the basaltic eugeosynclinal Mistamisk Formation at Lake Colombet at about latitude 57°N in the Labrador Trough (B. Dressler, personal communication, 1984; see also Dressler, 1979).

Mineral occurrences

Mineral occurrences in the Lac Guillaume-Delisle area (Fig. 1) have been the object of intermittent attention, but none is at present economically viable. As mentioned in the introduction to this report Chandler (1984) has endeavoured to fit them within a tectonic framework. He divided the Aphebian rocks of the eastern Hudson Bay region into three tectosomes, that is associations of rocks each characterized by a distinct tectonic regime during formation. They were as follows: thermal doming-related arkoses, downfaulted into the later Richmond Gulf Graben (Richmond Gulf Group); the mioclinal sequence of carbonates and quartzites (Nastapoka Group); and the convergence-related flysch-molasse sequence. This last sequence is best represented in the upper part of the Belcher Group in the Belcher Islands 120 km to the west of Lac Guillaume-Delisle, and only the basal parts remain on the coastal islands on the east shore of Hudson Bay.

Apatite and sedimentary copper in the Richmond Gulf Group

An occurrence of redbeds cemented by apatite and quartz was found (Chandler, 1984) at the base of the Richmond Gulf Group. Within the mioclinal

carbonates occurs at least one horizon of galena-sphalerite mineralization. Within both the Richmond Gulf Group arkoses and the overlying carbonates of the Nastapoka Group close to the unconformity separating them occurs disseminated chalcopyrite and traces of erythrite. Pyritization of all units occurs immediately beneath the unconformity and bleaching of the arkose is well developed also at this level. A higher part of the mioclinal sequence is well exposed on the offshore Nastapoka Islands, 3.5 km off the mainland coast in Hudson Bay, on Belanger Island (Chandler, 1982). It consists of marine quartzite and siltstone capped by iron formation associated with a rhodochrosite bed 60 cm thick. The iron-manganese unit is probably equivalent to thicker iron formation (Kipalu Formation) in the Belcher Islands and occurs at the transition from mioclinal sedimentation to the convergent tectonic regime.

Because available information on these mineral occurrences is already published elsewhere, what follows is a brief summary and introduction to the salient literature.

The apatite in the Richmond Gulf Group, together with quartz and hematite, cements a basal subarkose of the Pachi Formation. It is of unknown extent because it was discovered during petrographic examination of a grab sample. The occurrence is unusual because of its age and in that most sedimentary apatite deposits are believed to have been deposited under reducing marine conditions, whereas in this case the host rock is oxidized and is believed to be alluvial in origin. This type of occurrence may yet prove to be fairly common because very recently other Proterozoic apatite-cemented redbeds have been discovered in Canada (Chandler, 1984).

Available information on the disseminated copper mineralization at the base of the Nastapoka Group has been summarized by Chandler (1984) who as well as Stevenson (1968) noted several occurrences in the cliffs along the west shore of the gulf both in feldspathic sandstone at the top of the Qingaaluk Formation and in laminated dolomite (member B) at the base of the unconformably overlying the Nastapoka Group. Erythrite fracture coatings were found in the latter type of occurrence.

These occurrences are interpreted to occur in a failed arm. Raybould (1978) felt that mineralization was caused by thermal effects of the rifting. In the Lac Guillaume-Delisle area uplift, erosion of the Richmond Gulf Group and deposition of mioclinal carbonates, the latter dependent on removal of the area from the thermal anomaly related to rifting, all intervened between rifting and copper sulphide formation, so Raybould's (1978) idea is probably not applicable in this case.

At present the writer envisages the following model for the formation of the copper occurrences. Erosion of the subaerial basalt of the Persillon Formation that underlies the Qingaaluk Formation yielded basaltic debris to the basal part of the Qingaaluk Formation (Fig. 23, 27). Unlike the case of many Proterozoic copper deposits which occur at the boundary between redbeds and overlying marine carbonates, e.g. Ruelle (1982), there is no convincing evidence of a dry climate or the evaporites which it would give rise to, unless the lead-bearing zone (member F) is a solution-collapse breccia. Thus the abundant evaporite-derived chloride ion invoked by many as a contributor to the mobility of copper in redbeds (Rose, 1976) was probably not available.

A depositional site for the metal is not lacking. It exists in the form of a thick (up to 200 m) bleached pyritic zone in the Qingaaluk Formation immediately beneath the Nastapoka Formation carbonates. It is a mappable unit and was recorded as such along the northern half of the west shore of Lac Guillaume-Delisle (Chandler, 1979). Similarly, clearly biogenic carbonates of the lower biolaminite at the base of the Nastapoka Group, represent an obvious site for formation of reduced sulphur species by organic sulphate reduction. It is very likely that downward migration of these reduced sulphur species into the underlying black sand- bearing Qingaaluk Formation formed the pyritic zone by sulphurization of the black sand grains (Chandler, 1984, Fig. 4f).

It would seem that if causes for the poor development of copper mineralization at Lac Guillaume-Delisle are sought, one might be the apparent absence of evaporites and the hot dry climate that commonly leads to them.

Weathering of basaltic volcanics during the formation of alluvial redbeds and later oxidizing diagenesis may be important in contributing much of the copper to redbed- copper deposits. Although the first process clearly affects the Persillon Formation the amount of basalt in the sequence is not great. But it should be mentioned that less basalt appears to be associated with the copper deposits of the Redstone Copper Belt (Ruelle, 1982, p. 704). Also, apart from its basal member which is a detrital redbed, the bulk of the Qingaaluk Formation is not strongly oxidized. This suggests that extensive migration of oxidized solutions between the Persillon Formation and the site of the mineralization has not occurred.

Lead-zinc in the Nastapoka Group

Sphalerite and argentiferous galena in carbonates of the Nastapoka Group were reported by Bell (1879) in a 7.5 m thick band traced 80 km from Lac Guillaume-Delisle south to Passe Manitounuk. Stratigraphic sections including the band were published by Low (1902). Parks (1949) noted an upper mineralized bed 1.5 m thick and a lower one 2.5-25 m thick in which pyrite had replaced stromatolites and vugs were lined with quartz and carbonate.

At the southwest corner of Lac Guillaume-Delisle the algally laminated Nastapoka Group carbonates are about 100 m thick. Features listed above indicate a periodically exposed peritidal regime (see also Chandler, 1982). Sixty-five metres above the base of the carbonates a 12 m thick pyrite-rich zone is centred on unusually rich stromatolite development. Distinctive branched digitate stromatolites (Fig. 61) are restricted to the strongly brecciated (Fig. 59) and markedly cavernous middle 5 m of the zone, which from the presence of disoriented blocks (Fig. 60) of stromatolitic dolomite, is probably of collapse origin. Although evidence of evaporite minerals was sought none was found. The middle part contains disseminated and cavity filling galena and sphalerite, and abundant vitreous drusy quartz and white dolomite crystals. Mudcracks in the upper part of, and within 8 m beneath, the mineralized zone are evidence of exposure during deposition of the host carbonate.

The richest mineralization (Fig. 1) forms three ore bodies over the southern part of the graben (Chandler, 1984, Fig. 3), the Ruby Lake Deposit at 525 000 t of 1.26% Zn and 1.02% Pb; the Nancy Island Deposit at 267 000 t of 2.15% Zn and 0.72% Pb and the Monte Lake Deposit with 120 000 t of 1.75% Pb and some silver (Franklin and Thorpe, 1982; Chandler et al., 1982). The relation of the lead-zinc-bearing zone to the apparently unmineralized, presumably karstified, carbonate of the Belcher Islands and the Sutton Ridges is unknown.

Iron formation and manganese in the Nastapoka Group

Superior-type iron formation up to 125 m thick (the Kipalu Formation) occurs in the Belcher Group (Young, 1922; Jackson, 1960; Ricketts and Donaldson, 1981) and is broadly correlative with the iron formations of the Labrador Trough. Thinner iron formation with associated manganese occurs on the islands margining the east coast of Hudson Bay (Bell, 1879; Low, 1902, 1903; Lee, 1965) and in the Sutton Inlier west of James Bay (Bostock, 1971). Ricketts and Donaldson (1981) divided the iron formation in the Belcher Islands into micrite and argillite facies, both interpreted as deep water deposits, and a granular facies deposited in shallow agitated water. A steel blue weathering noted on the argillite facies may indicate a significant manganese content.

A detailed composite section of the thinner stratigraphic equivalent, 7 m thick at Belanger Island, one of the Nastapoka Group 120 km east of the Belcher Islands opposite Lac Guillaume-Delisle, was examined by Chandler (1982). The iron formation lies near the top of an upward- fining 200 m section of possibly storm-influenced tidal marine quartzite and siltstone. The iron formation itself was deposited as ripple-bedded magnetite-quartz-minnesotaite granules, separated by drapes of fine grained magnetite. These structures suggest periodic deposition of the granules by weak traction currents in a deepening suspension- dominated environment (Chandler, 1982, 1984).

From the vast literature on Precambrian iron formations (Eichler, 1976; Semenenko, 1973; James and Sims, 1973) emerge two major views on the source of the constituent iron and silica. From the common association of volcanic rocks with Archean iron formations it is generally agreed that volcanism is a likely source for these elements (Beukes, 1973; Goodwin, 1973). The tenuous (Gross, 1973) or cryptic (Gole and Klein, 1981) association of many Proterozoic iron formations with volcanic rocks prompted division of Precambrian iron formations into Algoma (Archean) and Superior (Proterozoic) type (Gross, 1965), and lent credence in the latter case to a lateritic weathering origin for the iron (James, 1954; Sakamoto, 1950) under an oxygen-poor atmosphere (Drever, 1974) or oxygeniferous atmosphere (Alexandrov, 1955). Other variants of the nonvolcanogenic model have been presented by Lepp and Goldich (1964), Windley (1977) and Govett (1966).

Moore (1918) advocated a weathering hypothesis for the iron formation (Kipalu Formation) of the Belcher Islands. Leith (1910) regarded equivalent iron formation in the Nastapoka Islands as derived ultimately from a basaltic volcanic unit lying about 200 m beneath it ("caprock" of Woodcock, 1960; unit 7, in Fig. 1) in the Nastapoka Group. He regarded the intervening clastic rocks as fragmental material, however, much of this sandstone is quartz arenite and abundant microcline is present among the feldspars. Ricketts and Donaldson (1981) favoured a restricted-basin model for the Kipalu Formation, considering tuffs in the upper part of the formation to be genetically unimportant.

If the lateritic weathering hypothesis were correct for this iron formation, one would expect other iron formations somewhere in the 6-9 km thick Belcher Group and in the several hundred metre thick Richmond Gulf and Nastapoka groups, which

together represent a wide range of depositional environments. There are two possible examples. One would be Low's (1902) iron formation at Lac Guillaume-Delisle. But this probably is not an iron formation but is the basal redbed of the Qingaaluk Formation, derived from subaerial weathering of the basaltic Persillon Formation. The other example is 1 m of granular lean iron formation immediately above the up to 900 m thick subaerial basaltic Eskimo Formation in the Belcher Group (Dimroth et al., 1970; Ricketts, 1979). This may have a similar origin. The presence of diagenetic and other redbeds on the earlier Pachi Formation indicated that red weathering products are possible, although those seen by the writer at Lac Guillaume-Delisle are quite different from iron formation. Wide areal extent of the iron formation in Hudson Bay (8500 km2, Ricketts and Donaldson, 1981) and association with quartzite, carbonate and argillite on a wide continental shelf, are attributes of a Superior-type iron formation (Gross, 1965). Yet several writers (Bell and Hofmann, 1974; Ricketts and Donaldson, 1981; Baragar and Scoates, 1981) have pointed out that the Kipalu Formation and equivalents, in widely dispersed parts of the Hudson Bay region (Bostock, 1971; Dimroth et al., 1970; Bell, 1879; Low, 1903) lie at the boundary between an underlying miogeosynclinal and an overlying eugeosynclinal sequence. In the Belcher Islands, where this sequence is thickest and most complete, the iron formation is directly overlain by upto 2 km of possibly arc- related basalt, volcanogenic turbidites and contains tuff (Ricketts and Donaldson, 1981), all characteristics of an Algoma-type iron formation.

Gross (1973, 1980) thought that Precambrian iron formation is of volcanic-exhalative origin, that near-surface water circulation transported much of the silica and iron, and that the apparent distinction between Algoma and Superior- type iron formations is due to operation of one set of hydrothermal processes in different sedimentary environments, an idea taken up by Gole and Klein (1981). Thus these difficulties in deciding between the Algoma and Superior type are resolved if the iron and silica are regarded as produced hydrothermally and transported into a range of sedimentary-tectonic environments by large scale marine currents.

The volcanic exhalative model for the genesis of Precambrian iron formation is receiving support from current work on sulphur isotopes (Cameron, 1983) and from work on mid-ocean ridges (Bolger et al., 1978; Corliss et al., 1979; Rona, 1980) which shows that hot springs on the ridges are a substantial source of sedimentary silica, iron and manganese. The Kipalu iron formation and the overlying volcanic Flaherty Formation thicken to the west; further the Flaherty was derived from the west (Dimroth et al., 1970). It may be of some significance that 150 km west of the Belcher Islands lies the postulated continental suture (Mukhopadhyay and Gibb, 1981) along which lies the Circum-Superior Foldbelt. But although the above argues for a volcanic-exhalative origin for the Kipalu and correlative iron formation, some of the data suggest a rifting environment, a point made generally by Burke and Dewey (1972) who thought that iron formation ought to be related to accreting plate margins because a tensional tectonic environment would permit easy movment of fluids. This conclusion was applied to the Kipalu Formation by Baragar and Scoates (1981) from their review of the regional geology of the Circum-Superior Belt.

But Ricketts and Donaldson (1981, p. 235) viewed the Belcher Supergroup as consisting, in sequence, of miogeocline, flysch and molasse with the volcanic rocks associated with the iron formation of arc origin. Clearly, for metallogenic modelling, it is important to decide the role of rifting and compressive tectonics in the genesis of this and by extensions other Proterozoic iron formations. Thus an important contribution would be to clarify the tectonic environment of the Flaherty Formation (see also section on Aphebian regional tectonics and correlation with the Belcher Foldbelt).

Although many accept Proterozoic iron formation to be marine in origin, Eugster and Chou (1973), Govett (1966) and Sakamoto (1950) developed lacustrine models. Sedimentary structures in clastic rocks associated with the iron formations in Hudson Bay support a marine depositional environment.

The paucity of Proterozoic-type iron formations younger than about 1.8 Ga, the occurrence of presumably detrital pyrite and uraninite, and the rarity of substantial redbeds in the Early Proterozoic suggested to Cloud (1972) that these iron formations were formed by transport of iron under an oxygen-free atmosphere. The rarity of such deposits after 1.8 Ga was caused by sudden biogenic oxidation of the ocean that swept it free of ferrous iron and curtailed the surface transport of iron (Goldich, 1973) and led to a peak of development of iron formation about that time (Cloud, 1968; Eriksson and Truswell, 1978). This hypothetical peak is becoming less apparent as some iron formations are being discovered to be significantly earlier (Gole and Klein, 1981). Also oxygenation of the atmosphere at about 1.8-2.0 Ga has its critics, e.g. Clemmey (1982). Further Dimroth and Kimberley (1976) have presented evidence of an oxygeniferous Archean atmosphere, as well as of redbeds in the Labrador Trough older than the iron formations of that region. Formation of hematite in redbeds of the Pachi Formation and formation of a 6 m thick red weathering zone on the Persillon Formation predate the iron formation of Hudson Bay and occurred a

possible 200 Ma before it, if Boillot's (1981) estimate of the evolution of passive continental margins is correct. These data indicate an oxygen-bearing atmosphere before the formation of the Kipalu and equivalent iron formations.

Discussion

Aphebian geological history of the Richmond Gulf Graben

Alluvial arkose of the Pachi Formation was transported from a granitic source in the west and north. It was deposited on the Archean granitic craton on the west coast of New Quebec in the Lac Guillaume-Delisle region on a little- weathered basement of some relief. Evidence of relief includes a scattered paleocurrent pattern (Fig. 76), thickness variation in the Pachi Formation, presence of lacustrine units only in the northern part of the area, and local exposure of granitic basement during deposition of overlying units. Slopes were probably gentle as is suggested by the thin and patchy distribution of basal conglomerate, certainly not fault scarps which would have shed breccia and conglomerate close to the now visible major faults.

Limited data suggest a paleoslope dipping to the east at the time of extrusion of the conformable Persillon Formation (Fig. 80). Its widespread occurrence indicates subdued topography, but local absence of the basalt points to a relief of at least 70 m, the thickness of the flow unit (Fig. 28). The Persillon Formation is normally conformable on the Pachi. Rare bodies of sand, but no previously lithified sandstone clasts, were incorporated into the base of the volcanic unit. A generally massive base, rare pillow-like structures and some pipe amygdules indicate that the surface of the Pachi alluvial plain was generally dry, but was locally damp and supported small water bodies at the time of Persillon basalt basalt extrusion. Reddening of some flow tops, and presence of local interflow mudcracked clastic sediments, in one case 14 m thick, are evidence of significant time lapse between outflows. The generally massive nature of the flow unit, position between two alluvial sandstone formations, the mudcracked interflow clastics and red weathering at the top of the unit, all point to a subaerial environment of extrusion.

The red weathering zone on the surface of the unit has isolated by spheroidal weathering (Fig. 19) mature-looking boulders from the otherwise rather cryptic columnar jointing of the basalt. These clasts together with blocks (Fig. 23) form a lag conglomerate, commonly no more than a metre thick, that Woodcock (1960) took as evidence of a phase of faulting and formation of an unconformity separating the Persillon and Qingaaluk formations. Such a phase ought to have stripped the Persillon Formation and yielded fault talus from available units, but no such record was seen by the writer. Instead, because of the conformable relation of the Pachi, Persillon and Qingaaluk formations, the lithological similarity of the two sandstone formations, and the undisturbed Richmond Gulf Group paleoslope, it is felt that the extrusion of the Persillon Formation represents merely an eruption onto an otherwise tranquil alluvial plain, the monotony of which was broken locally by granite hills. The presence of such basement monadnocks is inferred from local granite boulders in the overwhelmingly basaltic conglomerate overlying the Persillon Formation. One such hill in existence during Qingaaluk time is visible at the outlet of the Gulf (Fig. 70).

The Persillon Formation and its thin conglomerate mantle of "core-stones" and blocks was covered by alluvial arkose shed from a source more obviously in the west. The greater simplicity of the paleocurrent pattern of the 80 m thick redbed unit at the base of the Qingaaluk Formation (Fig. 77) could be related to a progressive smoothing of the topography. The basal part of the formation is coloured deep maroon by fine grained debris shed from the immediately underlying weathered basalt and as such is an example of an early Proterozoic detrital redbed.

Deposition of the Qingaaluk Formation continued with increasingly pebbly sandstone, a trend perhaps stronger in the south of the area. This coarsening-upward trend is also weakly shown in the Pachi Formation. Clasts continue to be composed of granite and quartz.

The uppermost preserved unit of the Qingaaluk Formation is a beach grit and tidal marine sandstone that is preserved in a gentle syncline in the east-facing cuestas on the west shore of Lac Guillaume-Delisle. This unit reflects the first depression and marine flooding of the area recorded in the Richmond Gulf Group.

The Richmond Gulf Group lies at present in a graben. The question arises; was the group deposited in the graben or was it part of a more extensive sheet of arkose and basalt preserved from erosion by being dropped into a structure that formed later? The group is extensively cut by east-west normal listric faults, a common fault style of graben- formation (Illies, 1981). There is no evidence of post- Archean faulting other than that affecting the whole group. No coarse clastic facies of the arkoses occur near any graben-bounding or host-margining faults. Nor are paleocurrent patterns affected by any of these faults. Therefore one must conclude that the graben was formed after deposition of the Richmond Group.

Mafic dykes, dominantly east-striking, associated possible diatreme breccia and mafic sills are present in the Richmond Gulf Group. These coincide with an east-trending positive gravity anomaly (Gibb et al., 1983) in the axial region of the graben. Some of the intrusives cut the Qingaaluk Formation and many are offset by the faulting discussed above, but none cut the excellently exposed overlying Nastapoka Group. Preservation of the marine tidal member at the top of the Qingaaluk Formation in a syncline, only in this region, points to maximum downwarp of the graben in this zone (Chandler, 1982, p. 2). These data argue that deeply reaching tensional stress, perhaps tapping the mantle, was focussed in the axial deepest zone of the graben after deposition of the Richmond Gulf Group and before the deposition of the Nastapoka Group.

The next event recorded is the uplift and erosion of the Lac Guillaume-Delisle area and creation of a locally jagged landscape (Fig. 49, Chandler, 1982, Fig. 1.6, 1.9) upon the Richmond Gulf Group in the graben.

Deposited on this surface (with gentle angular unconformity, Fig. 75) and upon the granitic rocks margining the graben (Fig. 72), carbonates of the Nastapoka Group record a second marine transgression and, on the basis of wide-ranging stratigraphic correlation (Chandler and Schwarz, 1980, Fig. 6.2), a widespread downwarp. Erosion of the Richmond Gulf Group at this unconformity raises the question of what unrecorded stratigraphic section might have been lost. There are no clasts in the thin conglomerates at the base of the Nastapoka Group that would suggest units different from those presently exposed. The overlying stratigraphic record is of much greater extent than the Richmond Gulf Group. It is continued in the Nastapoka Group, and its equivalent in the Belcher Islands, the Sutton Ridges of James Bay, and on the eastern shore and islands in eastern Hudson Bay (Dimroth et al., 1970; Ricketts and Donaldson, 1979; Baragar and Scoates, 1981). A consideration of the regional stratigraphic framework discussed by these authors brings one to the realm of tectonics, a subject of wider scope, more properly dealt with in the following section of this report.

Aphebian regional tectonics and correlation with the Belcher Foldbelt

Early views on the Aphebian tectonic evolution of the Circum-Superior Foldbelt in the Hudson Bay region are summarized by Chandler and Schwarz (1980). There are two groups of views on the nature of the tectonic cycle that gave rise to the foldbelt. One group involves rifting, formation of a significantly wide ocean and its collapse (Wilson Cycle; Chandler, 1984; Mukhopadhyay and Gibb, 1981; Ricketts and Donaldson, 1981; Wilson, 1968). The other (see also Taylor, 1982) accepts that rifting was involved, but no ocean, or at most an incipient ocean, formed, (Baragar and Scoates, 1981; Dimroth, 1981; Wardle and Bailey, 1981).

Both Chandler and Schwarz (1980) and Ricketts and Donaldson (1981) subscribe to the triple junction-Wilson Cycle model for the Belcher Foldbelt, but probably because the first two writers worked in the Lac Guillaume-Delisle area and the second two worked on the Belcher Islands, two variants of the model have emerged. The Richmond Gulf Group is regarded by the former writers as a pre-aulacogen west-derived thermal doming-related alluvium. The latter writers consider it an east-derived aulacogen-filling fluviodeltaic complex. The key factor separating the variants is which part, if any, of the Belcher Group is the sequence at Lac Guillaume-Delisle to be correlated with (Fig. 84).

The stratigraphy of the Belcher Group was first worked out by Jackson (1960; in Dimroth et al., 1970). Bell and Hoffman (1974) interpreted it in terms of a geosynclinal cycle, refined and couched later in plate tectonic language by Ricketts and Donaldson (1981). The model, given at its simplest, divides the Belcher Group into a sequence of three tectofacies; a west-facing mioclinal carbonate prism, a thick sequence of basalts of arc origin (Flaherty Formation) with reversal of paleoslope, and a southeast-transported volcanogenic flysch and cratogenic molasse (Fig. 84).

The earliest correlations between the Belcher Group and the Richmond Gulf and Nastapoka groups (Fig. 84) by Dimroth et al. (1970) were slightly modified by Ricketts and Donaldson (1981). The general correlation of most of the Belcher Group, i.e. the mioclinal carbonates and the overlying Flaherty Formation basalt and associated Kipalu iron formation, with partial homotaxial sequences around the south and east shore of Hudson Bay is at present widely accepted (Baragar and Scoates, 1981; Dimroth et al., 1970; Lee, 1965; Chandler and Schwarz, 1980; Ricketts and Donaldson 1981).

As mentioned above, important differences of opinion arise with correlation of the Richmond Gulf Group. Dimroth et al. (1970) believed the Richmond Gulf Graben to exist as an "embayment" during the deposition of the Kasegalik Formation, and the Pachi Formation to be a nearshore facies equivalent of the Kasegalik, even though the base of the Belcher Group is not seen and the two formations are of very different lithology. They correlated the Eskimo Formation with the Persillon Formation, partly because of the thin local iron formation believed to be present on these basalts. However Chandler and

Schwarz (1980, p. 64) felt the latter iron formation to be a detrital redbed unit formed by subaerial weathering of the Persillon Formation. It was logical for Dimroth et al. (1970) to correlate the Fairweather and Qingaaluk (Richmond Gulf) formations because of their stratigraphic positions, their differences in lithology being explained by facies variation.

The above correlations coupled with correlation of the Kipalu iron formation with that of the Nastapoka Islands (Chandler, 1982, Fig. 1, 8) by Dimroth et al. (1970) present a problem. With which unit should the up to 230 m thick basalt flows in the Nastapoka Group on the mainland, Woodcock's (1960) "caprock", be correlated? Dimroth et al. (1970) solved the problem as best they could by correlating it with argillite and quartzite in the Laddie Formation.

Ricketts and Donaldson (1981) were aware of the difficulties of correlating the contrasting lithologies described above over a distance of 120 km. Assuming the Richmond Gulf Group to have been deposited in an already present Richmond Gulf Graben as a west-facing fluvial-deltaic complex they (ibid., p. 250) saw difficulty in the absence of any arkosic material in the supposedly "offshore" carbonate Kasegalik Formation (ibid., p. 248). This was resolved by their suggestion that the Pachi Formation is perhaps older than the Kasegalik Formation, a relationship at variance with their Figure 14-7.

Ricketts and Donaldson (1981) equated the Persillon and Qingaaluk formations with the Eskimo Formation, even though concerned that the period of block faulting and erosion following the Qingaaluk at Lac Guillaume-Delisle appears absent from the mutually conformable Belcher Group. They resolved the difficulty by suggesting that arkose in the Fairweather Formation, overlying the Eskimo, came from erosion of the Richmond Gulf Group.

Ricketts and Donaldson's (1981) stratigraphic and sedimentological studies in the Belcher Islands led them to the postulate that the Richmond Gulf Graben is an aulacogen related to the Wilson Cycle that formed the Belcher Foldbelt, an idea independently derived by Chandler and Schwarz (1980) from their interpretation of the rocks at Lac Guillaume-Delisle. Rickett's and Donaldson's (1981) interpretation of the rocks at Lac Guillaume-Delisle led to the following conclusions. The Richmond Gulf Group formed by westward fluvial transport and deposition as a west-facing fluviodeltaic complex in the graben. Sedimentation commenced with the Pachi Formation that may have predated the Kasegalik Formation. Then came reactivation of the rift involving block -faulting, erosion, effusion of the Persillon Formation and continued progradation of clastics (Qingaaluk Formation) of the fluviodeltaic complex along the graben. The Nastapoka Group was correlated with the McLeary and later formations of the mioclinal part of the Belcher Group.

The writer's fieldwork at Lac Guillaume-Delisle requires a correlation and interpretation different from the above. As outlined earlier (Chandler and Schwarz, 1980) and indicated herein, the Richmond Gulf Group arkoses are older than the graben. Their facies and paleocurrent patterns convincingly preclude their interpretation as a fluviodeltaic complex developing westward along the graben. Correlation with any part of the internally conformable carbonate-rich mioclinal part of the Belcher Group is equally unlikely as an exposed granitic terrane is required to the north and west during deposition of the carbonates on the site of the Belcher Islands.

Given the above, it follows that the correlation of the Eskimo Formation with the Persillon Formation is also suspect. The volcanic unit in the Nastopoka Group (see Fig. 1, in pocket) was tenuously correlated with clastics of the Laddie Formation of the Belcher Group (Dimroth et al., 1970). Both this unit and the Eskimo Formation lie within broadly correlated mioclinal carbonate sequences and both are subaerial to very shallow water volcanic basalts. The writer (Chandler and Schwarz, 1980) has already suggested that a reasonable case exists for correlating the Eskimo Formation with the Nastapoka basalt ("Caprock" of Woodcock, 1960).

One difficulty with the Wilson Cycle model is the abundance of mafic and ultramafic igneous rocks and the paucity of calc-alkaline intermediate and felsic igneous rocks over much of the foldbelt (Baragar and Scoates, 1981). Baragar and Scoates would derive these mafic rocks during rifting, having them intrude and pour out over the mioclinal carbonates. But some Recent continental rift shoulders are elevated 1.2-3 km above sea level (Seidler and Jacoby, 1981, p. 56, 57). It is difficult to see how in a rifting environment a thickness of 2 km of mioclinal carbonate of the Belcher Group could have been deposited and preserved (Chandler, 1984). Also, it is hard to see why a foldbelt formed from tectonic processes involving only "possible initiation of subduction" (Baragar and Scoates, 1981) should choose to lie at the boundary of a craton of similar age and an earlier craton.

Thus one question that should be solved in establishing the correct model for the tectonics of the Belcher Foldbelt and, by extension, of the Circum-Superior Foldbelt is the tectonic significance of the thick mafic volcanics of the Flaherty Formation and of its equivalents.

Another important question (see section on iron formation and manganese in the Nastapoka Group) that awaits interpretation of the Flaherty Formation is that of a tectonic environment for the iron formation (Kipalu Formation and equivalents) which are widespread in the Aphebian sequence of Hudson Bay.

Chandler (1984) felt that the weight of evidence favoured a hydrothermal origin for the Kipalu and correlative iron formations. As noted above opinions favour both extensional and compressive tectonic regimes during the deposition of the Kipalu Formation. Hoffman (1981) observed that voluminous basaltic magmatism followed shortly after the foundering of the continental terrace of the 2.1-1.8 Ga Wopmay Orogen and was due to the ability of Proterozoic subducting lithosphere to release magma in trenches. Chandler (1984), because of the homologous tectono- stratigraphic position of the magmatism in both the Wopmay Orogen and in the Belcher Supergroup, suggested that this variant on the compressive model should be considered in modelling the genesis of the Kipalu iron formation.

Implications of the Richmond Gulf Graben for the Archean tectonics of northern Quebec

The Richmond Gulf Graben, striking east into the Archean craton of northern Quebec between latitudes 56 and 56°30'N, was interpreted by Chandler and Schwarz (1980) as an aulacogen related to the formation of the Circum-Superior Foldbelt.

To the east, on the other side of the craton at the same latitude, the Castignon Lake Graben strikes west from the Labrador Trough into the interior of the Archean craton. This graben was interpreted by Burke and Dewey (1973) as an aulacogen. It contains east-transported redbeds of the lower Seward Subgroup that tie it to the rifting phase of the Labrador Trough (Wardle and Bailey, 1981). Both the Richmond Gulf and Castignon Lake grabens have been interpreted as Aphebian. Chandler (1984) has speculated on a mid-Aphebian age for the former. If these two grabens that seem to strike into each other do indeed represent a failed attempt to rupture the Superior Craton along a line of latitude just north of latitude 56°N then the location of these grabens may indicate a major crustal dislocation or line of weakness along this line.

Examining the Archean geology of the Superior Craton on either side of this line, using Eade (1966) and Stevenson's (1968) one million-scale geological maps of northern Quebec, shows a general contrast on crustal composition (Fig. 85) across a line connecting Richmond Gulf and Castignon Lake grabens west at latitude 70°N. To the north a gneiss terrane contains abundant granulites. To the south, west of longitude 72°W massive granitic rocks are abundant in the gneiss terrane and granulites are sparse.

As shown by the tectonic map of Canada (Stockwell, 1969) this lithological contrast coincides with one in structural grain. To the north the grain strikes north and to the south, the trend is east. This structural pattern is brought out more clearly in the coloured aeromagnetic compilation maps of northern Quebec. Similarly the gravity map of Canada (Earth Physics Branch, 1980) shows a decrease in the Bouguer anomaly southward across northern Quebec, but the resolution of the map does not reveal a zone of high gradient to be identified that might be correlated with a crustal boundary.

The metamorphic map of Canada (Fraser et al., 1978) shows that retrograded granulites are abundant south of the limit suggested by Eade's (1966) and Stevenson's (1968) maps. R.K. Herd, compiler of that part of the metamorphic map (personal communication, 1982), puts little faith in the distribution of granulites shown by the metamorphic map owing to the absence of detailed magnetic maps for the region north of latitude 55°N during its compilation.

Of interest here is a pair of contiguous circular lakes 25 and 30 km across that lie on strike with Richmond Gulf Graben, about 125 km inland. The western lake contains a concentric ring of islands of dacite and volcanic breccia of Late Carboniferous age. Both cryptoexplosion and astrobleme hypotheses exist for the origin of these rocks, (Bostock, 1965).

It is a common view that cratons tend to rupture under stress along old lines of weakness (e.g. Illies, 1981, p. 251; Milanovsky, 1981, p. 216). An example of such a line is the Atlantic coast of North America which, over the last 1400 Ma, has been the margin of at least three oceans. The geological and geophysical maps discussed above indicate division of the Archean craton of northern Quebec into two subdomains with a boundary approximately along latitude 56°N. Formation of the Richmond Gulf and Castignon Lake grabens on this boundary could be explained as a mid-Aphebian attempt at rifting along this line of weakness during initial rifting on the Circum-Superior Foldbelt. If the Clearwater Lakes formed by cryptoexplosion rather than by meteorite impact their location on this already twice disturbed postulated zone of weakness is quite fitting.

If we accept that pyroxene-bearing granulites and charnockites generally represent formation at a deeper level in the crust than do pyroxene-free granites and granitic gneisses (e.g. granulites form at a depth of ca. 30 km, R.C. Newton, personal

communication, 1983), a boundary such as that discussed above could separate a deeply eroded northern terrane from a less eroded southern terrane. Inspection of Eade's (1966) map suggests, on account of the large zone of granulites to the east of the southern terrane, that the terrane had been up-tilted in the east. (see also Douglas et al. 1969, and Fig. 85). But when could this erosion of the northern terrane have taken place? Chandler and Scharz (1980) suggested that the Richmond Gulf Group alluvial arkoses were shed eastward from a thermal dome in Hudson Bay. Examination of three regional paleocurrent maps (Fig. 76-78) which, based on fluvial rocks, must also reflect paleoslope, demonstrates a significant component of southward flow in the paleocurrents. A second piece of information comes from the thickness variations in the Nastapoka Group across Lac Guillaume-Delisle. The carbonates thin northward and finally pinch out near the northern tip of Lac Guillaume-Delisle. This trend is also seen in the group as a whole as it is traced northward from near Poste-de-la-Baleine, about 100 km south of Lac Guillaume- Delisle (Ciesielski et al., 1983) to the Hopewell Islands, about 200 km to the north of Lac Guillaume-Delisle (Lee 1965). Over this distance the thickness of the sedimentary part of the Nastapoka Group diminishes from 400 m at the Neilsen Island drill hole to the Hopewell Islands where only 80 m of section, admittedly incomplete, represent the Nastapoka Group. But Lee's map (1965) suggests that the exposed 80 m is almost the complete section, if unfaulted. Lee (1965) suggested that the section is stratigraphically equivalent to the 5 km thick lower part of Belcher Group that lies beneth the Flaherty Formation basalts. The Neilson Island section on the other hand (Ciesielski et al., 1983) represents that part of the Nastapoka Group that lies beneath a volcanic unit (see map, Fig. 1, in pocket) correlated by Chandler and Schwarz (1980) with the Eskimo Formation of the Belcher Group, a volcanic unit some distance beneath the Flaherty Formation (Fig. 84). Near Richmond Gulf, in the Nastapoka Islands, at least 200 m of section lie above this second volcanic unit and beneath the equivalent of the Flaherty Formation, that has been eroded. Consequently that part of the Nastapoka Group of probably shallow marine sediment beneath the Flaherty Formation is considerably thicker (at least 600 m) in the region of Poste-de-la-Baleine and Lac Guillaume-Delisle than it is in the region of the Hopewell Islands to the north (ca. 80 m).

Thus the data from the Proterozoic Richmond Gulf Group suggest that a sedimentary source area lay to the northwest. The northward thinning of the overlying marine Nastapoka Group along the coast suggests greater downwarp in the south during deposition of the Mioclinal lower part of the Nastapoka Group. These data fit with the idea of erosion, during mid? Aphebian time, of a land mass to the north, and help to explain why a deeper crustal level appears to be exposed to the north of latitude 56°N than to the south.

Chandler and Schwarz (1980) and Burke and Dewey (1973) suggested that the Richmond Gulf and Castignon Lake grabens were connected with triple junctions that lay to the west and east respectively of the presently exposed grabens. If indeed these two grabens exploited a linear Archean zone of weakness that continued to the west and east beyond the present limits of the Superior Craton of northern Quebec, it is possible that this zone determined the site of the postulated triple juncitons as well as the related grabens.

If a major Archean crustal dislocation does trend across the Archean shield of northern Quebec at latitute 56°N what is its significance? Do the lithological and structural differences tell us that the craton has been ruptured and that the northern part has been elevated relative to the southern part which has been down-tilted to the northwest? Could the difference in structural grain mean that two originally separate terranes came together (collision?) during the Archean. Could the abundance of massive granitic rocks in the southern terrane indicate that some analogue of collisional reactivation occured in the southern terrane? Unfortunately the only geochronology available to the writer is of K-Ar type and yields only Kenoran ages over the whole region.

In order to resolve these intriguing questions perhaps an area transecting the proposed terrane boundary zone could be examined by mapping at a scale of 1:250 000. A north-south gravity traverse might reveal density or thickness contrasts across the boundary. Geochronology including dates from plutons from which original paleomagnetic data could be collected could be used to test for age differences across the boundary as well as for relative movement during the Archean.

A suitable area for such a study would be the well exposed region running east from the west coast to include the Clearwater Lakes, and extending north and south well into the lithologically and structurally contrasted terranes. This area is suitable also because the Aphebian geology of the Richmond Gulf Graben is well documented by recent studies by the writer and co-workers. As well as focussing on the question of an Archean crustal boundary, such an area could also yield information on the problem of the origin of the Clearwater Lakes.

REFERENCES
(Includes references cited in the Appendices)

Alexandrov, E.A.
1955: Contribution to studies of origin of Precambrian banded iron ores, Economic Geology, v. 50, p. 459-468.

Allen, J.R.L.
1982: Sedimentary Structures, their Character and Physical Basis; Developments in Sedimentology, v. 30A(v. 1), 593 p.northern Quebec, it is possible that this zone determined the site of the postulated triple junctions as well as the related grabens.

Assereto, R.L. and Kendall, G.C. St.C.
1977: Nature, origin and classification of peritidal tepee structures and related breccias, Sedimentology, v. 24, p. 153-210.

Baragar, W.R.A. and Scoates, R.F.J.
1981: The Circum-Superior Belt: a Proterozoic plate margin?; in Precambrian Plate Tectonics, ed. A. Kroner; Developments in Precambrian Geology, 4, p. 297-330, Elsevier, 781 p.

Bell, R.
1879: Report on an exploration of the east coast of Hudson's Bay; Geological Survey of Canada, Report of Progress for 1877-78, p. 1c-37c.

Bell, R.T. and Hofmann, H.J.
1974: Investigations of the Belcher Group (Aphebian), Belcher Islands, N.W.T.; in Program Abstracts, 3rd Circular, Geological Association of Canada, p. 8.

Beukes, N.J.
1973: Precambrian iron-formations of Southern Africa; Economic Geology, v. 68, p. 960-1004.

Bhattacharji, S. and Smith, C.H.
1964: Flowage differentiation; Science, v. 145, p. 150-153.

Blatt, H., Middleton, G., and Murray, R.
1972: Origin of Sedimentary rocks; Prentice-Hall, Inc., 634 p.

Boillot, G.
1981: Geology of the continental margins; English translation of French original, 1978; Longman, 115 p.

Bolger, G.W., Betzer, P.R., and Gordeev, V.V.
1978: Hydrothermally-derived manganese suspended over the Galapagos Spreading Center; Deep Sea Research, v. 25, p. 721-733.

Bostock, H.H.
1965: Clearwater Complex, New Quebec; Geological Survey of Canada, Paper 64-45, 17 p.
1971: Geological notes on Aquatuk River map-area, Ontario, with emphasis on the Precambrian rocks; Geological Survey of Canada, Paper 70-42, 57. p.

Bott, M.H.P.
1981: Crustal doming and the mechanism of continental rifting; Tectonophysics, v. 73, p. 1-8.

Burke, K. and Dewey, J.F.
1972: Orogeny in Africa; in African Geology, ed. T.F.J. Dessauvagie and A.J. Whiteman; Ibadan University Press, p. 583-608.
1973: Plume-generated triple junctions: key indications in applying plate tectonics to old rocks; Journal of Geology, v. 81, p. 406-433.

Cameron, E.M.
1983: Genesis of Proterozoic iron-formation; sulphur isotope evidence; Geochimica et cosmochimica Acta, v. 47, p. 1069-1074.

Carmichael, I.S.E., Turner, F.J., and Verhoogen, J.
1974: Igneous Petrology; McGraw-Hill, 739 p.

Chandler, F.W.
1973: Clastic dykes at Whitefish Falls, Ontario and the base of the Huronian Gowganda Formation; in Huronian Stratigraphy and Sedimentation; Geological Association of Canada, Special Paper no. 12, p. 199-209.
1978: Geological environment of Aphebian redbeds of the northern half of Richmond Gulf, New Quebec; in Current Research, Part A, Geological Survey of Canada, Paper 78-1A, p. 107-110.
1979: Geology of the Aphebian supracrustal rocks, Lac Guillaume Delisle, Quebec; Geological Survey of Canada, Open File 600 (2 bedrock geological maps, scale 1:50 000).
1982: The structure of the Richmond Gulf Graben and the geological environment of lead-zinc mineralization and of iron-manganese formation in the Nastapoka Group, Richmond Gulf area, New Quebec _ Northwest Territories; in Current Research, Part A, Geological Survey of Canada, Paper 82-1A, p. 1-10.
1984: Metallogenesis of an early Proterozoic foreland sequence, eastern Hudson Bay, Canada; Geological Society of London, Journal, v. 141, p. 299-313.

Chandler, F.W. and Schwarz, E.J.
1980: Tectonics of the Richmond Gulf area, northern Quebec _ a hypothesis; in Current Research, Part C, Geological Survey of Canada, Paper 80-1C, p. 59-68.

Chandler, F.W., Ciesielski, A., and St. Michel, R.
1982: Geological map of the southern margin of the Richmond Gulf Graben, New Quebec; Geological Survey of Canada, Open File 840 (map, scale 1:50 000).

Ciesielski, A., St-Michel, R., et Hamel, C.
1983: Géologie d'une portion sud de l'arc Nastapoka, Baie Hudson, Québec; Geological Survey of Canada, Open File 896 (map, scale 1:250 000).

Clemmey, H.
1982: Oxygen in the Precambrian atmosphere: an evaluation of the geological evidence, Geology, v. 10, p. 141-146.

Cloud, P.
1968: Atmospheric and by hydrospheric evolution on the primitive earth; Science, v. 160, p. 729-736.
1972: A working model of the primitive earth; American Journal of Science, v. 273, p. 537-548.

Cloud, P.E., Jr. and Semikhatov, M.A.
1969: Proterozoic stromatolite zonation; American Journal of Science, v. 267, p. 1017-1061.

Collinson, J.D.
1978: Alluvial sediments; in Sedimentary Environments and Facies, ed. H.G. Reading; Elsevier, p. 15-60.

Collinson, J.D. and Thompson, D.B.
1982: Sedimentary Structures; Allen and Unwin, 194 p.

Corliss, J.B., Dymond, J., Gordon, L.I., Edmond, J.M., Von Herzen, R.P., Ballard, R.D., Green, K., Williams, D., Bainbridge, A., Crane, K., and Van Andel, T.H.
1979: Submarine thermal springs on the Galapagos Rift; Science, v. 203, p. 1073-1083.

Curray, J.R.
1956: The analysis of two-dimensional orientation data; Journal of Geology, v. 64, p. 117-131.

Dewey, J.F. and Burke, K.C.A.
1973: Tibetan, Variscan and Precambrian basement reactivation: products of continental collision; Journal of Geology, v. 81, p. 683-692.

Dimroth, E.
1981: Labrador Geosyncline: type example of early Proterozoic cratonic reactivation; in Precambrian Plate Tectonics, ed. A. Kröner; Developments in Precambrian Geology, v. 4, p. 331-352.

Dimroth, E., Baragar, W.R.A., Bergeron, R., and Jackson, G.D.
1970: The filling of the Circum-Ungava Geosyncline; in Symposium on Basins and Geosynclines of the Canadian Shield, ed. A.J. Baer; Geological Survey of Canada, Paper 70-40, p. 45-142.

Dimroth, E., and Kimberley, M.M.
1976: Precambrian atmospheric oxygen: evidence in the sedimentary distribution of carbon, sulfur, uranium, and iron; Canadian Journal of Earth Sciences, v. 13, p. 1161-1185.

Donaldson, J.A.
1976: Paleoecology of **Conophyton** and associated stromatolites in the Precambrian Dismal Lakes and Rae Groups, Canada; in Stromatolites, ed. M.R. Walter; Developments in Sedimentology, v. 20, Elsevier, p. 523-534.

Douglas, R.J.W.
1969: Geological Map of Canada; Geological Survey of Canada, Map 1250A, scale 1:5 000 000.
1970: Geology and Economic Minerals of Canada; Geological Survey of Canada, Economic Geology, Report no. 1, 838 p.

Dressler, B.
1979: Region de la Fosse du Labrador (56°30'-57°15'); Ministère des Richesses Naturelles du Quebec, Rapport géologique 195, 117 p.

Drever, J.I.
1974: Geochemical model for the origin of Precambrian banded iron formations; Geological Society of America, Bulletin, v. 85, p. 1099-1106.

Eade, K.E.
1966: Fort George River and Kanapiskau River (West Half) map-areas, New Quebec; Geological Survey of Canada, Memoir 339, 82 p.

Earth Physics Branch
1980: Gravity Map of Canada; Gravity and Geodynamics Division, Earth Physics Branch, Department of Energy, Mines and Resources, Canada; scale 1:5 000 000.

Eichler, J.
1976: Origin of the Precambrian banded iron- formations; in Handbook of Stratabound and Stratiform Ore Deposits, ed. K.H. Wolf; Regional Studies and Specific Deposits, v. 7, Au, U, Fe, Mn, Hg, Sb, W and P Deposits, p. 157-201.

Eisbacher, G.H.
1970: Contemporaneous faulting and clastic intrusions in the Quirke Lake Group, Elliot Lake, Ontario; Canadian Journal of Earth Sciences, v. 7, p. 215-225.

Eley, B.E. and Jull, R.K.
1982: Chert in the middle Silurian Fossil Hill Formation of Manitoulin Island, Ontario; Canadian Society of Petroleum Geologists, Bulletin, v. 30, p. 208-215.

Eriksson, K.A. and Truswell, J.F.
1974: Tidal flat associations from a Lower Proterozoic carbonate sequence in South Africa; Sedimentology, v. 21, p. 293-309.
1978: Geological processes and atmospheric evolution in the Precambrian; in Evolution of the Earth's Crust, ed. D.H. Tarling; Academic Press, p. 219-238.

Esquevin, J. and Menendez, R.
1973: Geochronology of Aphebian sediments from eastern Hudson Bay; Fortschritte der Mineralogie, v. 50, p. 68-70 (abstract).

Eugster, H.P. and Chou, I-M
1973: The depositional environments of Precambrian banded iron-formations; Economic Geology, v. 68, p. 1144-1168.

Franklin, J.M. and Thorpe, R.I.
1982: Comparative metallogeny of Slave, Superior and Churchill provinces; in Precambrian Sulphide Deposits, H.S. Robinson Symposium Volume, ed. R.W. Hutchinson and J.M. Franklin; Geological Association of Canada, Special paper 25, 791 p.

Fraser, J.A., Heywood, W.W., and Mazurski, M.A.
1978: Metamorphic Map of the Canadian Shield; Geological Survey of Canada, Map 1475A, scale 1:3 500 000.

Fryer, B.J.
1972: Age determinations in the Circum-Ungava Geosyncline and the evolution of Precambrian banded iron-formations; Canadian Journal of Earth Sciences, v. 9, p. 652-663.

Gebelein, C.D.
1969: Distribution, morphology and accretion rate of recent subtidal algal stromatolites, Bermuda; Journal of Sedimentary Petrology, v. 39, p. 49-69.
1976: Open marine subtidal and intertidal stromatolites (Florida, The Bahamas and Bermuda); in Stromatolites, ed. M.R. Walter; Developments in Sedimentology, v. 20, Elsevier, p. 81-388.

Gibb, R.A. and Thomas, M.D.
1976: Gravity signature of fossil plate boundaries in the Canadian Shield; Nature, v. 262, p. 199-200.

Gibb, R.A. and Walcott, R.I.
1971: A Precambrian suture in the Canadian Shield; Earth and Planetary Science Letters, v. 10, p. 417-422.

Gibb, R.A., Chandler, F.W., and Fogarasi, S.
1983: The Richmond Gulf gravity anomaly, northern Quebec-Northwest Territories; in Current Research, Part B, Geological Survey of Canada, Paper 83-1B, p. 53-56.

Goldich, S.S.
1973: Ages of Precambrian banded iron-formations; Economic Geology, v. 68, p. 1126-1134.

Gole, M.J. and Klein, C.
1981: Banded iron-formations through much of Precambrian time; Journal of Geology, v. 89, p. 169-183.

Golubic, S.
1976: Organisms that build stromatolites; in Stromatolites, ed. M.R. Walter; Developments in Sedimentology, v. 20, Elsevier, p. 113-126.

Goodwin, A.M.
1973: Archean iron-formations and tectonic basins of the Canadian Shield; Economic Geology, v. 68, p. 915-933.

Govett, G.J.S.
1966: Origin of banded iron formation; Geological Society of America, Bulletin, v. 77, p. 1191-1212.

Gross, G.A.
1965: Geology of Iron Deposits in Canada, Volume 1. General Geology and Evaluation of Iron Deposits; Geological Survey of Canada, Economic Geology Report, No. 22, 181 p.
1973: The depositional environment of principal types of Precambrian iron-formation; in Genesis of Precambrian Iron and Manganese Deposits, Proceedings of the Kiev Symposium, 1970, ed. M.P. Semenenko; UNESCO, Earth Sciences, v. 9, p. 15-21.
1980: A classification of iron formations based on depositional environments; Canadian Mineralogist, v. 18, p. 215-222.

Hardie, L.A. and Ginsburg, R.N.
1977: Layering: the origin and environmental significance of lamination and thin bedding; in Sedimentation on the Modern Carbonate Tidal Flats of Northwest Andros Island, Bahamas, ed. L.A. Hardie; Johns Hopkins University, Studies in Geology, No. 22, p. 50-123.

Harms, J.C., Southard, J.B., Spearing, D.R., and Walker, R.G.
1975: Depositional environments as interpreted from primary sedimentary structures and stratification sequences; Society of Economic Paleontologists and Mineralogists, Lecture Notes for Short Course No. 2; 161 p.

Harwood, T.A.
1949: The lead-zinc deposits of Richmond Gulf; unpublished B.A. Sc. thesis, University of Toronto, 45 p.

Haslett, P.G.
1976: Lower Cambrian stromatolites from open and sheltered intertidal environments, Wirrealpa, South Australia; in Stromatolites, ed. M.R. Walter; Developments in Sedimentology, v. 20, p. 565-584.

Hews, P.C.
1976: An Rb-Sr whole-rock study of some Proterozoic rocks, Richmond Gulf, Nouveau Quebec; unpublished M.Sc. thesis, Carleton University, 64 p.

High, L.R., Jr. and Picard, M.D.
1974: Reliability of cross-stratification types as paleocurrent indicators in fluvial rocks; Journal of Sedimentary Petrology, v. 44, p. 158-168.

Hoffman, P.F.
1973: Evolution of an early Proterozoic continental margin: the Coronation Geosyncline and associated aulacogens of the northwest Canadian Shield; Royal Society of London, Philosophical Transactions, A. 273, p. 547-581.
1976a: Stromatolite morphogenesis in Shark Bay, Western Australia; in Stromatolites, ed. M.R. Walter; Developments in Sedimentology, v. 20, p. 261-271.
1976b: Environmental diversity of middle Precambrian stromatolites; in Stromatolites, ed. M.R. Walter; Developments in Sedimentology, v. 20, p. 599-611.
1981: Wopmay Orogen: a Wilson Cycle of Early Proterozoic age in the northwest of the Canadian Shield; in The Continental Crust and its Mineral Deposits, ed. D.W. Strangway; Geological Association of Canada, Special Paper 20, p. 523-549.

Hoffman, P., Dewey, J.F., and Burke, K.
1974: Aulacogens and their genetic relation to geosynclines, with a Proterozoic example from Great Slave Lake, Canada; in Modern and Ancient Geosynclinal Sedimentation; Society of Economic Paleontologists and Mineralogists, Special Paper 19, 380 p.

Illies, J.H.
1981: Mechanism of graben formation; Tectonophysics, v. 73, p. 249-266.

Irvine, T.N. and Baragar, W.R.A.
1971: A guide to the chemical classification of the common volcanic rocks; Canadian Journal of Earth Sciences, v. 8, p. 523-548.

Irving, E. and McGlynn, J.C.
1976: Proterozoic magnetostratigraphy and the tectonic evolution of the Laurentia; Royal Society of London, Philosophical Transactions, Series A, v. 208, p. 243-265.

Irving, E. and McGlynn, J.C.
1981: On the coherence, rotation and paleolatitude of Laurentia in the Proterozoic; in Precambrian Plate Tectonics, ed. A. Kroner; Developments in Precambrian Geology, v. 4, p. 561-598.

Jackson, G.D.
1960: Belcher Islands, Northwest Territories 33M, 34D, E; Geological Survey of Canada, Paper 60-20, 13 p. (with Map 28-1960, scale 1 inch to 2 miles).
1967: Interpretation of G.S.C. samples 65-83 to 65-87; in Age Determinations and Geological Studies, K-Ar Isotopic Ages, Report 7, ed. R.K. Wanless, R.D. Stevens, G.R. Lachance, and C.M. Edmonds; Geological Survey of Canada, Paper 66-17, 119 p.

James, H.L.
1954: Sedimentary facies of iron-formation; Economic Geology, v. 49, p. 235-293.

James, H.L. and Sims, P.K. (ed.)
1973: Precambrian Iron-formations of the World; Economic Geology, v. 68, no. 7, p. 913-1220.

Kinsman, D.J.J. and Park, R.K.
1976: Algal belt and coastal sabkha evolution, Trucial Coast, Persian Gulf; in Stromatolites, ed. M.R. Walter; Developments in Sedimentology, v. 20, p. 421-433.

Klein, G. de Vries
1977: Clastic Tidal Facies; Continuing Education Publishing Company, Champaign, Illinois, 149 p.

Kranck, E.H.
1951: On the geology of the east coast of Hudson Bay and James Bay; Acta Geographica, Societas Geographica Fenniae, v. 11, p. 1-71.

Lee, S.M.
1965: Inussuaq-Pointe Normande area, New Quebec; Quebec Department of Natural Resources, Geological Report No. 119, 134 p.

Leeder, M.R.
1980: On the stability of lower stage plane beds and the absence of current ripples in coarse sands; Geological Society of London, Journal, v. 137, p. 423-429.

Leith, C.K.
1910: An Algonkian basin in Hudson Bay – a comparison with the Lake Superior Basin; Economic Geology, v. 5, p. 227-246.

Lepp, H. and Goldich, S.S.
1964: Origin of Precambrian iron formations; Economic Geology, v. 59, p. 1025-1060.

Logan, B.W.
1961: Cryptozoon and associate stromatolites from the Recent of Shark Bay, Western Australia; Journal of Geology, v. 69, p. 517-533.

Logan, B.W., Hoffman, P., and Gebelein, C.D.
1974: Algal mats, cryptologal fabrics and structures, Hamelin Pool, Western Australia; in Evolution and Diagenesis of Quaternary Carbonate Sequences, Shark Bay, Western Australia; American Association of Petroleum Geologists, Memoir 22, p. 140-194.

Logan, B.W., Rezak, R., and Ginsburg, R.N.
1964: Classification and environmental significance of stromatolites; Journal of Geology, v. 72, p. 68-83.

Long, D.G.F.
1978: Proterozoic stream deposits: some problems of recognition and interpretation of ancient fluvial sandy systems; in Fluvial Sedimentology, ed. A.D. Miall; Canadian Society of Petroleum Geologists, Memoir 5, p. 313-341.

Loughnan, F.C.
1969: Chemical Weathering of the Silicate Minerals; Elsevier, 154 p.

Low, A.P.
1889: Report on explorations in James Bay and country east of Hudson Bay drained by Big, Great Whale and Clearwater rivers; Geological Survey of Canada, Annual Report, v. 3, pt. 2, p. 1J-62J.
1902: Report on an exploration of the east coast of Hudson Bay from Cape Wolstenholme to the south end of James Bay; Geological Survey of Canada, Summary Report, v. XII, pt. D, p. 5D-80D.
1903: Report on the geology and physical character of the Nastapoka Islands, Hudson Bay; Geological Survey of Canada, Summary Report, v. XIII, pt. D.D., p. 5DD-31DD.

MacDonald, G.A.
1953: Pahoehoe, aa and block lava; American Journal of Science, v. 251, p. 169-191.
1972: Volcanoes; Prentice-Hall, 509 p.

Middleton, G.V.
1965: Primary sedimentary structures and their hydrodynamic interpretation; Society of Economic Paleontologists and Mineralogists, Special Publication 12, 265 p.

Milanovsky, E.E.
1981: Aulacogens of ancient platforms: problems of their origin and tectonic development; Tectonophysics, v. 73, p. 213-248.

Miller, A.R.
1978: Uranium reconnaissance in the northern Richmond Gulf area; in Current Research, Part A, Geological Survey of Canada, Paper 78-1A, 558 p.

Milliman, J.D.
1974: Marine Carbonates; Springer-Verlag, 375 p.

Monty, A.
1977: Evolving concepts on the nature and the ecological significance of stromatolites; in Fossil Algae, Recent Results and Developments, ed. E. Flügel; Springer-Verlag, 372 p.

Moore, E.S.
1918: The iron-formation on Belcher Islands, Hudson Bay, with special reference to its origin and its associated algal structures; Journal of Geology, v. 26, p. 412-438.

Mukhopadhyay, M. and Gibb, R.A.
1981: Gravity anomalies and deep structure of eastern Hudson Bay; Tectonophysics, v. 72, p. 43-60.

Parks, T.
1949: A report on the geology of the Nastapoka Group of sediments (Hudson Bay) with its contained lead and zinc-bearing strata; unpublished B.A.Sc. thesis, Univ. of Toronto.

Playford, P.E. and Cockbain, A.E.
1976: Modern algal stromatolites at Hamelin Pool, a hypersaline barred basin in Shark Bay, Western Australia; in Stromatolites, ed. M.R. Walter; Developments in Sedimentology, v. 20, Elsevier, p. 389-411.

Ramberg, I.B. and Smithson, S.B.
1975: Gridded fault patterns in a late Cenozoic and a Paleozoic continental rift; Geology, v. 3, p. 201-204.

Raybould, J.G.
1978: Tectonic controls on Proterozoic stratiform copper mineralization; Institution of Mining and Metallurgy, Transactions, v. 87, Series B, p. B79-86.

Read, J.F.
1976: Calcretes and their distinction from stromatolites; in Stromatolites, ed. M.R. Walter; Developments in Sedimentology, 20, Elsevier, p. 55-71.

Reineck, H.E. and Singh, I.B.
1980: Depositional Sedimentary Environments, with Reference to Terrigenous Clastics; Springer- Verlag, 2nd edn., 549 p.

Reinhardt, E.W.
1972: Occurrences of exotic breccias in the Petitot Islands (85H/10) and Wilson Island (85H/15) map areas, East Arm of Great Slave Lake, District of Mackenzie; Geological Survey of Canada, Paper 72-25, 43 p.

Ricketts, B.D.
1979: Sedimentology and stratigraphy of eastern and central Belcher Islands, Northwest Territories; unpublished Ph.D. thesis, Carleton University, 314 p.

Ricketts, B.D. and Donaldson, J.A.
1979: Stone rosettes as indicators of ancient shorelines: examples from the Precambrian Belcher Group, Northwest Territories; Canadian Journal of Earth Sciences, v. 16, p. 1887-1891.
1981: Sedimentary history of the Belcher Group of Hudson Bay; in Proterozoic Basins of Canada, ed. F.H.A. Campbell; Geological Survey of Canada, Paper 81-10, p. 235-254.

Rona, P.A.
1980: TAG hydrothermal field: mid-Atlantic Ridge crest at latitude 26°N; J. Geological Society of London, Journal, v. 137, p. 385-402.

Rose, A.W.
1976: The effect of cuprous chloride complexes in the origin of redbed copper and related deposits; Economic Geology, v. 71, p. 1036-1048.

Ruelle, J.C.L.
1982: Depositional environments and genesis of stratiform copper deposits of the Redstone copper belt, Mackenzie Mountains, N.W.T.; in Precambrian Sulphide Deposits, H.S. Robinson Memorial Volume, ed. R.W. Hutchinson, C.D. Spence, and J.M. Franklin; Geological Association of Canada, Special Paper 25, p. 701-737.

Russell, R.J.
1968: Where most grains of very coarse sand and fine gravel are deposited; Sedimentology, v. 11, p. 31-38.

Sakamoto, T.
1950: The origin of the pre-Cambrian banded iron ores; American Journal of Science, v. 248, p. 449-474.

Sathyanarayan, S. and Muller, G.
1980: Origin of nodular chert in the carbonate rocks of the Kaladgi Group (younger Precambrian), Karnataka, India; Sedimentary Geology, v. 25, p. 209-221.

Schwarz, E.J. and Fujiwara, Y.
1981: Paleomagnetism of the Circum-Ungava Fold Belt II: Proterozoic rocks of Richmond Gulf and Manitounuk Islands; in Proterozoic Basins of Canada, ed. F.H.A. Campbell; Geological Survey of Canada, Paper 81-10, p. 255-267.

Seidler, E. and Jacoby, W.R.
1981: Parameterized rift development and upper mantle anomalies; Tectonophysics, v. 73, p. 53-68.

Semenenko, M.P. (ed.)
1973: Genesis of Precambrian Iron and Manganese Deposits, Proceedings of the Kiev Symposium, 1970; UNESCO, Earth Sciences, v. 9, 382 p.

Sengör, A.M.C., Burke, D., and Dewey, J.F.
1978: Rifts at high angles to orogenic belts: tests for their origin and the upper Rhine graben as an example; American Journal of Science, v. 278, p. 24-40.

Serebryakov, S.N.
1976: Biotic and abiotic factors controlling the morphology of Riphean stromatolites; in Stromatolites, ed. M.R. Walter; Developments in Sedimentology, v. 20, Elsevier, 790 p.

Shinn, E.A.
1968: Practical significance of birdseye structures in carbonate rocks; Journal of Sedimentary Petrology, v. 38, p. 215-223.
1969: Submarine lithification of Holocene carbonate sediments in the Persian Gulf; Sedimentology, v. 12, p. 109-144.

Simone, L.
1981: Ooids: a review; Earth Science Reviews, v. 16, p. 319-355.

Smith, D.B.
1974: Origin of tepees in upper Permian shelf carbonate rocks of Guadalupe Mountains, New Mexico; American Association of Petroleum Geologists, Bulletin, v. 58, p. 63-70.

Stevenson, I.M.
1968: A geological reconnaissance of Leaf River map- area, New Quebec and Northwest Territories; Geological Survey of Canada, Memoir 356, 112 p.

Stockwell, C.H.
1969: Tectonic Map of Canada; Geological Survey of Canada, Map 1251A, scale 1:5 000 000.
1982: Proposals for time classification and correlation of Precambrian rocks and events in Canada and adjacent areas of the Canadian Shield, Part I: a time classification of Precambrian rocks and events; Geological Survey of Canada, Paper 80-19, 135 p.

Taylor, F.C.
1982: Reconnaissance geology of a part of the Canadian Shield, northern Quebec and Northwest Territories; Geological Survey of Canada, Memoir 399, 32 p.

Wanless, R.K.
1970: Isotopic Age Map of Canada; Geological Survey of Canada, Map 1256A, scale 1:5 000 000.

Wardle, R.J. and Bailey, D.G.
1981: Early Proterozoic sequences in Labrador; in Proterozoic Basins of Canada, ed. F.H.A. Campbell; Geological Survey of Canada, Paper 81-10, p. 331-358.

Warren, J.K.
1983: Tepees, modern (South Australia) and ancient (Permian-Texas and New Mexico) — a comparison; Sedimentary Geology, v. 34, p. 1-19.

Waters, A.C.
1960: Determining direction of flow in basalts; American Journal of Science, Bradley Volume, v. 258A, p. 350-366.

Windley, B.F.
1977: The Evolving Continents; John Wiley & Sons, 385 p.

Wilson, J.T.
1968: Theories on the origin of Hudson Bay. Part III: comparisons of the Hudson Bay arc with some other features; in Science, History and Hudson Bay, ed. C.S. Beals; v. 2, p. 1015-1033.

Woodcock, J.R.
1960: Geology of the Richmond Gulf area, New Quebec; Geological Association of Canada, Proceedings, v. 12, p. 21-39.

Young, C.A.
1922: Iron bearing rocks of Belcher Islands, Hudson Bay; Geological Survey of Canada, Summary Report, 1921, Part E, 61 p.

APPENDIX 1

DESCRIPTION OF THREE VERTICAL FACIES SEQUENCES FROM SANDSTONES OF THE QINGAALUK FORMATION

The first facies sequence

This sequence (Fig. 30) consisting of a set of three complete and two incomplete fining upward cycles is exposed in fine grained sandstone (Fig. 32) in the basal redbeds on the east side of Lac Guillaume-Delisle (56°27'N, 76°20'12"W). They usually commence with trough crossbedded medium grained sandstone lying on a scoured base. A complete cycle would continue up through current-lineated and rippled finer grained sandstone to a mudcracked mud layer or a layer of mud curls. These cycles are probably representative of much of the basal redbed member because in less well-exposed parts of the area facies similar to parts of these sequences are very common. Apart from the planar crossbed (Fig. 35) which could show sediment transport direction at a high angle to the flow direction of the channel (High and Picard, 1974, p. 165) all other indicators indicate an eastward flow of low variance, falling between azimuths 060 and 087°, fitting with many more widely collected data from crossbeds (Fig. 77) and ripple marks (Fig. 82) and one observation of current crescents (Fig. 86). The cycles can be explained as unidirectional waning-current cycles (Harms et al., 1975) terminating with exposure and desiccation. Absence of bimodal or polymodal paleocurrent patterns and of lithologies suggestive of marine depositional environments from these and enclosing sedimentary rocks fit their interpretation as alluvial fining upward cycles.

The second facies sequence

This was measured in well rounded but poorly sorted microcline-rich coarse grained arkose and grit, containing quartz and granite pebbles, at the exposure shown in Figure 33. From four accurate measurements of trough- crossbed orientations and a dozen or so imprecise other measurements sediment transport is concluded to have been toward the southeast.

Unit 1, the lowest unit (81 cm thick), pinches out 30 m to the west. It is composed of pink quartzofeldspathic sand and grit and overlies a scoured surface cut into medium grained sandstone. It contains several sets of trough crossbeds up to 35 cm thick. Dispersed pebbles include granite, up to 1 cm in size, and angular mud clasts up to 5 cm in size.

Unit 2, 19 cm thick, is traceable 10 m southward and contains alternating fine- to coarse-grained lenticular sandstone layers 0-1.5 cm thick and massive mudstone layers 1-1.5 cm thick. The sole of the unit is obscured and the top is overlain sharply by the third unit or passes gradually to unit 3 via a 5 cm thick red and green mud-clast layer. A tendency for upward-grading from the sand sublayers to succeeding mudstone sublayers was noted in two instances. Thicker examples of the mudstone layers are mudcracked and thinner ones are broken into mud chip layers (see detail in Fig. 35).

Unit 3, 4 m thick, is an upward-coarsening set of six non-parallel, wavy bedded, orange-weathering medium grained beds of crossbedded sandstone to grit, ranging from 0.3 to 1 m in thickness. One bed was traced 30 m south until it pinched out. Soles lie within gentle scour troughs up to 5 cm deep. The unit is entirely crossbedded on a scale of 7-60 cm. Most forms seem to be troughs. Pebbles up to 3 cm long of white quartz, light coloured aphanitic and porphyritic clasts (felsic volcanic?), pink granite and much larger unabraded mud clasts lie scattered or form wedge- shaped pockets on foresets.

Unit 4, 1.5 m thick, ranges from mud to coarse sand size. It consists of a lower part, a finer grained and smaller scaled variant of unit 3, with crossbeds up to 18 cm thick. It has a plum-coloured upper part

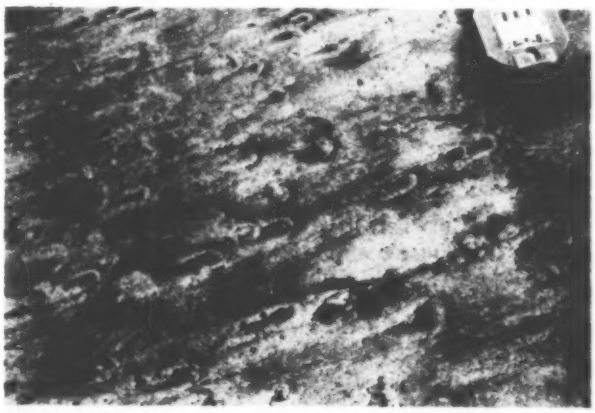

Figure 86. Current crescents in fine grained sandstone, second (redbed) member, Qingaaluk Formation. Flow was to azimuth 090° (56°27'27"N, 76°20'29"W; GSC 03264-I).

of similar thickness with two interlayered components. In the first component bunches of mudcracked and mud-curl layers and layers of rippled and laminated fine grained sandstone alternate with massive sand layers (reminiscent of unit 2). The second component is composed of crossbedded units up to 15 cm thick.

Unit 5, 1.3 m thick, composed of wavy bedded salmon- coloured coarse grained pebbly sandstone, was traced to a pinch-out at 60 m. Pebbles include white quartz, up to 2.5 cm long, felsic volcanic and some rounded mud clasts up to 7 cm across. Smaller mud clasts are imbricated in crossbed foresets. The sole of the unit is defined by a 10 cm deep scour with an amplitude of 1 m.

Unit 6, 20-40 cm thick, could be regarded as a fine grained (coarse-medium grained) upper part of unit 5, with corresponding decrease in thickness of crossbeds (up to 20 cm), similar pebble composition (up to 1.8 cm long), but it differs in containing two mud layers, 46 cm and 2 m long, and 3 and 1.5 cm thick respectively.

Unit 7, 30-135 cm thick, was traceable 50 m where it split into several units similar to unit 6. Planar crossbeds lie upon a gently undulose base. Crossbeds are both planar and of trough type and thin upward from 54 to 8 cm in thickness with a concomitant decrease in grain size from grit to coarse sand. Pebbles include pea-sized quartz and thin tabular black mud clasts up to 5 cm long scattered on foreset laminae.

Unit 8, 3.55 m thick, is a set of units similar to those stratigraphically below but alternating on a smaller scale, hence they are grouped as one unit. The unit consists of five subunits of orange-pink weathering crossbedded sandstone and fine grained green-grey units. The sandstone subunits, finer than those already described, i.e. units 1, 3 and 5, range from 10-50 cm in thickness and contain laminated coarse- to fine-grained sand of 1-4 crossbedded layers up to 16 cm thick. These subunits lie with gently undulose basal contacts on desiccation-cracked mudstone or on the fine grained dark sand of the alternating subunits. The fine grained subunits are similar to finer grained units already described, e.g. the upper part of unit 4, and are rippled and mudcracked.

The third facies sequence

A third facies sequence in the Qingaaluk Formation was seen in the bleached upper part of the coarse grained arkose on a northeast-facing bluff (Fig. 34, 56°24'30"N, 76°27'W). Here the sandstone consists of three facies. Facies A consists of trough crossbedded light pink to grey coarse grained sandstone. Facies B forms thinner units of generally finer grained mid-green sandstone to siltstone alternating with facies A. Facies C is a complex small-scale interbedding of facies A and B.

The facies were examined over about 5 m of vertical section. Facies A (number of beds = 4) is composed of fining- upward units of coarse- to fine-grained arkose containing rare quartz and feldspar pebbles, about 1 cm in size, and "tabular" dark green mudstone fragments up to 4 cm long. The scale of the trough crossbeds diminishes upward from a thickness of about 50 to 7 cm. Irregular "pinch and swell" bedding (wavy, nonparallel, Collinson and Thompson, 1982, p. 13) is caused by scour at the base of the trough crossbeds and those of succeeding units and by the preservation of the tops of some bedforms (Fig. 34).

Facies B (n = 3), is generally finer grained but ranges from coarse sand grade to silt sized. Units are generally traceable for several metres but here two examples were traced along strike for 30 and 40 m. Units terminate laterally by removal at the scoured base of an overlying trough crossbedded unit. The basal surface of these units is determined by the topography of the underlying unit and the top by basal scour beneath the succeeding trough crossbedded unit except in rare cases where planar crossbedded units are superposed. Sedimentary structures in facies B include symmetrical ripples, some with secondary crests in trough centres indicative of wave action in shallow water (Allen, 1982, p. 434), mudcracked siltstone, and fine grained current- lineated sandstone. The facies also includes isolated sand waves up to 1 m x 10 cm in vertical section.

An intimate mixing of facies A and B gave rise to units of intermediate thickness which could be designated a separate facies, facies C. Several trough crossbeds measured in this sequence suggested a southward sediment transport direction (azimuths 195, 195, 175, 225, 240, 195, 140 and 125°).

APPENDIX 2

STRATIGRAPHIC SECTIONS (1-12) THROUGH THE NASTAPOKA GROUP, WITH ILLUSTRATIONS

The following pages contain descriptions of twelve stratigraphic sections (Fig. 47), through the Nastapoka Group taken from the scarp slope of the coastal cuesta. The locations of the sections are shown in Figure 48.

The stratigraphic sections are subdivided into units on the basis of field characteristics. These units are numbered in ascending stratigraphic order, followed by thicknesses and descriptive notes. Correlation of all of these units between stratigraphic sections is not implied. At the level of study used by the writer, as already mentioned, ten units or sets of units could be traced between these sections and are designated as informal members, A-J on Figures 46, 47.

Stratigraphic section 1

This section was measured 60 km south of Lac Guillaume-Delisle to gain some feeling for long distance changes in the stratigraphy of the Nastapoka Group.

The group overlies granitic basement which shows evidence of pyritization 4 m beneath the contact. The contact is lost in a 4.5 m covered interval. In this section there are few characteristics that distinguish units, and subdivision is made mainly for the purpose of convenient description.

Unit 1; 6 m, consists of brown dolomite with 5% of tabular grey chert, edgewise laminite breccia, occasional low stromatolite mounds 25 cm across and 7 cm high.

Unit 2; 6 m, is similar but contains chert.

Unit 3; 1.5 m, contains prominent stromatolites and grey chert.

Unit 4; 2 m, consists of grey dolomite similar to that already seen but is weakly laminated.

Unit 5; 3 m, is of buff-weathered dolomite with sparse low stromatolite domes and grey chert layers.

Unit 6; 3 m, is a dolomite bluff with well developed lamination at a 1 mm scale, lenticular and tabular chert and very rare stromatolites.

Unit 7; 5 m, is of finely laminated dolomite with chert layers up to 30 cm thick. Isolated spherical stromatolites are preserved at the base of the unit in a 60 cm zone and others, some chertified, are scattered up through the unit. This rock is followed by 2 m of stromatolite-free but otherwise similar material.

Unit 8; 5 m, is of buff-weathering dolomite with layered grey chert and low stromatolite domes.

Unit 9; 4 m, is of light buff-weathering dolomite with light grey chert nodules, 15 cm across and 5 cm high, stromatolite spheres 10 cm across, and isolated domes 15 cm across and 5 cm high. At the top lies a 15 cm thick layer of 45 cm across low linked domes and 1 m of poorly exposed rusty dolomite.

Unit 10; 3 m, is of grey laminated dolomite with rare low stromatolite domes, some growing into 30 cm high columnar forms and little layered chert.

Unit 11; 3 m, is of laminated grey dolomite with 20% of black chert layers and 5 cm across spherical and low domal stromatolites separated by edgewise laminite breccia.

Unit 12; 3 m, is of dolomite with low domal stromatolites.

Unit 13; 3 m, consists of a zone of packed club-shaped stromatolites. In plan view these structures are circular in outline.

Unit 14; 18 m, a covered interval in which occurs limited outcrop of grey laminated dolomite with low domes and minor grey chert.

Unit 15; 12 m, is of sandy-weathered dolomite, finely laminated but chert-free. At the top of the unit is a 1 m zone of 1 cm across delicate upright branched stromatolites that is unique in the Lac Guillaume-Delisle area (Fig. 87). This unit is succeeded by 18 m of covered interval in which 60 cm of sandy-weathering poorly laminated dolomite (unit 15a) was visible 12 m from the base.

Unit 16; 3 m, is of alternating sandy and grey dolomite with a few low domal stromatolites and grey tabular chert.

Unit 17; 1 m, is of rusty carious-weathering dolomite full of low domal stromatolites and containing pyrite cubes.

Unit 18; 1 m, is pale grey laminated chert-poor dolomite with oncolites, possible spherical stromatolites, laminae truncated possibly by current scour and layers of edgewise laminite breccia.

Unit 19; 5 m, a bluff of grey dolomite, the top of which dips gently westward as a bedding-surface plateau 0.8 km across. Such a plateau, not as well developed, at this stratigraphic level in sections 2 and 3, is described below. The bluff and the plateau are scattered with abundant weathered limonitic gossan fragments, and are significant because they are formed by a lead-zinc bearing unit.

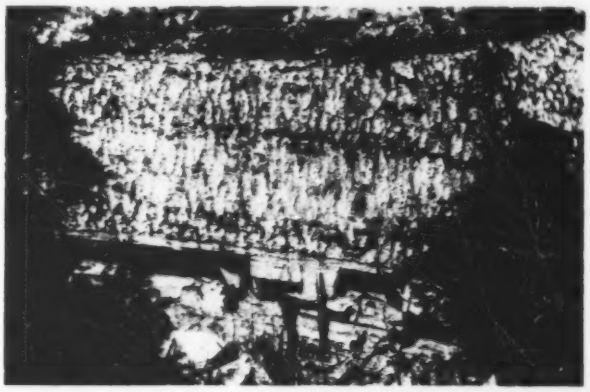

Figure 87. Unique zone of finger-shaped and finger-sized stromatolites, 1 m of which is exposed in poorly exposed section, unit 15, section 1, Nastapoka Group. (see Fig. 47; GSC 203895-O).

Within the bluff occurs a 60 cm thick zone of 15 cm wide, linked hemispherical stromatolites and associated pyrite nodules, calcite and quartz geodes. On the plateau domical stromatolites over a metre across and hemispherical stromatolites 10-15 cm across are associated with galena crystals 0.5-1 cm in size. Beyond this plateau a large swamp obscures a probable 10 m of section.

Unit 20; a 60 cm high outcrop is formed of wavy stromatolites and is a distinct marker unit (Fig. 62, 63). After this exposure a large swamp at the head of Passe Manitounuk was crossed. At this stage control of position in the section was lost.

Unit 21 consists of the remainder of the section seen from the base of a cliff that rises on the west side of the head of Passe Manitounuk. It consists, in ascending order, of an unknown thickness of dolomite with columnar stromatolites, 7 m of quartzite possibly of tidal origin, about 30 m of dolomite, about 30 m of quartzite and finally basaltic volcanics of the Nastapoka Group.

Stratigraphic section 2

This 160 m thick section was measured in the vicinity of the Ruby Lake lead occurrence (Chandler et al., 1982). It overlies, with slight unconformity, gently west-dipping crossbedded and limonite-stained feldspathic grit of the Qingaaluk Formation. The grit contains quartz and angular feldspar pebbles up to 2.5 cm across and rare granite pebbles up to 5 cm across.

Unit 1; 50 m, consists of a talus slope with 20% exposure of grey dolomite and tabular black chert. More detail on the facies in this unit can be had from the better- exposed unit 1 of stratigraphic section 3.

Unit 2; 6 m, is a massive breccia of black chert fragments, some tabular and up to 10 cm thick, set in a matrix of white quartz arenite.

Unit 3; 18 m, overlying 15 m of talus is a pale grey laminated dolomite with abundant tabular black chert. In the basal 3 m is a zone of 50 cm across spherical stromatolites. In the middle third of the unit low domal stromatolites are present.

Unit 4; 6 m, is a grey laminated dolomite with linked low domal and spherical stromatolites 50 cm across in the upper 1.5 m.

Unit 5; 12 m, consists of very limonitic and pyritic dolomite with cavernous weathering, rare digitate stromatolites associated with galena crystals up to 1 cm across, quartz geodes, and white encrustations on fracture surfaces that gave positive geochemical tests for both lead and zinc.

Unit 6; 3 m, overlies a 3 m thick covered interval and consists of wavy stromatolites (Fig. 62, 63) that define a stratigraphic marker zone above the lead-bearing zone.

Unit 7; 6 m, is a buff-weathering cream wavy-laminated dolomite with large irregular chert nodules.

Unit 8; 18 m, follows 24.5 m of basalt talus which probably covers much of the unit. The unit consists of grey- rusty weathering light grey fine grained sandstone, planar crossbedded on a 10 cm scale. Mudcracks and symmetrical ripples were noted in a loose block.

Above this unit lies basalt of the Nastapoka Group.

Stratigraphic section 3

This 160 m thick section was measured on a salient of the east-facing cliff 1.5 km to the north of section 2 because of poor exposure in the previous section. The Nastapoka Group in this section overlies massive rusty-weathering, dark grey feldspathic grit that passes down into pink crossbedded grit. The grey grit contains horizons of 2-3 cm quartz pebbles and scattered granitic pebbles up to 4 cm across and quartz pebbles up to 10 cm across.

Unit 1; 32 m, is not well exposed. Here, as in section 2, it is defined as including all the strata beneath the chert breccia (unit 2). Unit 1 consists of 12 m of covered section, 9 m of dolomite, 6 m of covered section and 3 m of carbonate in ascending order. The 9 m zone is laminated, contains several layers of tabular black chert, small low stromatolite domes separated by edgewise laminite breccia and many 2-3 cm thick laminite breccia zones.

Unit 2; 6 m, as in section 2, is a black chert breccia with rare fragments of buff dolomite set in a quartz arenite matrix (Fig. 55). It is overlain by 9 m of dolomite talus.

Unit 3; 2 m, is of buff-weathering laminated dolomite. Some of the laminae show minor (2 cm high) doming. Minor edgewise laminite breccia is present. This unit is succeeded by 6 m of talus.

Unit 4; 9 m, consists of 3 m of laminated dolomite with some ripple-like structures and rare 2 cm thick black chert layers. Two stromatolite domes 10 cm wide and 4 cm high are present. This 3 m zone is succeeded by 6 m of similar but poorly exposed rock.

Unit 5; an 18 m thick cliff-forming unit has a basal 3 m part packed with spherical stromatolites 50-100 cm across. In the upper 6 m occur 5% of black chert layers up to 15 cm thick.

Unit 6; 4 m, consists of fine grained weakly laminated otherwise featureless dolomite.

Unit 7; 4 m, is a laminated dolomite with edgewise laminite breccia and rare oncolites.

Unit 8; 4 m, is a dark grey, massive to laminated pyritic dolomite from which pyrite nodules have weathered out to leave a pitted surface. Some laminae appear to have undergone recumbent folding.

Unit 9; 3 m, weathers tan and contains club-shaped and spherical stromatolites. One or two stromatolites have a conophyton-like top.

Unit 10; 6 m, is a brecciated zone at the top of which is a wide plateau similar to that defined by the lead-bearing zone in stratigraphic section 1. The zone and the plateau at the level of its upper surface contains abundant limonitic rubble and limonite-cemented dolomite fragments. Quartz geodes are present and hematite stains fractures.

Unit 11; 1 m, consists of grey dolomite with a few 2 m wide stromatolite domes.

Unit 12; 2 m, is of sandy weathered laminated dolomite containing abundant light grey, tabular chert. Many tepee structures and layers of edgewise laminite breccia are present, some of which have been chertified.

Unit 13; 10.5 m, consists of a lower part, 7.5 m thick, that forms a brown-weathering bluff packed with wavy stromatolites (Fig. 62, 63) and quite abundant grey tabular chert. The upper 3 m zone differs in its weaker development of the wavy stromatolites. At the top of the unit a wide bedding plane plateau occurs.

Unit 14; 9 m, finely laminated brown-weathering dolomite that contains abundant mid-grey tabular chert. The unit is succeeded by 18 m of basalt talus.

Unit 15; 2 m, buff dolomite containing dolomite and quartz arenite ripples. Shaly laminae and 2-3 cm thick edgewise laminite breccia layers also occur. The unit is overlain by 3 m of overburden.

Unit 16 starts with 18 m of carbonate-cemented and quartz-cemented quartzite with tabular crossbeds about 10 cm thick. This is overlain by 9 m of sandstone and interbedded rusty and black shale with mudcracks. One 2 m thick shale unit coarsens upward. The unit is overlain by basalt of the Nastapoka Group.

Stratigraphic section 4

Study of this 55 m thick section was started with identification of the lead-bearing zone (unit 12 of section 5) and the overlying transition zone. In this exposure the succeeding zone weathers sandy rather than white as in section 5 (see unit 13, section 5). Because here the cliff faces north, rather than southeast as in section 5, differently oriented cliffs of several stratigraphic units were examined. This led to the firm conclusion that the weathering colour of the dolomite units depends on orientation except in the case of the very pyritic zones that are strongly coloured brown by weathering of pyrite to limonite. Stratigraphic section 4 was divided into 6 units.

Unit 1; 3 m, consists of dolomite, well-laminated on a scale of a millimetre to a centimetre, and containing about 5% of grey chert layers, tepee structures with ruptured apices, oncolites 7.5 cm across, isolated stromatolite buns up to 30 cm across, and 4-10 cm thick edgewise laminite breccia layers.

Unit 2; 10 m, is correlative with the upper exposed part of unit 13 of section 5, packed with wavy stromatolites. Oncolites and a small amount of edgewise carbonate breccia were seen in the lower 3 m of the unit.

Unit 3; a 4 m cliff, contains 5-10% of irregularly layered tabular chert. The lowest third is massive and contains an edgewise laminite breccia bed 5 cm thick, some stromatolite buns and pyrite nodules. The central and upper thirds are well laminated with parallel to faintly crinkly laminae. In the top third, small isolated buns, clubs and a chertified tepee structure are visible.

Unit 4; 8 m of laminated dolomite. In the lower 2.5 m occur a few isolated buns and rare 1 cm across pyrite nodules. In the upper 5.5 m less than 5% of tabular chert layers are present. There is a weak development of low stromatolite buns, unusually large and abundant oncolites, one of which measures 37x7.5 cm, and a few 15 cm thick layers of wavy stromatolites. Some of these stromatolites grew on lenses of edgewise breccia.

Unit 5; 3 m, a feldspathic sandstone with varied amounts of dolomitic cement, represents transition to a sandstone environment.

Unit 6; 24.5 m, white-weathering feldspathic sandstone, is well parallel-bedded on a 10-15 cm scale and abundantly crossbedded. All crossbeds

suggest sand transport more or less to the west. There are a few beds throughout the unit, 5-10 cm thick, that are dolomite-cemented and a few symmetrical (wave?) ripples. The sandstone is poorly sorted and subarkosic to arkosic in composition. Cement is usually quartz but patches of carbonate occur. The contact with the overlying basalt of the Nastapoka Group is sharp. No spiracles that could be used in determining paleoflow direction of the overlying basalt were found.

Stratigraphic section 5

This 121 m thick partial section is exposed in a 400 m high southeast-facing cliff that falls sheer to the waters of the gulf and is best examined by boat. The upper part is inaccessible and was examined in a separate stratigraphic section (4) 7.5 km to the south.

The section overlies, with gentle angular unconformity, a sharp topography cut into the tidal member of the Qingaaluk Formation (Fig. 49). Within the valleys formed by the unconformity surface lie two lenticular units, a lower turbidite-like unit and an overlying crossbedded quartz arenite unit (Fig. 59).

Unit 1; the turbidite-like unit, is up to 16 m thick and commences with about a metre of massive quartzite cobble conglomerate with clasts similar in composition to the underlying tidal sandstone. The rest of the unit consists of laminated silty carbonate with bed thickness and grain size increasing upward. Bedding scale increases from laminae at the base to a scale of 50 cm at the top where the beds appear to have been disrupted by slumping. Apart from well developed plane parallel bedding, sedimentary structures are not prominent. In the lower part they include very common fine lamination, contorted and slumped laminae and current ripples. One 12 cm interval contains the sequence in ascending order; massive sand, laminated fine grained sand, slumped silt, rippled siltstone, massive siltstone, laminated siltstone; a set of structures reminiscent of a turbidite bed.

Within the lower part of the turbidite-like unit at least three massive pebble conglomerates occur. They are composed of green chert and quartzite and twisted laminated siltstone fragments similar to enclosing strata. Beneath the thickest conglomerate, drag folds in the laminated carbonates indicate downslope drag. Blocks of tidal sandstone from beneath the unconformity enclosed within the turbidite-like sequence (Chandler, 1982, Fig. 1.9) have tumbled down the unconformity surface during deposition of unit 1. The upper part of the unit (Fig. 53) consists of alternating grey sandstone beds and black mudstone beds. Many sand beds are boudinaged, some forming load casts.

Unit 2; the quartz-dolomite arenite unit, is conformable on the turbidite-like unit. It is texturally very mature. It contains mainly monocrystalline quartz grains and at least 30% of well-rounded micritic carbonate grains of similar size that contain siliciclastic silt and framework grains cemented by carbonate. It is trough crossbedded on a 10-20 cm scale, and parallel-laminated. The unit tends to part on a 30 cm scale and contains pyritic stylolites. Grain size ranges from very coarse grained sand to rippled fine grained sand. The unit was probably deposited as subaqueous dunes. Transition to unit 3 is via 4 m of conformable pyritic crossbedded quartz arenite with pyrite nodules. Associated facies include rippled and syneresis-cracked black siltstone, limestone and dolomite conglomerate beds and some boudinaged metre-long, 10 cm thick boudins of carbonate, possibly beach rock.

Unit 3; 2 m, consists of laminated carbonate. Laminae are truncated, probably by current scour. Also present are a 70 cm thick carbonate-pebble conglomerate layer, 2.5 cm thick grit layers and layers of black chert.

Unit 4; is a 6 m thick laminated carbonate layer of grey dolomite with carious weathering caused by solution of pyrite nodules up to 1 cm across. It contains laminite breccia zones, 2-10 cm thick, tabular black chert layers, poorly preserved ripples and a 15 cm thick layer of low domal stromatolites.

Unit 5; is a 4 m thick, massive black chert breccia with a pale grey pyritic quartzite matrix seemingly identical to the chert breccia seen in stratigraphic sections 2 and 3. The base of the breccia is unconformable, cutting down into unit 4 up to 3 m. The top metre of unit 4 is brecciated to a depth of 1 m (Fig. 56).

Unit 6; 7 m thick, consists of a lower part of 4 m of alternating carbonate and sandstone and an upper part 3 m thick of siltstone and quartzite. The carbonate of the lower part is laminated, pyritic, with 5 cm thick laminite breccia zones containing chert fragments. It contains layered black chert, ripples with scoured bases, and mudcracks filled with quartz arenite. Within the carbonate also occur low domal stromatolites 2 m across and 30 cm high, of which the surfaces are draped with alternating layers of fine grained quartz arenite and black mudcracked mudstone-siltstone. At the top of the 4 m thick part of the subunit the depressions between the stromatolite mounds are filled with tiny stromatolites about 2-3 cm in size. The succeeding 3 m of the subunit consists of grey rippled siltstone coarsening up to 2 m of quartz arenite. The siltstone contains chert pebble breccia. The quartzite is crossbedded on a 5 cm scale, contains asymmetric wave-ripples and contains 7 cm thick beds of

laminite-chert breccia in a quartz arenite matrix. This unit passes up through 1 m of grey rippled siltstone with 7 cm thick beds of carbonate pebble breccia to the succeeding unit.

Unit 7; consists of grey laminated dolomite with interlaminated black shale. Wrinkled laminae are preserved in black replacement chert layers. Isolated stromatolite domes, 4.5 cm high by 5 cm across, are present.

Unit 8; 5 m thick, consists of rhythmic alternation in 6 cycles of buff stromatolitic dolomite (60 cm) with grey massive mudcracked siltstone-shale (15 cm). The carbonate layers are a mass of stromatolites ranging from low buns 4.5 m across (Fig. 88) to 30 cm spheres with interdome depressions filled with edgewise laminite breccia. The upper and lower limits of the siltstone-shale units contain carbonate ripples.

Unit 9; consists of 6 m of well laminated grey dolomite with a basal 0.5 m thick stromatolite zone, and a second 2.5 m up into the unit. The lower stromatolite layer consists of spheres separated by edgewise laminite breccia. The upper stromatolite layer consists of a single layer of low domes and spheres 10 cm high, separated by edgewise laminite breccia (Fig. 89). Black chert layers up to 8 cm thick range, from composing 5% of the rock in the lower part of the section, to comprising 10% in the upper part. Other features of the unit include a 30 cm thick edgewise laminite breccia layer, chert breccia layers, oncolites up to 20 cm long, a 5 cm thick massive carbonate grit layer and ripples.

Unit 10; 3 m thick, contains abundant pyrite nodules and is affected by cavernous weathering. It contains stromatolites that are abundant in the middle metre. There is a tendency for the scale of the stromatolites to increase upward (Fig. 90).

Unit 11; 13 m thick. The lower 10 m is light cream and laminated, with a flaggy parting. It is stromatolite- and chert-free and contains 2.5 cm thick edgewise laminite breccia zones and mudcracked symmetrical ripples. The upper 3 m is a cavernous-weathered rusty dolomite containing abundant 60 cm-1 m across stromatolite buns.

Unit 12; the lead-bearing zone, is 5 m thick, very cavernous and rusty. It is abundantly stromatolitic, including 30 cm high club-shaped stromatolites, and low domes 30 cm across. Some delicate digitate forms were also noted. Many stromatolites are disoriented, lying on their sides. The zone also contains 60 cm across cavities filled with cream calcite crystals 2-4 cm across, vugs filled with euhedrally terminating clear quartz crystals and pyrite encrustations (Fig. 57, 58). The zone

Figure 89. Detail of layer of spherical stromatolites (S) with interdome edgewide laminite breccia (B), Nastapoka Group, unit 9, section 5, Figure 47. (GSC 203264-V)

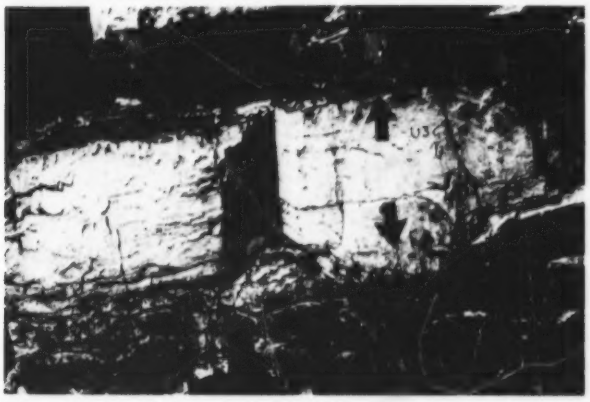

Figure 88. Stromatolite bun, 150 cm across (width of photograph), top and base arrowed, U in lower biolaminite, Nastapoka Group, unit 8, section 5, Figure 47. (GSC 203902-X)

Figure 90. Stromatolite-rich dolomite layer with pyrite nodules (black, large nodule arrowed), Nastapoka Group, unit 10, section 5, Figure 47. (GSC 203895-C)

(Fig. 59) appears to represent a broken and collapsed rubble of stromatolitic material.

At the top of the lead-bearing zone lies a transition zone 5 m thick. It is less brecciated and disturbed. Carious weathering is less severe and quartz and calcite are less abundant. Pyrite seems restricted to the larger stromato- lites. Mudcracks and inverted stromatolites (Fig. 60) occur two-thirds of the way up the zone. In the upper part of this zone stromatolites are draped by laminated dolomite.

Unit 13; the highest accessible unit in this cliff section is a white-weathering dolomite of which 12 m are exposed. Due to difficult access and cover by basalt talus, examination of the cliff was discontinued at this stratigraphic level. Unit 13 contains several per cent of evenly distributed grey chert layers several centimetres thick. At the base of the unit occurs a layer, 30 cm thick, of stromatolite buns with associated edgewise laminite breccia.

Five metres up into the unit a zone of wavy stromatolites (Fig. 62, 63) begins. At this level occurs a 15 cm thick, 1 m long, crossbedded lens of arenite. Although the arenite now consists of microcrystalline dolomite and quartz, circular structures with radial internal substructure resemble altered oolites. Little else occurs in the wavy stromatolite zone except a second arenite lens (an isolated sand wave?) with a rippled top and a small amount of laminated carbonate with a few ripples. Inspection of the surrounding cliffs indicated that unit 13 is overlain in succession by about 20 m of buff-weathering dolomite, about 50 m of well bedded sandstone and lastly by basalt. In order to complete study of the section these inaccessible units were examined 7.5 km to the south at stratigraphic section 4.

When seen from a distance the carbonates of the Nastapoka Group in the east-facing cliffs in the southern half of Lac Guillaume-Delisle (Fig. 49) consist mainly of two white-weathering zones separated by a buff-weathering zone. In section 5 the lower white zone consists of units 9, 10 and 11. The buff-weathering zone consists of the lead- bearing unit 12 stained by limonite released by weathering of its abundant pyrite. The upper white zone is composed of unit 13 which is better described as units above the lead- bearing zone, and leading up to the "wavy" stromatolite zone in several stratigraphic sections (Fig. 47). A similar set of coloured zones is shown by units 6-8 of stratigraphic section 6.

Stratigraphic section 6

Like sections 4 and 5, this 145 m thick section is almost continuously exposed and consequently was examined in detail. The section overlies an irregular surface cut into sandstone of the locally, gently west-dipping Qingaaluk Formation (Fig. 91), similar to the topography of the unconformity underlying section 5. As Figure 91 shows, clastic units like those of section 5 are draped in the valleys of the unconformity surface.

At section 6 the unconformity surface is draped by about 3 m of massive carbonate conglomerate. Above this a 9 m interval is obscured.

Unit 1; 5 m, interlayered crossbedded sandstone and black fissile shale (Fig. 92) similar to unit 1 of section 5. The sandstone occurs as lenticular bodies with straight bases except where draped over undulose surfaces of similar bodies that are formed into sand waves. The sands are fine grained with rippled tops. Some ripples have a wavelength of 15 cm. The "shale" consists of wavy to lenticular bedded quartz silt and black shale (Fig. 92).

Unit 2; 9 m, well-sorted and rounded quartz arenite with 30% of dolomicrite clasts and a dolosparite matrix.

Unit 3; 3 m, interlayered quartz arenite and black shale. The arenite has a high textural roundness and great purity. It is rippled and crossbedded and the shale is lenticularly bedded.

Unit 4; 12 m of grey laminated dark shaly carbonate with rippled and brecciated layers.

Unit 5; 9 m, distinguished by its buff weathering. It consists of 6 buff dolomite layers that

Figure 91. General view of the Nastapoka Group on the west shore of Lac Guillaume-Delisle, to show irregular unconformity surface (arrowed). In the depressions on the unconformity surface are draped lenticular units of interbedded quartzite and shale (member BO and overlying quartz arenite (member C). The unconformity is cut here into member 3, arkose of the Qingaaluk Formation. The exposure is located 1 km east of section 6, Figure 47. (GSC 203265-X)

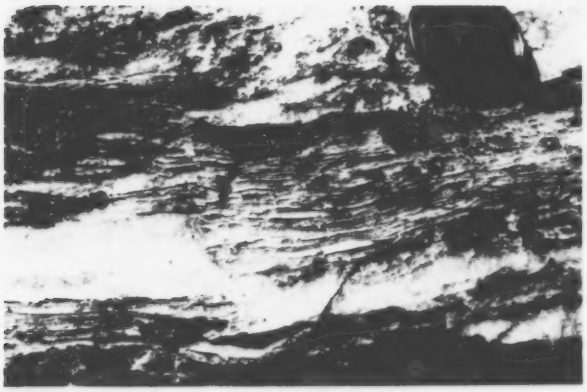

Figure 92. Vertical section of crossbedded and rippled quartz arenite interbedded with lenticularly bedded siltstone-shale, unit 1, section 6, Nastapoka Group, Figure 47. (GSC 203895-F).

decrease in thickness downward, from about 1 m to about 30 cm. Black shale interbeds are about 15 cm thick and the unit becomes increasingly shaly downward. The dolomite beds contain low domal stromatolites, medium grained quartzite layers about 2.5 cm thick, layers of edgewise laminite breccia and tepee structures.

Unit 6; 12 m, a distinctive white-weathering porous unit, the lower of two such white units in the section. It is divisible into 4 subunits in ascending order.

Unit 6a, 3 m thick, is of generally fine grained dolomite with dark grey chert lenses, ripples, a 15 cm oolite bed and low domal stromatolites.

Unit 6b, 3 m thick, is composed of pale grey, parallel-laminated dolomite, with many lenticular chert bodies and an unusually large tepee structure 1 m high (Fig. 93). At the base of the subunit lies a 60 cm thick zone of spherical stromatolites (Fig. 94).

Unit 6c, 3 m thick, is similar to the underlying subunit 6a. Ripples, parallel lamination and grey chert were noted.

Unit 6d, 4 m thick, is finely laminated, contains oncolites, edgewise laminite breccia, current-type ripples 0.5 cm high, and a 30 cm zone of structures resembling climbing ripples or perhaps wavy stromatolites.

The succeeding unit 7, 7 m thick, is distinguished by its grey weathering colour. It contains a lower porous subunit, 7a, and an upper brecciated unit, 7b.

Subunit 7a, 3 m thick, is fine grained and evenly laminated with wavy laminae. It contains pores probably formed by the weathering-out of pyrite. The only other structures discerned in this subunit were a zone of domal stromatolites at the top.

Figure 93. Vertical section of 1 m high tepee structure in unit 6, section 6, lower biolaminite, Nastapoka Group, Figure 47. (GSC 203895-H)

Subunit 7b, 4 m thick, is much broken into blocks that are surrounded by, and cemented by, pyrite, drusy quartz and calcite crystals. Traces of fine laminar structure, domal stromatolites and chert layers are also present. One metre- high area showed branched columnar stromatolites (Fig. 61) that seem restricted to the lead-bearing zone. No galena was seen in this subunit.

Overlying the grey unit 7 lies a white unit, 8, 7.5 m thick. It contains low domal linked stromatolites, i.e. wavy stromatolites similar to those shown in Fig. 62, oncolites (Fig. 96), cavities filled with drusy quartz and black and grey chert lenses. Some of the stromatolites and edgewise laminite breccia are obviously replaced by chert.

Unit 9, at least 15 m thick, is distinguished by its buff weathering. It is divisible into 5 parts.

The unit commences with a 2 m zone, subunit 9a, of club- shaped and conophyton-like stromatolites (Fig. 97), continues upward with a 2 m zone, subunit 9b, of buff dolomite with low domal stromatolites, tepee structures, edgewise laminite breccia, overthrust laminae, apparently resulting from the tepee-forming compression, and chert

Figure 94. Vertical section of 60 cm high single stromatolite layer, unit 6, section 6, lower biolaminite, Nastapoka Group, Figure 47. (GSC 203265-K)

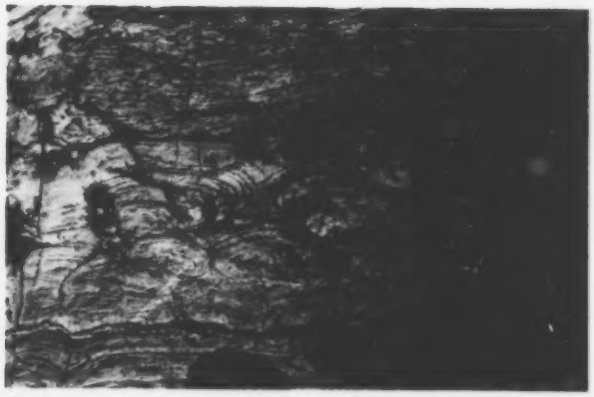

Figure 96. Oncolites in vertical section in wavy stromatolite member (member G), unit 8, section 6, Nastapoka Group, Figure 47. (GSC 203895-J)

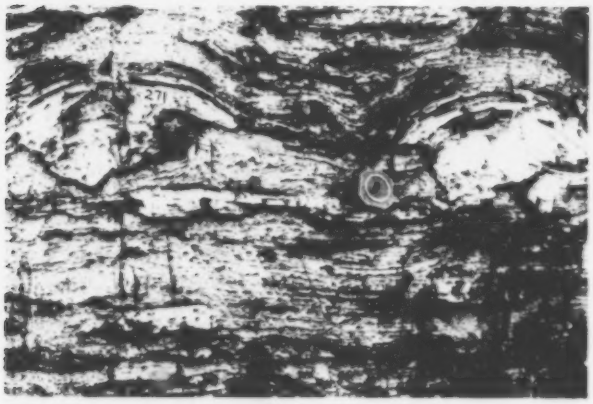

Figure 95. Vertical section of chertified low domal stromatolites growing on elevations of edgewise laminite breccia in biolaminite, unit 4, section 7, Nastapoka Group, Figure 47. (GSC 203264-B)

Figure 97. Fifty-five centimetre high vertical section of conophyton-like stromatolites, unit 9, section 6, Nastapoka Group, Figure 47. (GSC 203902-W)

layers that pinch and swell, in the order of 2-8 cm thick (Fig. 98). Above this subunit, 3 m of section are obscured.

Subunit 9c, 3m thick, is a light cream laminated dolomite with pockets of edgewise laminite breccia, some of which are chertified.

Subunit 9d, 2 m thick, contains the highest stromatolites in the section. These are in the form of low domes growing on mounds of edgewise laminite breccia (Fig. 64).

In subunit 9e, 6m thick, an abundantly rippled and laminated dolomite contains edgewise laminite breccia layers, wave ripple-topped quartz arenite layers 2-15 cm thick, and pale green horizontal chert lenses.

Unit 10, the topmost sedimentary unit in this section is 45 m of well parallel bedded light grey to buff subarkose. Beds are traceable and of even thickness for at least 100 m. The bedding scale is 15 cm or less. The unit is well crossbedded on a 5-10 cm scale. In this east-west cliff section (Fig. 65) all crossbeds suggest a westward paleotransport. Rare subunits of quartz-biotite-muscovite- feldspar siltstone and sandstone with wavy bedding up to 2 m thick occur within the unit.

The top 12 m of the unit appear texturally supermature. At the contact with the overlying basalt the sandstone appears baked and there are no vesicles, amygdules or directional structures in the basalt nor fragments of sandstone in the basalt.

Stratigraphic section 7

The 110 m thick section rests on a grey pebbly feldspathic sandstone of the Qingaaluk Formation that contains mudcracked and rippled siltstone. The upper 1 m of the sandstone is friable and rusty.

Figure 98. Laminated dolomite with low domal stromatolite domes, edgewise laminite breccia layers (E), and chert layers (C), upper biolaminite, unit 9, section 6, Nastapoka Group. (GSC 203902-S)

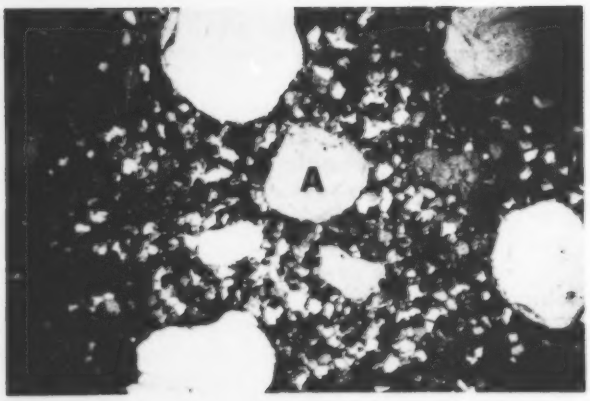

Figure 99. Photomicrograph of bimodal quartz arenite, unit 2, section 7, Nastapoka Group, Figure 47. Large clasts are quartz with minor micrite both set in a quartz, dolomite and minor feldspar matrix, nicols crossed. Grain "A" is 0.5 mm across.

Unit 1; 24.5 m thick, consists of a laminated rock with a platy parting and the appearance of a calcareous shale. Microscopic examination shows it to consist of hemicycles of quartzofeldspathic silt overlain by finely grained graded micritic dolomite topped by black wrinkled laminae (algal mat origin?). Increasing in importance and thickness (up to 30 cm) upward in the unit are buff dolomite layers. This nonfissile rock type is distinguished by the larger scale of the laminae and the greater abundance and continuity of the black laminae. The upper 7 m of unit 1 consists of an upward-coarsening quartz-rich siltstone with a matrix of about 30% of carbonate.

Unit 2; 3 m, dolomite-cemented crossbedded quartz arenite. The rock is bimodal (Fig. 99) with minor amounts of dolomicrite clasts containing quartz silt that are not dissimilar from that of unit 1.

Unit 3; 3 m, pure quartz arenite interlayered with dolomite-cemented quartz arenite.

Above unit 3, 15 m of covered section are littered with blocks of dolomite containing 30 cm high club-shaped stromatolites. These bodies are similar to 2 m of outcrop at the top of the covered interval.

Unit 4; 7.5 m, grey-buff weathered laminated dolomite with tabular chert nodules, some of which have silicified stromatolites that have grown on edgewise laminite breccia pockets (Fig. 95).

Unit 5; 8 m, straight-parallel and crinkly laminated dolomite with edgewise laminite breccia layers (Fig. 54). At the top of this unit lies a zone of poorly preserved stromatolites, probably of club form.

Unit 6; a 6 m zone of wavy stromatolites similar to those seen in other sections. This unit, terminating the carbonate section, has a fissured upper surface. The fissures are about 30 cm across and filled with sandstone similar to that overlying unit 6.

Unit 7; 36 m thick, crossbedded bimodally textured subarkose to arkose that underlies the basalts of the Nastapoka Group.

Stratigraphic section 8

The 29 m thick section overlies white-weathering grey pyritic arkose of the Qingaaluk Formation. The first unit (1) consists of 12 m of flaggy laminated micrite (Fig. 52; graded laminite) with isolated grains and microscopic pockets of quartzofeldspathic silt. Interlayered buff massive dolomite layers increase upward in thickness, up to 10 cm, at the expense of the laminated micrite. Nine metres of section are covered by basalt talus, above which is visible unit 2, 7.5 m of white-weathering microcline-rich, texturally bimodal arkose. Minor amounts of interbedded dolomite and shale are present in the arkose.

Stratigraphic section 9

The 18 m thick section lies unconformably upon white- weathering crossbedded arkose with mudcracked silty interbeds of the Qingaaluk Formation. Nearby the relief of the unconformity was seen to be at least 25 m.

Unit 1 of the Nastapoka Group is a carbonate-cemented crossbedded quartzose feldspathic grit of unknown thickness. It contains pebbles of the underlying sandstone.

Unit 2 is a laminated fissile dolomite, possibly up to 6 m thick, but poor exposure prevents estimation.

Unit 3; 3 m of light pink, coarse grained chloritic subarkose above which lies a 1.5 m thick covered interval.

Unit 4; 5.5 m, fine grained baked sandstone, a poorly sorted texturally bimodal arkose. It includes two crossbedded dolomitic layers each about 10 cm thick, about 1 m above the base of the unit. Fragments of wave-rippled siltstone were noted in loose debris from the subunit.

The unit is overlain by basalt displaying columnar jointing.

Two hundred metres along strike to the east the section consists of 6 m of flaggy sandstone with 3 discontinuous carbonate layers up to 10 cm thick and about 30 cm apart, lying 5 m above the base of the section.

Stratigraphic section 10

The 6 m thick section overlies almost horizontal rusty weathering, light grey poorly sorted arkosic grit-fine grained sandstone of the Qingaaluk Formation.

Sediments of the Nastapoka Group in this section are represented by buff- to red-weathering mainly fine grained sandstone and siltstone, with subordinate mudcracked maroon shale. A crossbedded calcareous sandstone occurs 2 m above the base of the section.

Stratigraphic section 11

This 10 m thick section is well exposed in a 100 m south-facing cliff (Fig. 69) where pink arkose is overlain by grey (reduced) arkose, both of the Qingaaluk Formation. The arkose has been downthrown against granitic basement. The faulted rocks are overlain with gentle discordance by undisturbed 10 m of light grey-pink feldspathic sandstone and overlying basalt of the Nastapoka Group.

Stratigraphic section 12

In this section 0-3 m of texturally immature crossbedded grey arkose is sandwiched between the basalt of the Nastapoka Formation and the granitic basement. It is assumed that the sandstone belongs to the Nastapoka Group.

MAPS
NOT
FILMED

CARTES
OMISES